

Republic of Iraq
Ministry of Higher Education & Scientific Research
University of Kerbala College of Engineering
Department of Mechanical Engineering



Construction of Driver's Seat Test Rig with Simulation Study of Linear Quadratic Control

A Thesis

Submitted to the Department of Mechanical Engineering – University of
Kerbala in Partial Fulfilment of the Requirements for the Degree of Master of
Science in

Mechanical Engineering

(Applied Mechanics)

By

Noor Abbas Hussein Al-Mosawi

(B.Sc. Mech. Eng. 2008)

Supervised By

Prof. Dr. Emad Qasem Hussein

Lecturer. Dr. Ali Ibrahim Al-Zughaibi

2022 A.D.

بِسْمِ اللَّهِ الرَّحْمَنِ الرَّحِيمِ

فَالْحَمْدُ لِلَّهِ
الْعَظِيمِ
الَّذِي
بَدَأَ
الْحَيَاةَ
الْأُولَى

الضحى، اية 5



The father.....

Who asks two stars from him,

and returns carrying the sky!!!

To

my father 

And

my daughter's father 


Supervisor's Certification

We certify that this thesis titled

**" Construction of Driver's Seat Test Rig with Simulation Study
of Linear Quadratic Control"**

has been prepared by (**Noor Abbas Hussein Al-Mosawi**) under our supervision the department of Mechanical Engineering, College of Engineering, University of Kerbala as partial fulfillment of the requirements for the Degree of Master of Science in Mechanical Engineering (Applied Mechanics).

Signature:



Name: **Prof. Dr. Emad Qasem Hussein**

Date:

Signature:




Name: **Lecturer. Dr. Ali Ibrahim Al-Zughaibi**


Date:

Examining Committee Certification


We certify that we have read this thesis entitled " **Construction of Driver's Seat Test Rig with Simulation Study of Linear Quadratic Control**" and as an examining committee, examined the student (**Noor Abbas Hussein Al-Mosawi**) in its content and that in our opinion, it meets the standard of a thesis and is adequate for the award of the Degree of **Master of Science in Mechanical Engineering / Applied Mechanics**.

Signature: 
Name: **Prof. Dr. Emad Q. Hussain**
Date: / / 2022


(Supervisor)

Signature: 
Name: **Asst. Prof. Dr. Wajdi Sadik Aboud**
Date: / / 2022

(Member)

Signature: 
Name: **Lecturer. Dr. Ali I. Al-Zughaibi**
Date: / / 2022

(Supervisor)

Signature: 
Name: **Lecturer. Dr. Muslim Muhsin Ali**
Date: 19 / / 2022

(Member)

Signature:

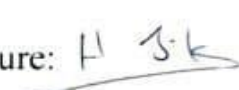


Name: **Prof. Dr. Mohsin A. AL-Shammari**

Date: / / 2022

(Chairman)

Approval of Mechanical Engineering Department

Signature: 

Name: **Asst. Prof. Dr. Hayder Jabber Kurji**

(Head of the Mechanical Engineering Department)

Date: / / 2022

Approval of Deanery of the College of Engineering / University of Kerbala

Signature: 

Name: **Prof. Dr. Laith Shakir Rasheed**

(Dean of the College of Engineering)

Date: / / 2022

Linguistic Certificate

I certify that the thesis entitled

**"Construction of Driver's Seat Test Rig with Simulation Study of
Linear Quadratic Control"**

which has been submitted by "**Noor Abbas Hussein Al-Mosawi**" has been prepared under my linguistic supervision. Its language has been amended to meet the English style.



Signature:

Linguistic advisor:

College of Engineering

University of Kerbala

Date: 14 / 12 / 2021

Abstract

There is an increasing concern to enhance the heavy-duty vehicle driver's seat suspension system to reduce the vibration transmitted to the driver's body. These vibrations are caused by the road condition and affect the driver's efficiency, performance, and health. Establishing and developing a driver's seat suspension system has been vital in the last years, which has great attention from researchers and companies to gain more ride comfort and ride safety.

Hence, this thesis has designed and built up a passive test rig seat by creating and assembling the parts with adopted some globally applicable models. An analysis of a passive seat suspension system was carried out. A comparison between the simulation and experimental results was achieved to check the validation of the test rig. It was found that the driver's seat test rig manufactured is active, suitable, and low cost.

To complete a full picture of the seat test rig, it is suggested to study and analysis an active seat system through designing a Linear Quadratic Regulator LQR controller and see whether how much the enhancement in the ride comfortably and road handling happen via reducing the vertical vibration transmitted to the seat pan through dropping the vertical seat pan acceleration. MATLAB/Simulink environments chosen for simulation works to check the performance of LQR controller design. Analysis of the driver's seat test rig model with a two degree of freedom was performed. The simulation results show that the LQR controller is robust, suitable, and has a better potential to reduce the vertical acceleration by an approximated range of 83% and achieve ride comfort, with low cost for this system; by means of considering an optimal value for control input weight matrix R and state weight matrix Q , they affected the control action. LQR controller within considering the control cost.

Acknowledgments

I would like to sincerely thank my supervisors, **Prof. Dr. Emad Qasem Hussein** and **Lecturer. Dr. Ali Ibrahim Al-Zughaibi**, for their most excellent support and endless help during each stage of this research, they have always motivated me to improve my academic skills, encouragement, much-respected enthusiasm towards the field, and complete this work successfully. And special thank to the examiners: **Prof. Dr. Mohsin A. AL-Shammari**, and **Asst. Prof. Dr. Wajdi Sadik Aboud**, and **Lecturer. Dr. Muslim Muhsin Ali**.

I am grateful to thank Al-Furat Al-Awsat Technical University/Technical Institute of Al-Mussaib/Mechanic department, **Assist. Prof. Dr. Kamil J. Kadhim**, **lecturer. Dr. Zaid H. Rashid**, and the laboratory technician "**Laith Abdul Rahim**" and "**Haitham Hamid Al-Jubouri**" for the technical support and substantial help in performing experimental tests. Many thanks go to the **lecturer. Emad Jabr**, Technical College - Al-Mussaib.

It is an honor for me to thank Kerbala University/ Engineering College/Mechanical Department, **Assist. Prof. Dr. Hayder Kurji**, and **Assist. Prof. Dr. Mohammed Wahab**, for their providing departmental facilities and their continuous encouragement.

Finally, I am deeply grateful for the love and inspiration provided by my husband **Yasser**♥; this work would not have been possible without his support. And my daughter **Dania**♥, all of my love, efforts, and successes are for you.

Contents

Abstract	I
Acknowledgments.....	II
Contents	III
List of Figures	VI
List of Table.....	IX
List of Symbol	X
List of Abbreviations	XII
Chapter 1. Introduction	1
1.1 Introduction	1
1.2 Classification of Suspension System of Vehicles.....	3
1.2.1 Passive Suspension System	3
1.2.2 Active Suspension System	3
1.2.3 Semi-Active Suspension System	6
1.3 Aim of the Thesis.....	8
1.4 Steps for Achieving the Aim	9
1.5 Thesis Layout	10
Chapter 2. Literature Review.....	11
2.1 Introduction	11
2.2 Classification of Seat Suspension	11
2.2.1 Passive Seat Suspension System	11
2.2.2 Active Seat Suspension System	13
2.2.3 Semi-Active Seat Suspension System	17
2.3 Active Vibration Control Strategies	19
2.4 Concluding Remarks	20
Chapter 3. Establishing of Driver's Seat Test Rig.....	22
3.1 Introduction	22
3.2 Basic Simulation Model to Understand Seat Test Rig	22
3.3 Stages of Building Up Seat Test Rig.....	22
3.3.1 Input Unit	23
3.3.1.1 Iron Steel Structure Frame	23
3.3.1.2 AC Motor.....	23
3.3.1.3 Cam and Flower	24
3.3.2 Seat Structure.....	25

3.3.2.1 Seat Base Construction.....	25
3.3.2.2 Seat Pan	25
3.3.2.3 The Shock Absorber (Passive Suspension System)	26
3.3.2.4 Linear Slider	28
3.3.2.4.1 Linear Shaft Part.....	28
3.3.2.4.2 Linear Bearing (Slide Block Part)	28
3.3.2.5 Tow Lever Arm.....	29
3.3.3 Electronic Parts.....	30
3.3.3.1 Arduino Uno Board	30
3.3.3.2 Accelerometer and Displacement Sensors	31
3.3.4 Assembly of Seat Test Rig.....	32
3.3.4.1 GUI Window.....	33
3.4 Summary	34
Chapter 4. Theoretical Parts (Passive and Active Model).....	35
4.1 Introduction	35
4.2 Simulation Models	35
4.2.1 Model of the Passive Driver's Seat Test Rig	36
4.2.2 Model of the Active Driver Seat Test Rig	37
4.3 LQR Control Technique	38
4.3.1 Design of LQR Controller	44
4.3.2 Determination of the Weight Matrices	46
4.3.3 Controllability and Observability of the System.....	48
4.3.4 LQR Controller with Integral Compensation Action.....	49
4.4 Road Profile Generation	51
4.5 Summary	53
Chapter 5. Results and Discussion	55
5.1 Introduction	55
5.2 Passive Test Rig Seat Performance Validation.....	55
5.2.1 Simulation and Experimental Verification.....	55
5.2.1.1 Passive Suspension Response.....	57
5.3 Active System and LQR Controller Performance Validation	60
5.3.1 Active System with LQR Controller Without Disturbance.....	61
5.3.2 Active System with LQR Controller with Disturbance	65
5.3.3 LQR Controller with Integrator Compensation	69
5.4 Summary	76

Chapter 6. Conclusion and Recommendation	78
6.1 Conclusion	78
6.2 Recommendation	79
Reference	80
Appendix.....	86

List of Figures

Figure 1–1: Passive suspension system.....	3
Figure 1–2: a) Low bandwidth active systems b) High bandwidth active systems	4
Figure 1–3: Mercedes Benz low bandwidth active systems.....	.5
Figure 1–4: BOSE high bandwidth active systems.....	5
Figure 1–5: Semi active suspension system.....	6
Figure 1–6: MR damper sketch.....	7
Figure 1–7: ER damper sketch.....	7
Figure 2–1: Sketch diagram of a (Passive b (Active c (Semi-Active seat suspension system.....	11
Figure 2–2: a) Duplicate picture for a passive seat suspension system b) Sketch for the passive seat suspension system.....	12
Figure 2–3: Duplicate picture of a passive suspension system.....	13
Figure 2–4: Duplicate picture of heavy-duty truck test rig.....	14
Figure 2–5: a) Passive suspension prototype b) Sketch of an active suspension system..	15
Figure 2–6: Sketch of an active system.....	15
Figure 2–7: Sketch of an active suspension system.....	16
Figure 2–8: Boos Ride systems.....	17
Figure 2–9: a) Sketch of a semi-active suspension system b) Duplicate picture of the semi-active seat.....	18
Figure 2–10: Sketch of a semi-active system.....	18
Figure 2–11: Sketch of a semi-active suspension system.....	19
Figure 3-1: a) Sketch of the frame in SOLIDWORKS program b) Duplicated picture of the frame. c) Duplicated picture for the upper and lower plates.....	23
Figure 3-2: a) Sketch of the motor in SOLIDWORKS program b) Duplicated picture of the motor and gearbox.....	24
Figure 3-3: a) Sketch of an eccentric cam in SOLIDWORKS program b) Duplicated picture for the eccentric cam	24
Figure 3-4: a) Sketch of flower in SOLIDWORKS program b) Duplicated picture of the flower	24
Figure 3-5: a) Sketch of the seat base in SOLIDWORKS program b) Duplicated picture of the seat base.....	.25
Figure 3-6: a) Sketch of the seat pan in SOLIDWORKS program b- Duplicated picture of the seat pan.....	26

Figure 3-7: a) Sketch of damper and spring in SOLIDWORKS program b) Duplicated picture for the damper c) Duplicated picture for spring.....	27
Figure 3-8: Duplicated picture for the SM1000 universal testing machine.....	27
Figure 3-9: a) Duplicated picture for the spring test b) Duplicated picture for the damper test.....	28
Figure 3-10: a) Sketch of a linear shaft in SOLIDWORKS program b) Duplicated picture for the linear shaft part.....	28
Figure 3-11: a) Sketch of slide block in SOLIDWORKS program b- Duplicated picture for the slide block part.....	29
Figure 3-12: Duplicated picture for the linear slider.....	29
Figure 3-13: a) Sketch for two lever arms in the SOLIDWORKS program. b) Duplicated picture for two lever arms.....	30
Figure 3-14: a) Duplicated picture for Arduino Uno board b) Duplicated picture for relay	31
Figure 3-15: Duplicated picture for GY-61 DXL335 3-axis accelerometer.....	32
Figure 3-16: Duplicated picture for GY-VL53L0XV2 laser distance sensor.....	32
Figure 3-17: a) Sketch for the whole assembly of driver's seat test rig in SOLIDWORKS program b) Duplicated picture for the whole assembly of driver's seat test rig.....	33
Figure 3-18: GUI window control and monitoring.....	34
Figure 4-1: a) Sketch of the passive seat test rig b) Passive seat suspension system model c) Free body diagram for passive system.....	36
Figure 4-2: a) Model of the active seat suspension system b) Free body diagram for active system.....	38
Figure 4-3: The LQR block diagram.....	39
Figure 4-4: Poles-Zeroes map.....	40
Figure 4-5: Controller design in case of without disturbance.....	42
Figure 4-6: Controller design in case of adding disturbance.....	43
Figure 4-7: The test rig system with zero reference.....	49
Figure 4-8: Step response of the active test rig with LQR control.....	49
Figure 4-9: System with the LQR controller and integrator compensation	50
Figure 4-10: Step response of the active test rig with LQR control and integrator ...	51
Figure 4-11: Bump road profile.....	52
Figure 4-12: Random road profile.....	53

Figure 5–1: SIMULINK code of passive test rig model.....	56
Figure 5–2: a) Setup of Arduino Uno Board with displacement and acceleration sensors b) GUI window with monitoring data.....	57
Figure 5–3: Experimental and simulation of system input.....	58
Figure 5–4: Simulated and experimental seat pan displacement results.....	58
Figure 5–5: Experimental and simulation seat pan velocity results.....	59
Figure 5–6: Experimental and simulation seat pan acceleration results	59
Figure 5–7: Road profiles a) Bump b) Random.....	60
Figure 5–8: LQR control without disturbance for the active seat test rig... ..	61
Figure 5–9: Seat pan displacement for a) Bump profile b) Random road profile	62
Figure 5–10: Seat pan velocity for a) Bump profile b) Random road profile	63
Figure 5–11: Seat pan acceleration for a) Bump profile b) Random road profile	64
Figure 5–12: Seat suspension travel for bump profile	65
Figure 5–13: LQR control with disturbance for the active seat test rig..... ..	66
Figure 5–14: Seat pan displacement for a) Bump profile b) Random road profile	66
Figure 5–15: Seat pan velocity for a) Bump profile b) Random road profile	67
Figure 5–16: Seat pan acceleration for a) Bump profile b) Random road profile..... ..	68
Figure 5–17: Seat suspension travel for bump profile	69
Figure 5–18: LQR control with integrator compensation for the active seat test rig	70
Figure 5–19: Seat pan displacement of a) Bump profile with LQR Control b) Bump profile with LQR and an Integrator c) Random road profile with LQR control d) Random road profile with LQR and an Integrator.....	70
Figure 5–20: Seat pan velocity of a) Bump profile with LQR control b) Bump profile with LQR and an Integrator c) Random road profile with LQR control d) Random road profile with LQR and an Integrator.....	71
Figure 5–21: Seat pan acceleration of a) Bump profile with LQR control b) Bump profile with LQR and an Integrator c) Random road profile with LQR control d) Random road profile with LQR and an Integrator.....	72
Figure 5–22: Seat suspension travel of a) Bump profile with LQR control b) Bump profile with LQR and an Integrator	73

List of Table

Table 1- 1: Comparative Between Active, Semi-Active and Passive System.....	8
Table 4 1: The Description of The Active Model Symbol.....	37
Table 5-1: The Value of Parameters of the Active Seat Suspension.....	57
Table 5-2: Performance of the System in Term of Acceleration, Velocity, Suspension Travel	74
Table 5-3: Performance of the System in Term of Rising time, Settling time, Percentage Overshoot.....	74
Table (5-4) : the RMS value of vertical acceleration for passive and active with LQR controller	75
Table (5-5): Uncomfortable reaction level to vibration values according to IOS 2631-1..	75

List of Symbol

Symbol	Description	Unit
a_w	Frequency Weighted Vertical Acceleration	m/s ² (RMS)
c_{sp}	Seat pan suspension damper	(N.s/m)
k_{sb}	Seat base stiffness	(N/m)
k_{sp}	Seat pan suspension stiffness	(N/m)
m_{sb}	Seat base mass	(Kg)
m_{sp}	Seat pan mass + driver's mass	(Kg)
X_b	Body excitation displacement	(m)
X_{sb}	Vertical displacement of seat base	(m)
X_{sp}	Vertical displacement of seat pan	(m)
C_m	Controllability	----
J_{LQR}	LQR performance index	----
K_I	Integrator gain	----
K_{LQR}	the LQR control gain	----
O_m	Observability	----
$x_r(t)$	road displacement	(m)
ϑ_n	random phase angel	(rad)
$\Phi(\Omega_n)$	power spectral density	(rad/m)
A	state matrix	----
a	bump height	(m)
A_n	the amplitudes	(m)
B	input matrix	----
C	output matrix	----
D	disturbance matrix.	----
F_a	Control force	(N)
L	the wavelength	(m)

Q	State weight matrix	----
R	Control input weight matrix	----
u	Feedback control law	----
$x(t)$	State-space vector	----
Ω	angular spatial frequency	(rad/m)
ρ	positive constant	----

List of Abbreviations

Abbreviations	Description
2DOF	Two Degree of Freedom
ABC	Active Body Control
ANNC	Artificial Neural Network
EOM	Equation of Motion
FBD	Free Body Diagram
FLC	Fuzzy Logic
FSTPID	Fuzzy-Self-Tuning PID
GA PID	Genetic Algorithm PID
ICs	Intelligent controllers
LMS	Least-Mean-Square
LQ	Linear Quadratic
LQG	Linear Quadratic Gaussian
LQR	Linear Quadratic Regulator
LTI	Linear Time Invariant
OICA	Organization of Motor Vehicle Manufacturers
PA	Pole Assessment
PD	Proportional Derivative
PI	Proportional Integral
PID	Proportional Integral Derivative
RMS	Root Mean Square
SMC	Sliding Mode Control
H_{∞}	H-Infinity

Chapter One

Introduction

Chapter 1. Introduction

1.1 Introduction

Vehicle occupants, especially drivers in heavy-duty vehicles, are exposed to vibrations. These vibrations are caused by road disturbances, and affect driver's performance, and lead to health risks. The vibrations are transmitted to drivers through the vehicle suspension system. The enhancement of the driver's seat suspension system has an increasing concern to reducing the vibration transmitted to the driver body. The crucial aspect of the suspension design is being reliable and safe and having good performance to remove road excitation. The preferred vehicle's suspension system has a good performance in reducing the high-frequency vibrations caused by bumpy roads. Despite significant enhancement in suspension system design, still have poor isolate performance in the low-frequency vibrations, which surely leads to deep thinking of developing seat suspension systems to reduce the vibration in low frequencies.

A driver seat suspension system was developed to increase driver comfortable and reduce health risks while driving. The driver seat acts as an insulator and reducer of vertical vibrations that are transmitted to the seat. The essential aspects should be involved in seat suspension design, low cost, suitable to cancel the road excitation. From the literature, the seat suspension systems are classified into **passive**, **active**, and **semi-active**.

The first type is the passive system, in which the insulation is achieved through using of spring with dampers and cushions. The springs support the seat's body by acting as an energy reservoir, while the damper is a dispersive energy element. It has been called passive because neither the springs nor the damper can add energy to the system. The second type is an active system, which

consists of spring and damper, in addition to a factor that supplies energy to the system called an actuator with sensors to measure force, motion, and acceleration. The actuator controls the system and is considered an essential part of the active system of the seat. The force of the actuator is the main responsible for isolating and canceling the vibrations. Many types of actuators have been developed in past years, including hydraulic, pneumatic, electrohydraulic, electromagnetic, and stacked piezoelectric actuators.

The semi-active suspension system is medley between the passive and active suspension systems. Such systems provide the best performance better than a passive system because the passive element can be adjusted using control strategies requiring specific active devices such as electrorheological and magnetorheological fluid dampers. The semi-active systems represent the plainness of passive suspension systems and the excellent performance of the active suspension systems with high costs.

The active suspension system is characterized by changing road condition results as adjusted continuously, so many control strategies were employed to produce a controlled force for an active suspension system to obtain a more comfortable and safer ride. The optimal control is one of these strategies. Linear Quadratic Regulator (LQR) is a technique of the optimal strategy, the LQR control is full state feedback control, designed to minimize the energy that associated with performance index. It will be used in this thesis to generate control forces to achieve a safe and comfortable ride.

Recently, many researchers have great attention to developing driver seats, and they are interested in building up a seat test rig to develop its suspension system and control strategies. The manufacturing process of the test rig has a high contribution because the researchers need to know how to build up the test rig that will help undertake their research and develop the rig to be used later in the industry field.

1.2 Classification of Suspension System of Vehicles

The suspension system of vehicles can be classified into Passive, active, and sim-active according to their required energy to complete their works.

1.2.1 Passive Suspension System

A passive suspension system consists of a spring with a shock absorber (damper), as shown in Figure (1-1). The spring is a major component in the passive system, which acts as a storage-energy element for impulse force from above. In contrast, the spring absorbs vibration energy while deforming and supporting the car body. The damper acts as a dissipate-energy element and controller to the road input transmitted to the vehicles [1]. The passive suspension system cannot add energy to the system or require energy to complete its function, so, identified as passive [2].

The selection of the passive system specification should be achieved the compatibility between road comfort and road holding under various road conditions [3][4].

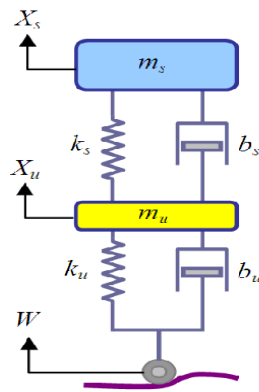


Figure 1–1: Passive suspension system [5]

1.2.2 Active Suspension System

The active suspension system consists of a passive element, spring, and damper, with additional factors that supply energy to the system, called an

actuator (e.g., electrical linear motor or hydraulic cylinder); this actuator generates a controlled force [6]. The active suspension system classification to slow active suspension systems (also called low bandwidth active systems) and fully active suspension systems (also called high bandwidth active systems), as displayed in Figure (1-2) [7].

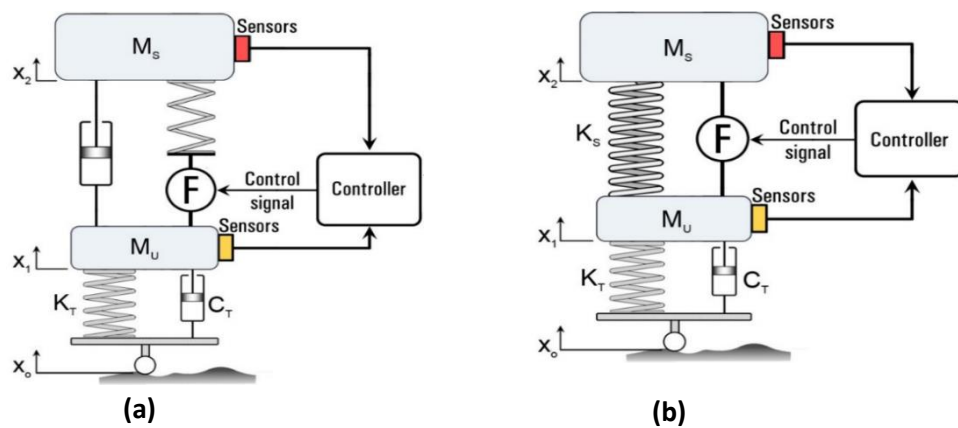


Figure 1–2: a) Low bandwidth active systems b) High bandwidth active systems [8]

The slow active suspension systems are also called low bandwidth active systems. The feature of this system is to add actuator combined in series to the spring and generate suspension forces separate from the relative motion of the chassis and wheels[9].

The concept of low bandwidth active system is employed by Mercedes Benz company which is developed Active Body Control (ABC) which is used in the Mercedes Benz S-class, the coupe CL-class since 1999 and since 2001 in the SL roadster As shown in Figure (1-3) [10]. The bandwidth in this system is in a range of approximately 5 Hz.



Figure 1–3: Mercedes Benz low bandwidth active systems [10]

The fully active suspension system is also called the high bandwidth active suspension system, characterized by the passive element being replaced or complemented by an actuator combined in parallel with the spring[11]. The concept of high bandwidth active suspension systems has been worked on and developed by BOSE company since 1980 [12]. As presented in Figure (1-4).



Figure 1–4: BOSE high bandwidth active systems [12]

The request energy for a low active suspension system is in the range of 1–5kW, and for a fully active suspension system is in the range 4–20kW, which makes it expensive, which is considered the main disadvantage of this system[13]. An active approach is generally less reliable because it produces external control forces that make it unstable[14].

1.2.3 Semi-Active Suspension System

Semi-active suspension systems consist of spring and damper, which characteristics can be adjusted, as demonstrated in Figure (1-5). The control force is able to be generated by modulating the damping rate, and that achieve by using the semi-active hydraulic damper or magnetorheological dampers (MR damper); this damper is also called MagneRide, which is represented by Delphi [15], and Electrorheological dampers [16].

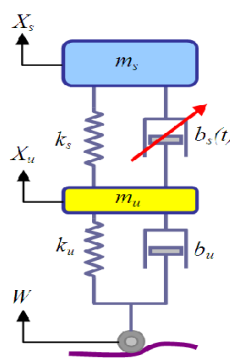


Figure 1–5: Semi-Active suspension system [5]

The hydraulic damper throttles hydraulic oil between the chambers inside the damper, which can dissipate the energy. So, to change the dissipation level, used the valves as a controller to adjust the cross-section of the opening between the chambers [17].

In magnetorheological dampers, it can be applied by a magnetic field changing the magnetorheological fluid's viscosity, which causes magnetic particles in the fluid to form chains[18]. Figure (1-6) shows the MR damper.

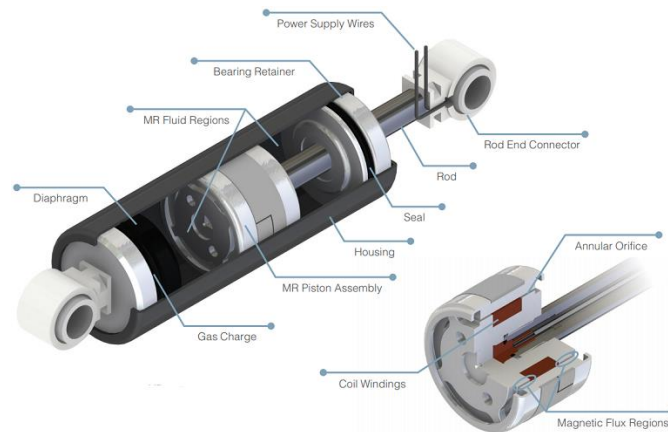


Figure 1–6: MR damper sketch [18]

Electrorheological dampers are used as an electrical field to form the particle chains of the fluid, leading to varying flow properties of the electrorheological fluids[19]; Figure (1-7) shows the ER damper. Semi-active dampers operate at a low power consumption of around 20 - 40 W and have a bandwidth of up to 40Hz [20].

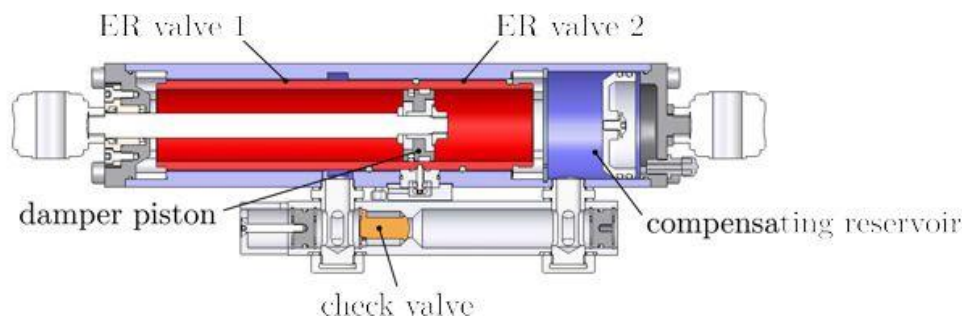


Figure 1–7: ER damper sketch [19]

Finally, a brief comparison between the three systems can be made in the table (1-1) as follows:

Table 1- 1: Comparative between active, semi-active, and passive system

Active system	Semi-active system	Passive system
✓ Dynamic behavior is good.	✓ Dynamic behavior is less than an active system.	✓ Passive dynamic behavior.
✓ The structure design is complex spatial in a hydraulic and pneumatic system.	✓ The structure design is also slightly complex.	✓ The structure design is simple.
✓ Handling and ride comfort are good spatially in the active electromagnetic system are the best.	✓ Handling and ride comfort is less than an active system.	✓ Handling and ride comfort is bad.
✓ Reliability is lower than passive, except for the active electromagnetic system, which has high reliability.	✓ Reliability is high.	✓ Reliability is the highest.
✓ The cost is the highest between the systems.	✓ The cost is lower than the active system.	✓ The cost is the lowest.
✓ Power request is higher than passive and semi-active systems	✓ Power request is less than an active system.	✓ Power request is the lowest.

1.3 Aim of the Thesis

This thesis aims to establish and develop a driver seat suspension system by building up a passive driver seat test rig and analyzing theoretically and

experimentally the passive seat responses. And suggesting a suitable active control force using a control strategy called LQR (Linear Quadratic Regulator) to reduce vertical vibration, enhance the system performance, and gain a ride comfortable. The reason for studying vertical vibration is that at low frequencies, the vertical vibration is the most dominant to the driver's body, which causes an uncomfortable ride. The test rig has been built up by creating and assembling the parts with adopted applicable models.

1.4 Steps for Achieving the Aim

The aim of the research will be achieved by representing the following objectives:

1. Building up experimentally the test rig for passive seat suspension.
2. Carry out an experimental test to show system responses.
3. Modelling the passive system of the practical test rig.
4. Verification of the results.
6. Modelling the active seat system.
7. Proposed and design a suitable controller based on LQR technique.
8. Analyzing data gain from simulation of active system and shows the system responses enhancement.

1.5 Thesis Layout

This thesis is composed of five themed chapters.

- Chapter one provides an introduction to the research subject review for vehicle suspension systems and the aim and objective of the thesis.
- Chapter two represents the literature review on the subject of this thesis.
- Chapter three represents the stages of test rig built-up with reviews each part details.
- Chapter four shows the theoretical description of the mathematical modeling of passive, active suspension systems, LQR controller design.
- Chapter five reviews the results and discussion with a conclusion.
- Chapter six reviews the conclusion with the recommendation.

Chapter Two

Literature Review

Chapter 2. Literature Review

2.1 Introduction

This chapter surveys the literature on seat suspension systems which are classified into three systems. Each type of classification was focused and reviewed on the assembly of the driver's seat after those active vibration control strategies were reviewed and concluding remarks.

2.2 Classification of Seat Suspension

The ride's comfortable and safe can be enhanced by developing seat suspension systems. The seats can be classified as in-vehicle suspension into **passive**, **active**, and **semi-active** suspension systems, as indicated in Figure (2-1).

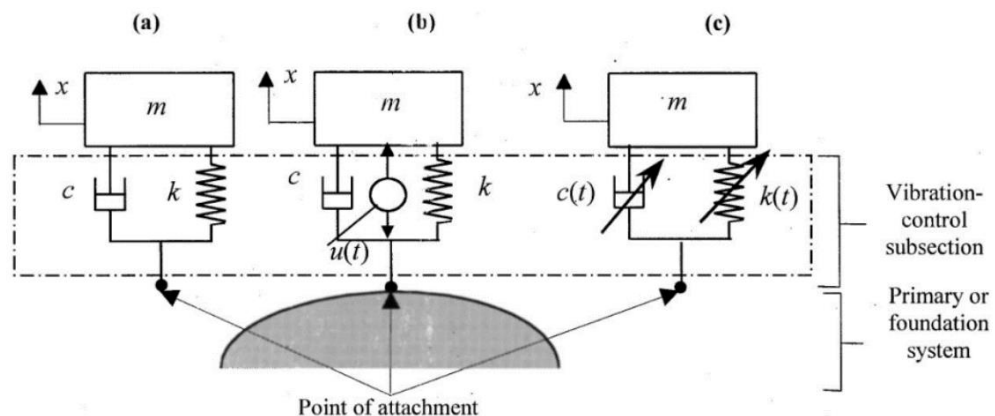


Figure 2–1: Sketch diagram of a (Passive b (Active c (Semi-Active seat suspension system [21]

2.2.1 Passive Seat Suspension System

This system consists of a spring and a damper as an in-vehicle suspension system see Figure (2-1 a). For having ride comfortable, the spring and damper coefficients are set usually to specific values.

The passive vibration isolated for most vehicles is achieved by using spring and damper with cushions. The standard material used in cushions can reduce high-frequency vibrations but simultaneously amplify vibration in low frequencies.

Ning. D, et al. in [22] proposed a suspension system for a passive seat to examine the seat's dynamic response to inputs. The seat structure consists of a spring with a hydraulic damper. Figure (2-2) shows a sketch of the passive seat suspension with a prototype picture.

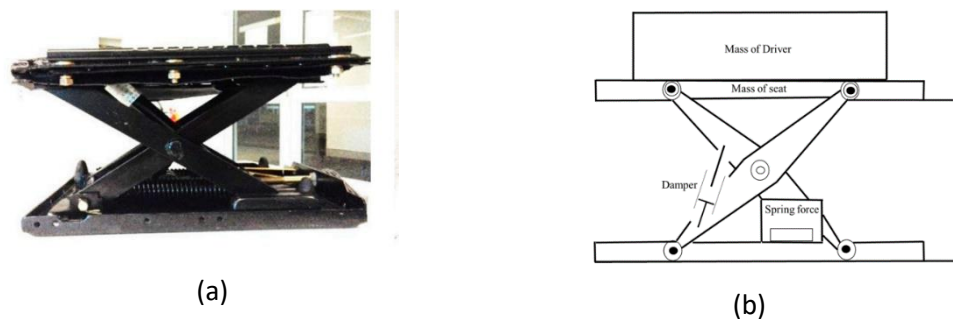


Figure 2–2: a) Duplicate picture for a passive seat suspension system b) Sketch for the passive seat suspension system [22]

Although some cushions materials in passive seat systems have been developed to reduce vibration in high frequencies, those materials lose their effectiveness in low frequencies and make significant relative motion [23]. The elastomer is one of the materials recently used to achieve the damping effect, and it can absorb mechanical vibration energy [24].

Adam, et al. [25] studied the performance of passive seat suspension to reduce vertical vibration for agricultural tractors seats, and the researchers suggested suspension with two linear springs with foam cushion. The results showed that changes in posture and vibration magnitude affect the vibration transmission of the suspension system, see Figure (2-3).



Figure 2–3: Duplicate picture of a passive suspension system [25]

In general, the vibration energy in the passive seat dissipates before the energy is transmitted to the occupant. The limitation of passive seat suspension, it is challenging to develop and perform poorly at low vibration frequencies.

2.2.2 Active Seat Suspension System

The active seat suspension system in which the passive element can be replaced or supported by a control element that supplies the force to the system, which is an actuator. With sensors to measure force, motion, and acceleration that indicate a vibration signal [26]. Figure (2-1 b) shows the active seat suspension system.

The actuator is the essential part of the active system, and it can be classified as a hydraulic actuator (with hydraulic servo), electromagnetic actuator (with linear motor), pneumatic actuator (with pneumatic spring). The actuators distinguishing characteristics are reliability, low cost, low power consumption, low noise [27].

The researchers and vehicle manufacturers companies are interested in developing an active seat suspension system because they were trying to

achieve good vibration isolation in low frequencies, leading to comfortable and safe rides.

M.Kawana, et al. [28] designed an active seat with a scissor structure test rig. The researchers proposed an active seat suspension system for heavy-duty trucks using an electric servo-motor spring to eliminate vertical vibration. Although the scissor structure had internal friction and allowed only vertical motion, it successfully reduced the vertical vibration in the seat. In addition, the suspension system did not need ample space.

Later Ning.D, et al.[29] developed the test rig by using a ball-screw mechanism and an additional actuator to reduce the vibration in roll direction and pitch direction (lateral vibration), As demonstrated in Figure (2-4). According to the results, WBV in the roll and pitch directions is reduced by 41.4 and 44.3 %, respectively. So, the suggestion system has a good performance, enhances vibration cancelation, and achieves a safe and comfortable ride. The disadvantage of these changes makes a structure complex and high cost.

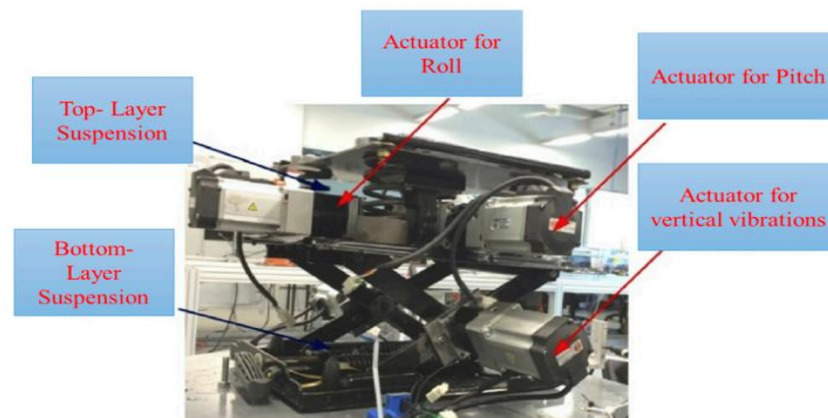


Figure 2–4: Duplicate picture of a heavy-duty truck test rig [29]

Braghin, et al.[30] modified a passive agriculture vehicle seat to active suspension by changing the hydraulic shock absorber with a hydraulic actuator. Furthermore, adding a PD regulator and modifying the air spring by adding a servo-valve. The suggested active system degrades the seat acceleration by 50%

in comparison with the passive seat. Figure (2-5) shows the passive and a sketch of the active system.

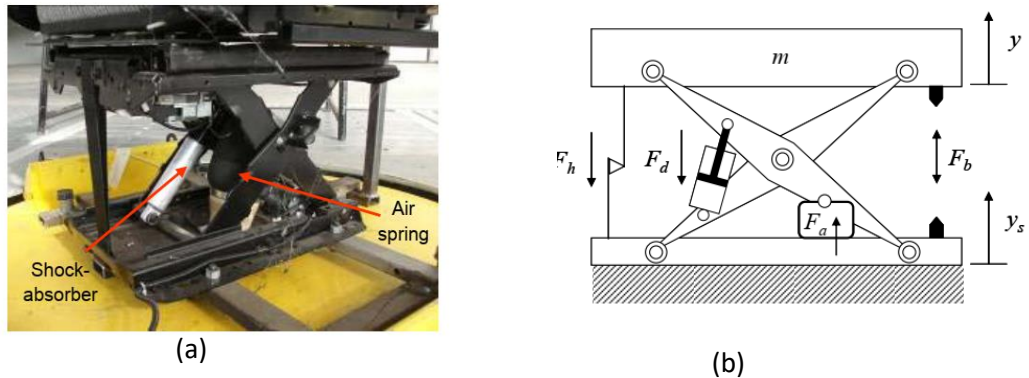


Figure 2–5: a) Passive suspension prototype b) Sketch of an active suspension system [30]

Stein, et al. in [31] developed an active system for off-highway equipment seats using a proportional electro-pneumatic transducer with a pneumatic spring to reduce vibration transmissibility. Figure (2-6) shows the sketch of an active system. This system successful to reduce the vertical acceleration by 30-40%.

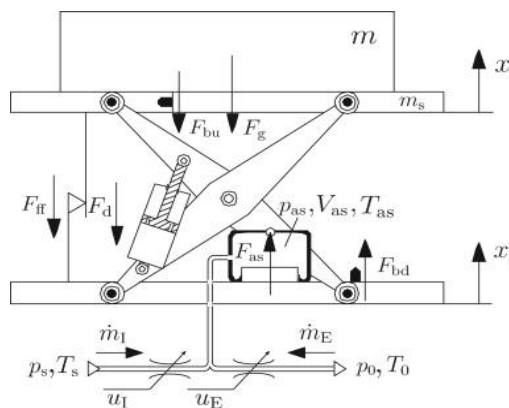


Figure 2–6: Sketch of an active system [31]

I. Maciejewski et al. [32] introduced a seat with the active suspension consisting of the hydraulic damper with a pneumatic spring. The researchers used a directional servo-valve to achieve the active control of airflow to the pneumatic spring. The modified seat suspension significantly improves the

seat's vibro-isolating properties in the 0–4 Hz frequency range. So, this system has a good vibration reduction and achieves an excellent dynamic response. The disadvantage of a pneumatic system is complex because the air pressure stowed in the source needs a large amount of energy.

In [33], Gan, et al built a test rig for an active seat suspension system. The author employed a passive suspension (with Elka-stage5 bicycle shock absorber) to carry the static load and an active suspension using electromagnetic linear actuators to generate the control force to reduce vertical vibration, as duplicated in Figure (2-7). Alfadhli [34] developed the seat using a ball bearing and the slide bearing to obtain rotational motion. The test rig succeeded in reducing the vertical vibration. From the results, the level of vibration absorption, with up to a 19.5 dB reduction throughout the HBSF range. The disadvantage of this test rig is the high cost and complexity of the data measurement system.

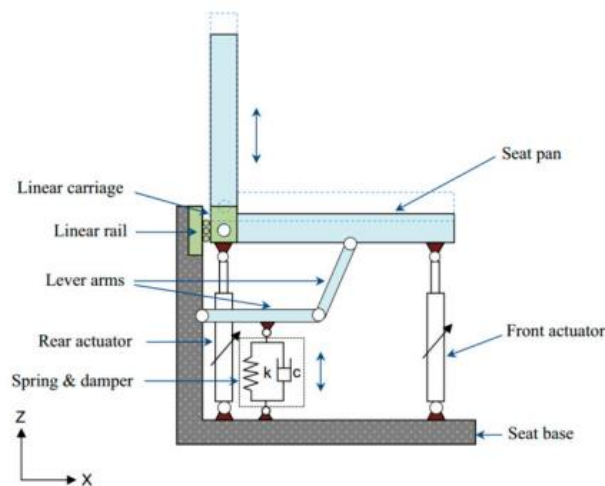


Figure 2–7: Sketch of an active suspension system [33]

The Bose Ride System for trucks is the successful use of an active seat suspension. The investigators used in their system a linear electromagnetic actuator [35]. The Bose Ride system represents safe and comfortable driving

over different road conditions, reducing driver pain and fatigue. Figure (2-8) shows Bose Ride system.



Figure 2–8: Boos Ride systems [35]

Using an active seat system is limited Because of the complexity and required high cost; therefore, this study will be limited to building up the passive seat test rig and simulating the active seat test rig.

2.2.3 Semi-Active Seat Suspension System

Although this study will consider only the passive and active seat system, it is still vital to cover as literature the semi-active seat system; the semi-active seat suspension system is distinguished by a passive element that can be adjustable. The damping characteristic can be modulated by applying an electric field to the electrorheological fluid damper (ER). Moreover, magnetic field to the magnetorheological fluid damper (MR) or modulating fluid flow orifices [36]. The semi-active system is displayed in Figure (2-1c).

The advantage of this system is the high reliability, low energy requirements, in addition to its cost compared to an active system, so it finds many semi-active seat suspension systems proposed in recent years [37].

Sun , et al in [38] proposed a semi-active seat system with a rotary MR damper with the best vibration cancellation performance, As shown in Figure (2-9).

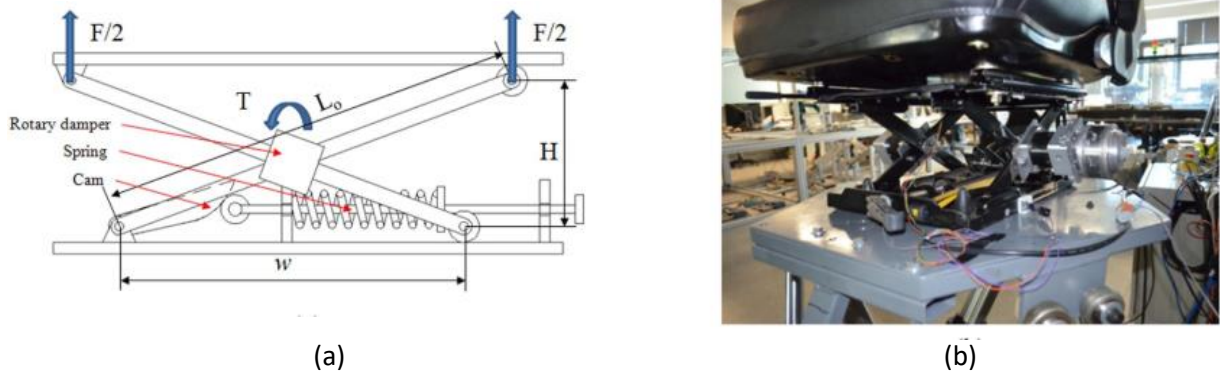


Figure 2–9: a) Sketch of a semi-active suspension system b) Duplicate picture of the semi-active seat [38]

In [39] X. Wu , et al. developed a semi-active seat suspension system to reduce the impact caused by high vibration rate or shocks in the occupant seat by using ER fluid damper

Also, in [40], Choi, et al. suggested semi-active seat suspension for commercial vehicles by using MR fluid damper to enhance vibration reduction, as shown in Figure (2-10). The developing system has an excellent dynamic performance.

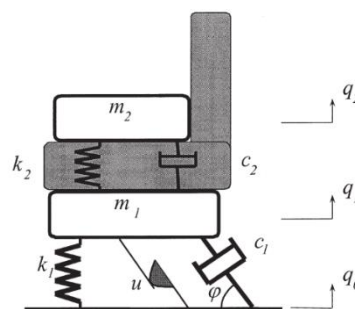


Figure 2–10: Sketch of a semi-active system [40]

S. J. MCMANUS, et al [41] estimated the semi-active seat suspension system performance to decrease vibration and shock to minimize the happening and seriousness of the end-stop impacts of seat suspension low natural frequency.

Hiemenz , et al [42] discuss that the occupant's comfort can be achieved when used MR damper in semi-active seat suspension system for helicopter crew seats, as shown in Figure (2-11).

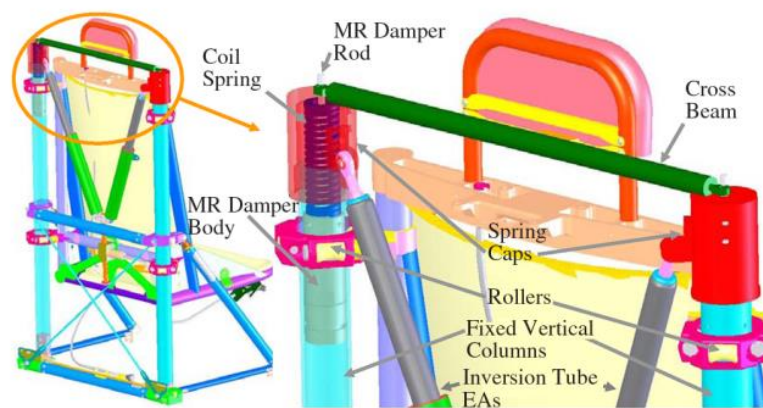


Figure 2–11: Sketch of a semi-active suspension system [42]

2.3 Active Vibration Control Strategies

Several control strategies can be utilized to control the active vibration system. In recent years, active seat suspension techniques were developed to reduce vibrations and to be comforted. For example, PID controller [43], Skyhook control [44] [45], robust control [46] like Robust H_∞ Controller [47] [48] and sliding mode control (SMC) [49], adaptive control [50] [51] like Least-Mean-Square (LMS) algorithm [52], Intelligent controllers (ICs) [53] like fuzzy logic (FLC) controller [54], and artificial neural network (ANNC) controller [55], and finally optimal control [56] Linear Quadratic Regulator (LQR).

Many researchers have developed a hybrid control algorithm. This algorithm combines two control strategies to maximize the system's performance.

Shaimaa A. Ali in [57] improved the performance of an active seat suspension by using the hybrid genetic algorithm PID (GA PID) and fuzzy-self-tuning PID (FSTPID) controllers to obtain comfort rides for pregnant women, and the suggested controls enhance the performance of the seat.

LQR technique is the most common form of an optimal control strategy that can optimize the system's feedback data to improve the performance index and obtain high stability to the system. The drawback of this technique is challenging to apply in the real case because it assumes that all system states are able to be measured. Linear Quadratic Gaussian approaches used the Kalman filter technique to overcome the drawback in the LQR technique and estimate the unavailable states. Emad, Q.Hueesin in [58] shows that when compared to the LQR controller technology, the LQG controller technique has excellent stability and response.

2.4 Concluding Remarks

This chapter introduces the literature review that deals with vehicle seat suspension systems, a review of the seat suspension systems with their advantage and limitation, and scoping on the manufacturing of seat test rigs. Most of these test rigs have a scissor structure which has a drawback like, first, allowing only the vertical motion; although the researchers added a ball-screw mechanism to obtain the roll and pitch direction, this made the structure complex with the high cost and big space. The second is the internal friction which can impede the performance of seat suspension. Furthermore, the advantage of this structure is the good vertical vibration reduction, and the scissor structure does not take a large space. However, Zengkang Gan represented the vertical structure for the seat suspension system in 2015. This structure's advantages are that it can achieve the motion in three directions

(vertical, roll, pitch) by changing the slide bearing. Also, the seat has low friction in comparison with scissor structures. In this thesis work, it developed a vertical seat suspension. Details for building up the test rig were represented in chapter three.

A summary of the active vibration control strategies was done; the LQR technique, the most common form of optimal control strategy, was decided to use for enhancing the system. More investigation on this technique is available in chapter four.

Chapter Three

Establishing of Driver's Seat Test Rig

Chapter 3. Establishing of Driver's Seat Test Rig

3.1 Introduction

This chapter shows how to create and produce each part for establishing the passive suspension system of the driver seat test rig. This is the basic ground of this study that will be helping to validate the mathematical system model by comparing with simulation results. The analysis of the study will be detailed in the next chapters. This chapter introduces information on all mechanical, electrical, and electronic parts relative to the practical seat test rig. To be more technical, after the test rig was established, simulation of the mathematical model was performed using MATLAB/Simulink environments to validate test rig design.

3.2 Basic Simulation Model to Understand Seat Test Rig

In order to have the basic information of the seat test rig, it should be using the literature simulation models that will be helped with designing and building up the test rig. For this purpose, the researcher has adopted the design used before for the test rig, such as [59] [60], it was found that helpful for building up the test rig process.

3.3 Stages of Building Up Seat Test Rig

The test rig is established through designing and creating parts and then assembling those parts to have a test rig. The test rig consists of three main units. The first unit stocks the input signal to the test rig system; the second is the seat's structure; the last is the measurement unit.

3.3.1 Input Unit

The input unit is designed to provide the input system signal. The applied force provides the movement of the seat test rig system. The input unit system consists of the following parts:

3.3.1.1 Iron Steel Structure Frame

As shown in Figure (3-1), the structure is made of two iron steel plates, upper and lower bases with dimensions are $[460 \times 640 \times 10]$ mm for every four columns (diameter is 80 mm for each) covered at the top by four smaller springs for supporting and distributing the plates weights.

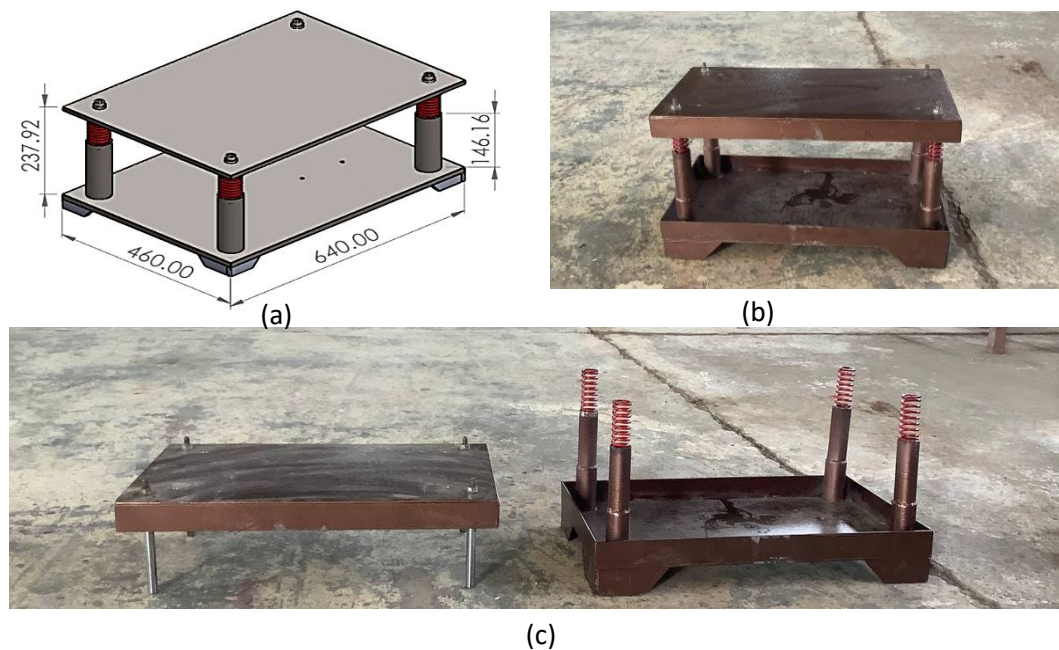


Figure 3-1: a) Sketch of the frame in SOLIDWORKS program b) Duplicated picture of the frame. c) Duplicated picture for the upper and lower plates

3.3.1.2 AC Motor

A three-phase electric motor was used with three hp -380V. The motor was connected to the gearbox to reduce the output cycle to 104 rpm, as shown in

Figure (3-2). the electric motor works to rotate the cams to obtain the required displacement [input signal].

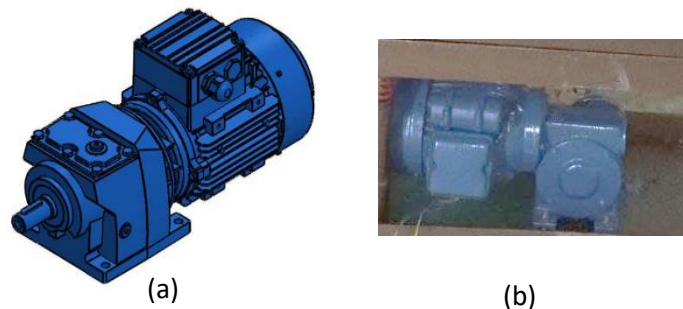


Figure 3-2: a) Sketch of the motor in SOLIDWORKS program b) Duplicated picture of the motor and gearbox

3.3.1.3 Cam and Flower

An eccentric cam is added to transmit the motion of the input signal to the system. This cam is with a circular shape and a diameter of (100 mm), which is illustrated in Figure (3-3), while the flower diameter is 40 mm, as shown in Figure (3- 4).

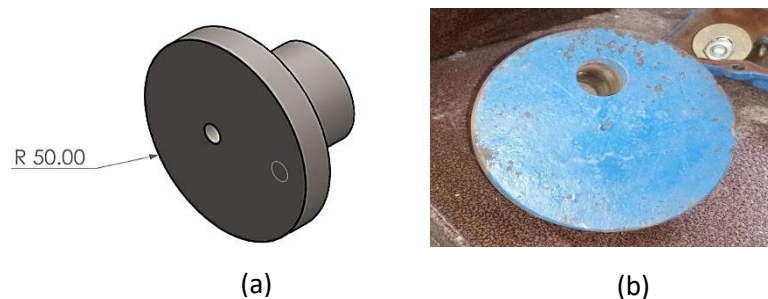


Figure 3-3: a) Sketch of an eccentric cam in SOLIDWORKS program b) Duplicated picture for the eccentric cam

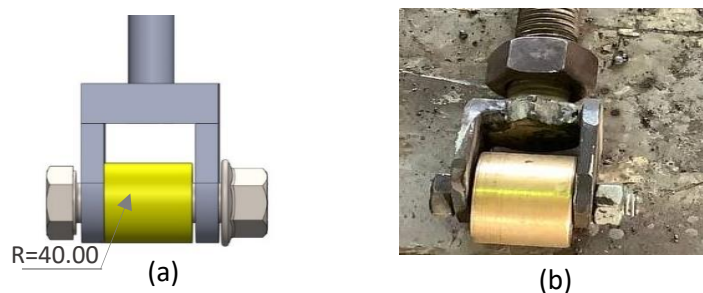
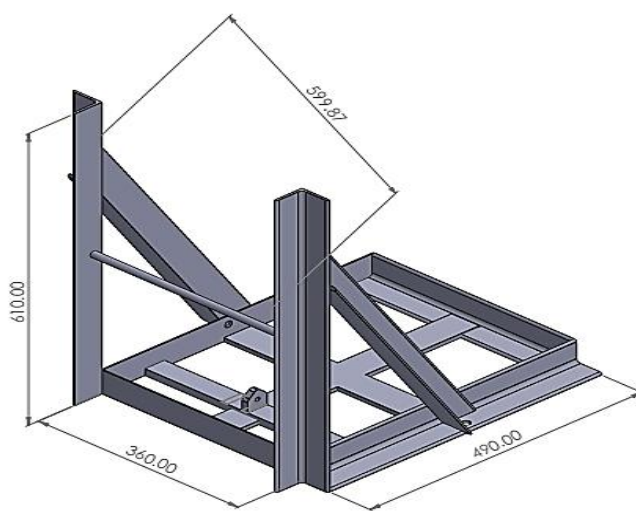


Figure 3- 4: a) Sketch of flower in SOLIDWORKS program b) Duplicated picture of the flower

3.3.2 Seat Structure

3.3.2.1 Seat Base Construction

The seat base is made of an angle –section iron steel bar in the form of L litter with dimensions of [610 ×360×490] mm, as shown in Figure (3-5). The seat base is connected directly with the eccentric cam unit to gain its movement relative to the system input signal.



(a)



(b)

Figure 3-5: a) Sketch of the seat base in SOLIDWORKS program b) Duplicated picture of the seat base

3.3.2.2 Seat Pan

The seat pan is also made of an angle section iron steel bar. The seat pan dimensions are [490×268×570]mm, and the pan is connected to the seat base through a suspension unit [damper and spring]. To ensure the movement of the seat pan is vertical, a linear bearing was added to the seat. The test sandbag was put on the seat pan, so a seat belt was used to secure the sandbag during the test. Figure (3-6) shows the seat pan.

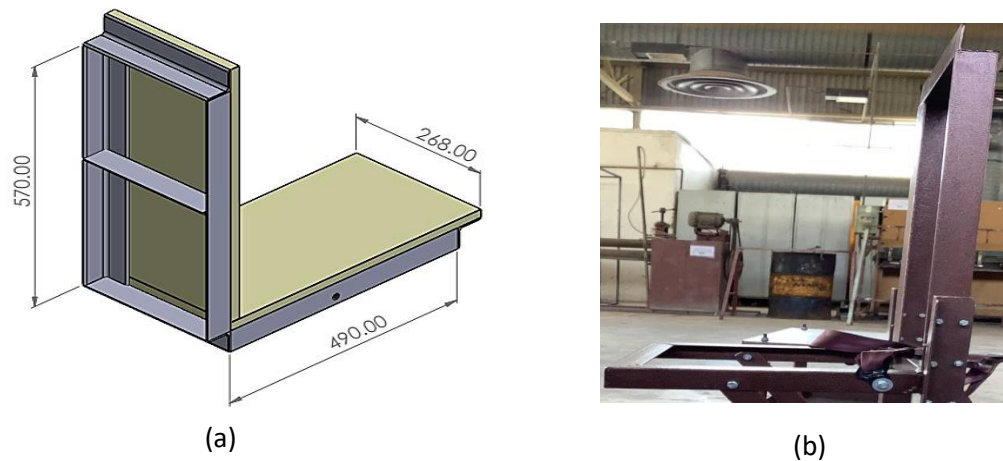


Figure 3–6: a) Sketch of the seat pan in SOLIDWORKS program b- Duplicated picture of the seat pan

3.3.2.3 The Shock Absorber (Passive Suspension System)

As shown in Figure (3-7), a GAOBIAO air shock absorber with a length of 200 mm from eye to eye was used for a passive suspension system for the driver seat. It consists of a coil spring and a pneumatic damper. The stiffness of the spring is calculated by using the SM1000 universal testing machine; the relationship between the compression force applied on the spring and the resulting displacement was studied, and it was equal to 20000 N/m.

For the pneumatic damper, the coefficient of damping was assumed the motion of the damper piston was linear to simplify the calculation of the damping coefficient using the SM1000 universal testing machine. The SM1000 universal testing machine is a hydraulic press connected to a manual hydraulic pump with load and displacement gauges. The manual hydraulic pump replaces by an electric pump to achieve a suitable measuring velocity, as shown in Figure (3-8).

The damping coefficient is calculated by using the relationship between the impacted load and piston velocity, and it was equal to 4000 N.s/m. Figure (3-9) illustrates the test for spring and damper.

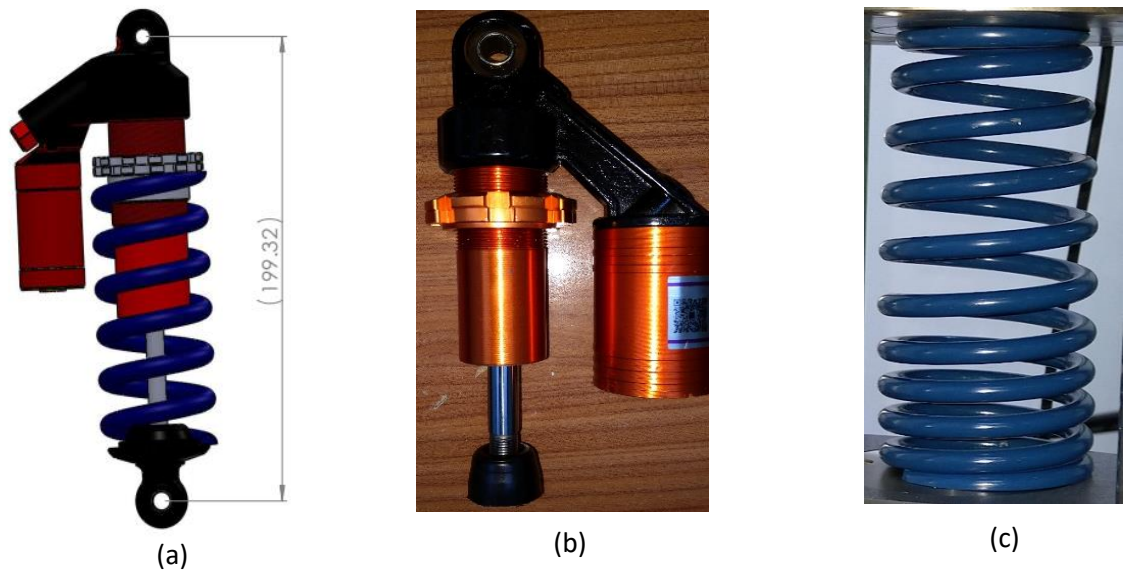


Figure 3-7: a) Sketch of damper and spring in SOLIDWORKS program b) Duplicated picture for the damper c) Duplicated picture for spring



Figure 3-8: Duplicated picture for the SM1000 universal testing machine

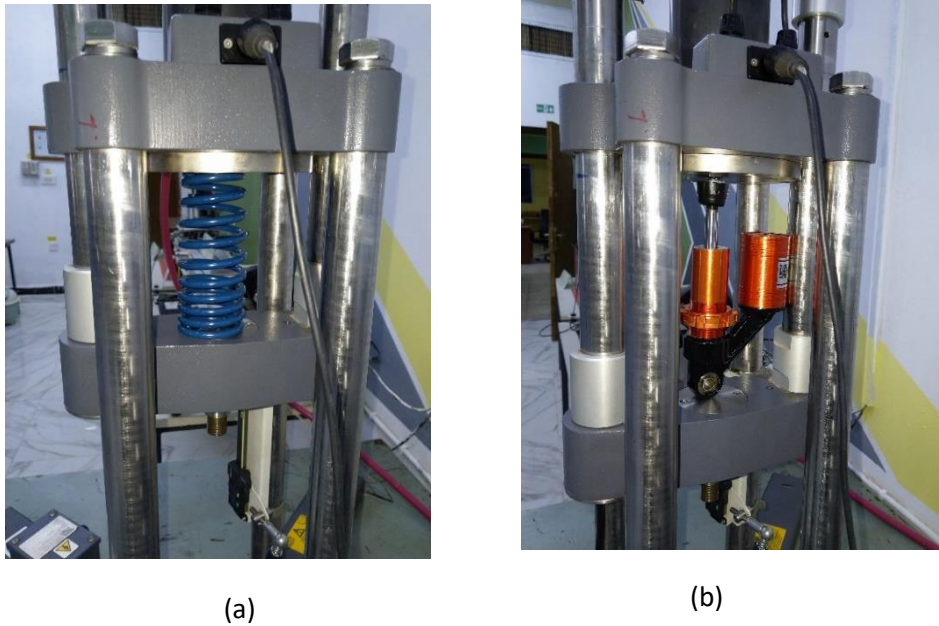


Figure 3-9: a) Duplicated picture for the spring test b) Duplicated picture for the damper test

3.3.2.4 Linear Slider

A linear motion slide is used to support and attach the seat pan to provide a smooth vertical movement. It consists of two pieces as follows:

3.3.2.4.1 Linear Shaft Part

This part is made of a chrome steel shaft connected to an aluminum rail, and it is clamped simply by bolts to the seat base. Figure (3-10) shows the linear shaft part.

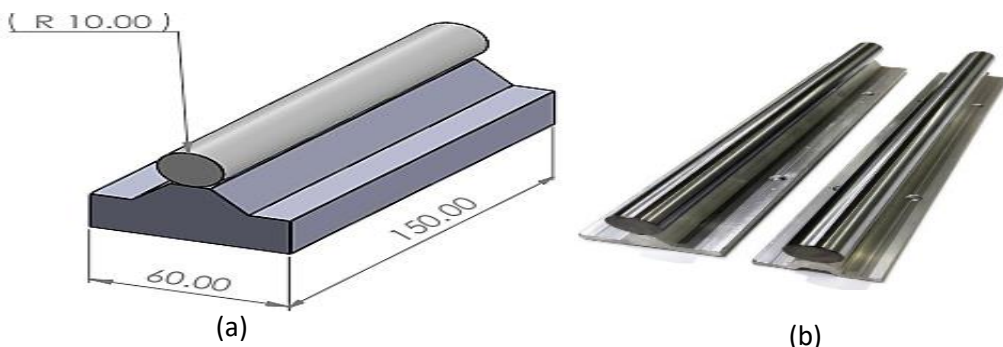


Figure 3-10: a) Sketch of a linear shaft in SOLIDWORKS program b) Duplicated picture for the linear shaft part

3.3.2.4.2 Linear Bearing (Slide Block Part)

This element is made of aluminum alloy material on rectangular form conjunction with cylinder axis carrying a small ball contact with the shaft. With low friction ball rotation, high accuracy smooth movement could be achieved low noise, low friction, and high precision. The slide can be lubricated by using oil grease through a designed aperture. The linear bearing links to the seat pan by bolts. Figure (3-11) shows the linear bearing part, and Figure (3-12) shows the photograph for the linear slider.

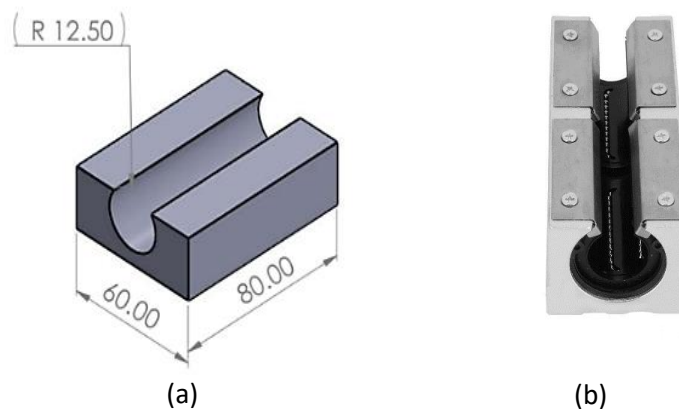


Figure 3-11: a) Sketch of slide block in SOLIDWORKS program b- Duplicated picture for the slide block part



Figure 3-12: Duplicated picture for the linear slider

3.3.2.5 Tow Lever Arm

Two lever arm works, linking the shock absorber (passive suspension system) to the seat pan. The advantage of the two lever arms is to carry the seat's static load and the sandbag test. Figure (3-13) shows the two-lever arm.

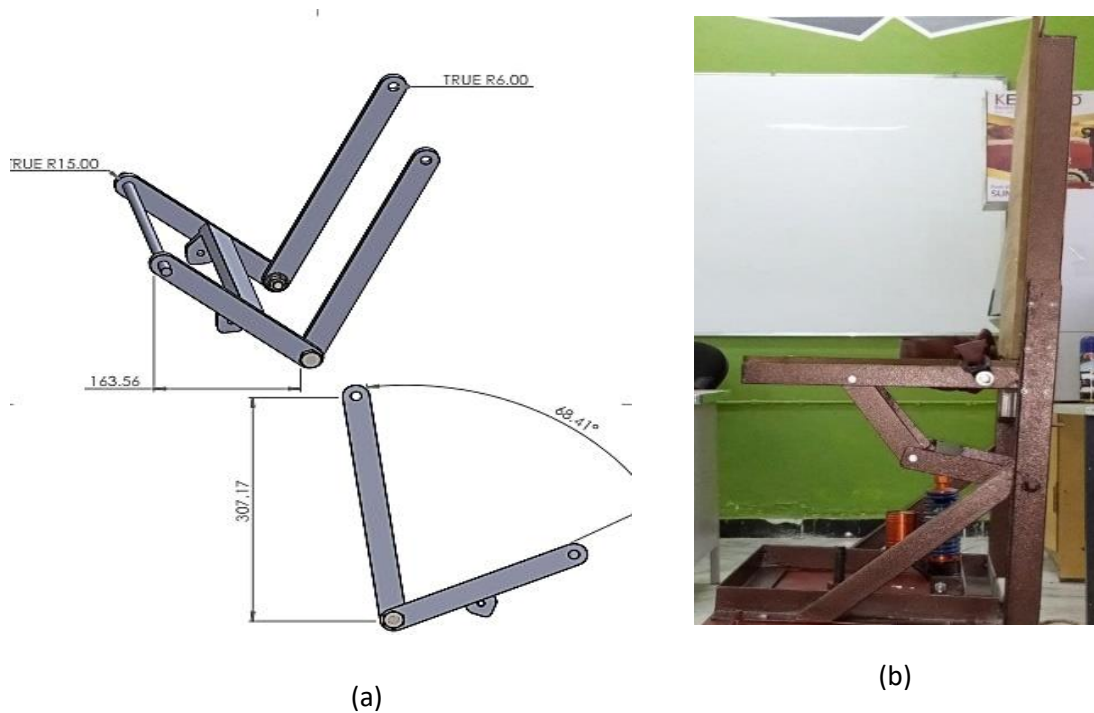


Figure 3-13: a) Sketch for two lever arms in the SOLIDWORKS program. b) Duplicated picture for two lever arms

3.3.3 Electronic Parts

The seat has been moved up and down caused by the motion of the cam linked to the electric motor. The displacement, velocity, and acceleration are measured and monitored using an Arduino **Uno** board and a GY-VL53L0XV2 Laser Distance sensor, with a GY-61 DXL335 3-Axis acceleration sensor through using a software program.

3.3.3.1 Arduino Uno Board

Arduino technology is an open-source electronics platform. Therefore, an Arduino Uno board is used by easily connecting the board with devices and sensors to expand the project possibilities. Fourteen digital input/output pins

and six analog inputs are available on the Arduino Uno. Electrical discharge USB connector with the 5–12-volt power jack, ICSP header, and red reset button. This board is simply to connect with a computer through USB or an AC-to-DC adaptor.

Moreover, the board is connected to 3 phase Relay to control the electrically operated switch. Figure (3-14) shows the Arduino Uno board and the relay. The specification of the Uno board is illustrated in Appendix.

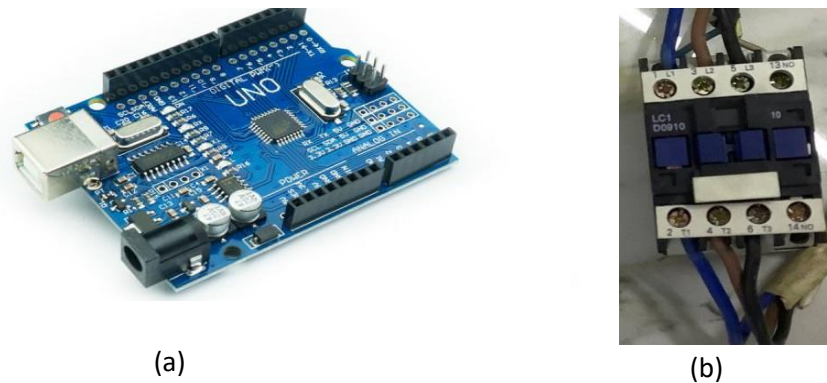


Figure 3-14: a) Duplicated picture for Arduino Uno board b) Duplicated picture for relay

3.3.3.2 Accelerometer and Displacement Sensors

Micro-Electro-Mechanical Systems (MEMS) are very small systems or devices with micro components ranging from 0.001mm to 0.1mm in size. These micro components are made of silicon, polymers, metals, or ceramics, and it is usually combined with a microcontroller to complete the system.

The GY-61 DXL335 3-Axis Accelerometer Module is based on the ADXL335 integrated circuit (Figure 3-15). The ADXL335 is a low-noise, low-power triple-axis accelerometer. The sensor measures $\pm 3g$. It can detect static acceleration from gravity and dynamic acceleration from motion, shock, or vibration. The specification of the acceleration sensor is shown in Appendix.



Figure 3-15: Duplicated picture for GY-61 DXL335 3-axis accelerometer

The sensors were calibrated to receive the data in m/s^2 and then added to the Arduino programming code to obtain acceleration results [61][62]. The calibration formula is illustrated in Appendix.

Figure (3-16) shows a GY-VL53L0XV2 laser distance sensor used to measure the displacement. The VL53LOX sensor has incorporated infrared eye-safe lasers, improved filters, and ultrafast photonic detection arrays for greater range, speed, and precision. The specification of the distance sensor is illustrated in Appendix.

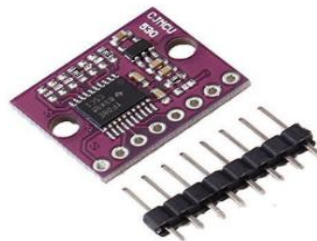


Figure 3–16: Duplicated picture for GY-VL53L0XV2 laser distance sensor

3.3.4 Assembly of Seat Test Rig

After the mechanical components have been designed and built, all mechanical, electrical, and electronic components have been assembled; therefore, the seat test rig will be ready to make a test to check the practical system responses. Figure (3-17) illustrates the whole assembly of the driver's seat test rig.

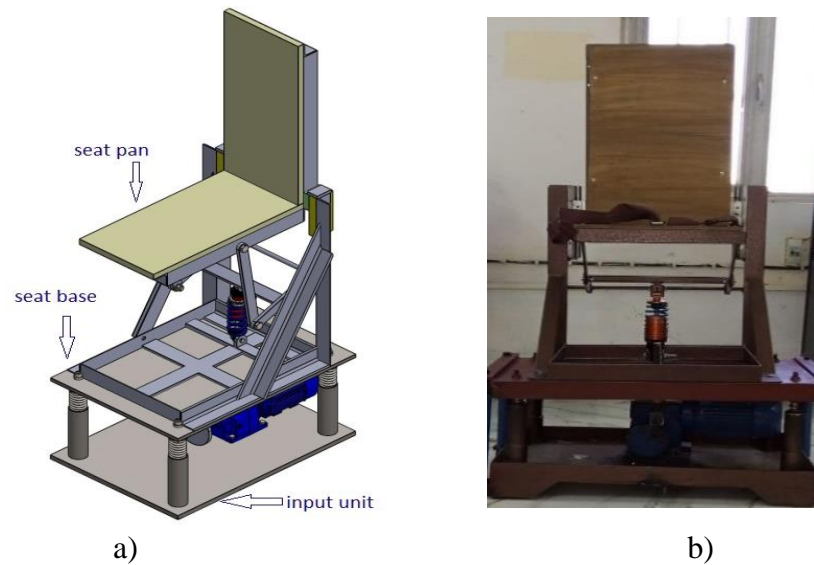


Figure 3–17 a) Sketch for the whole assembly of driver's seat test rig in SOLIDWORKS program

b) Duplicated picture for the whole assembly of driver's seat test rig

3.3.4.1 GUI Window

GUI [Graphical User Interface] is an input window design in MATLAB software for the experimental test rig. GUI is connected between m-file in MATLAB and Arduino code to monitor and control experimental results. Figure (3-18) shows the GUI window, which consists of the acceleration and displacement results box, where the resulting displacement and acceleration curves were blots. Moreover, the com port box connects the computer to the Arduino board, the run time box to put the operation time, and the ON/OFF box to start operation by giving the order to the relay to open/switch the electric motor. Finally, plot box to plot the data resulted in the result box and exported to an excel file.



Figure 3–18: GUI window control and monitoring

3.4 Summary

This chapter illustrated the design and manufacturing process of all parts of the driver seat test rig. As mentioned, the test rig consists of three main units. All parts are described in detail. After the mechanical parts were completed, the Arduino control unit was added to measure the acceleration, velocity, and displacement data for the seat pan ; the test rig is suitable to use different input profiles by changing the cam shape.

The next chapter (chapter four) will offer the constitutive mathematical model for the passive and active seat test rig with a scope of designing the LQR controller and making a validation through comparison with experimental work results. It will help us judge the test rig suitability, cost, and useability. It should be mentioned that the test rig could be remodeled in order to improve its response.

Chapter Four

Theoretical Parts

(Passive and Active Model)

Chapter 4. Theoretical Parts (Passive and Active Model)

4.1 Introduction

This Chapter describes how the simulation works for the active model with the suggested LQR controller agreeing with the passive system's experimental performance. As aforementioned in chapter three, the passive seat test rig was established. Therefore, start with making a suitable passive mathematical model depending on the experimental seat test rig. This model must be validated by comprising the behaviors between them. After that, depending on the passive validation model and generating the active mathematical model with the suggested controller, it was decided to use the most common optimal control technique, i.e., Linear Quadratic Regulator Controller (LQR) to drive the system. LQR is a well-known, full state feedback control technique that optimizes a quadratic performance index, is used to minimize the seat test rig vibration (acceleration) for modifying system response to be more comfortable and safely used. In addition, it is vital to model the input system and review how to generate in simulation different road profiles to check the controller robustness and suitability.

4.2 Simulation Models

In order to show the characteristics and examine the performances of passive and active suspension systems, mathematical models for a seat test rig suspension are conducted, as will be shown in the rest of this chapter. All of the models were in time domain.

4.2.1 Model of the Passive Driver's Seat Test Rig

The mathematical model is required to analyze and evaluate the dynamic response of the experimental passive test rig. It is well known that the seat suspension system derives its movement from the vehicle suspension; therefore, due to the complexity of constructing a vehicle suspension test rig, it was decided for research purposes to take the road excitation directly from the input unit to the seat test rig. A linear seat base and seat pan model with two DOF characterizes the test rig. This approach was used by Gan [33] to evaluate the performance of the driver seat suspension system. Figure (4-1) illustrates the modeling of the seat test rig passive suspension system.

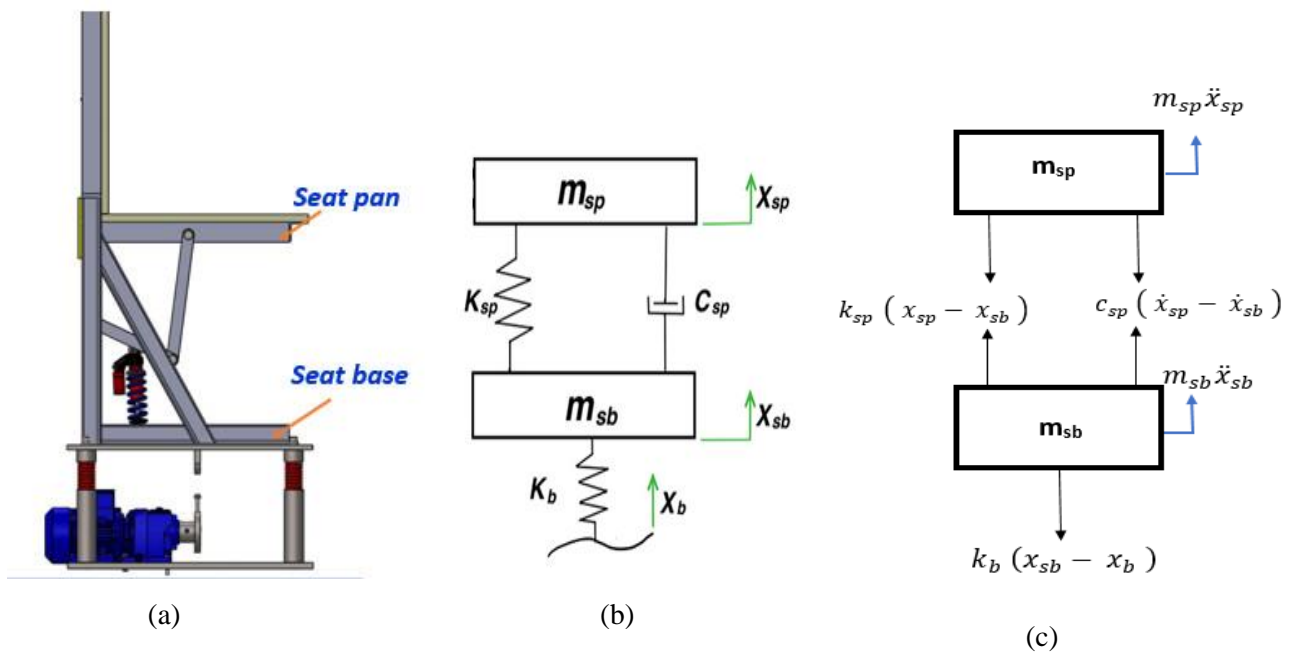


Figure 4–1: a) Sketch of the passive seat test rig b) Passive seat suspension system model

c) Free body diagram for passive system

As shown in Figure (4-1), the system parameters are defined as follows: m_{sp} and m_{sb} are seat pan and seat base masses, respectively. x_b is the body excitation displacement, while x_{sp} and x_{sb} are the displacements in a vertical direction of corresponding masses. The description of 2DOF model parameters is shown in Table (4-1).

Table 4-1: The description of the active model symbol

Symbol	Description	Symbol	Description
m_{sp}	Seat pan mass + driver's mass (Kg)	F_a	Control force (N)
m_{sb}	Seat base mass (Kg)	X_{sb}	Vertical displacement of seat base (m)
k_{sb}	Seat base stiffness (N/m)	X_{sp}	Vertical displacement of seat pan (m)
k_{sp}	Seat pan suspension stiffness (N/m)	X_b	Body excitation displacement (m)
c_{sp}	Seat pan suspension damper (N.s/m)		

The equation of motion EOM in the vertical direction for the passive test rig model was obtained by applying Newton's 2nd law of motion. Furthermore, by assuming the test rig suspension characteristics is linear, the dynamic behaviors of the system could be described by the two following equations[63]:

$$\ddot{x}_{sp} = \frac{1}{m_{sp}} \left[-c_{sp} (\dot{x}_{sp} - \dot{x}_{sb}) - k_{sp} (x_{sp} - x_{sb}) \right] \quad (4.1)$$

$$\ddot{x}_{sb} = \frac{1}{m_{sb}} \left[-k_b (x_{sb} - x_b) + c_{sp} (\dot{x}_{sp} - \dot{x}_{sb}) + k_{sp} (x_{sp} - x_{sb}) \right] \quad (4.2)$$

4.2.2 Model of the Active Driver Seat Test Rig

The active system was reviewed as mentioned in chapter two. The objective of the active system is to conserve all desired state variables at a zero reference when exposed to road disturbances because it considers working as a regulator.

Depending on the passive validation model, the active system model is generated by adding the control force. The characteristics of the test rig are assumed to be linear. The EOM in the vertical direction for the active driver seat system is derived through applying Newton's 2nd Law equation of motion on FBD as demonstrated in Figure (4-2).

$$\ddot{x}_{sp} = \frac{1}{m_{sp}} [-c_{sp} (\dot{x}_{sp} - \dot{x}_{sb}) - k_{sp} (x_{sp} - x_{sb}) + F_a] \quad (4.3)$$

$$\ddot{x}_{sb} = \frac{1}{m_{sb}} \begin{bmatrix} -k_b (x_{sb} - x_b) + c_{sp} (\dot{x}_{sp} - \dot{x}_{sb}) \\ +k_{sp} (x_{sp} - x_{sb}) - F_a \end{bmatrix} \quad (4.4)$$

As mentioned in the literature, many control strategies are used to generate the control force needed in an active system based on this system's states.

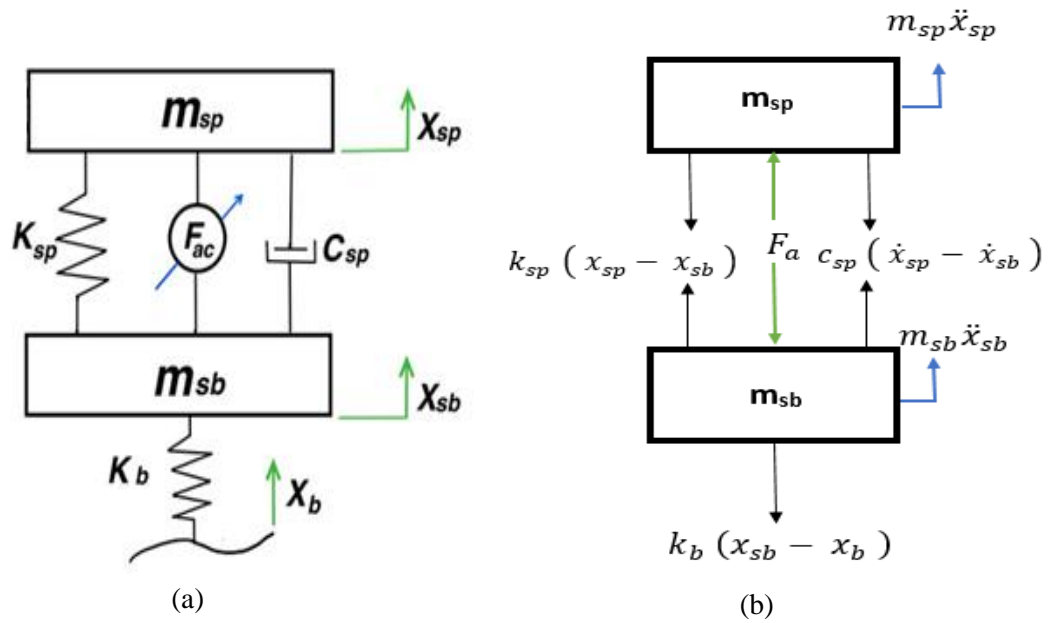


Figure 4–2: a) Model of the active seat suspension system b) Free body diagram of active system

The integrated active mathematical model is required to process the proposed control technique (LQR) concept, as will be shown in the next paragraph.

4.3 LQR Control Technique

It should be paid great attention to select the control strategies for the active system to generate the control force. This force is vital for the active system performance in reducing vibration, thus will help to improve the ride safety

and comfort. The concept of the optimal control strategy is to operate the dynamic system with minimum cost. LQ problems are associated with a linear time-invariant system represented by a quadratic function that follows a set of linear differential equations and a linear system with the state. The LQR control technique is a full state feedback control that is interesting only in the constraints connected with the system's states. The idea of the LQR control technique is to minimize the energy associated with a cost function[64]. That would provide optimal control feedback gain to enhance the close loop stability and give the system a good performance design [65].

The first researcher who applied LQR theory on the active suspension system of a quarter car is Thompson 1976. Figure (4-3) illustrates the LQR feedback block diagram.

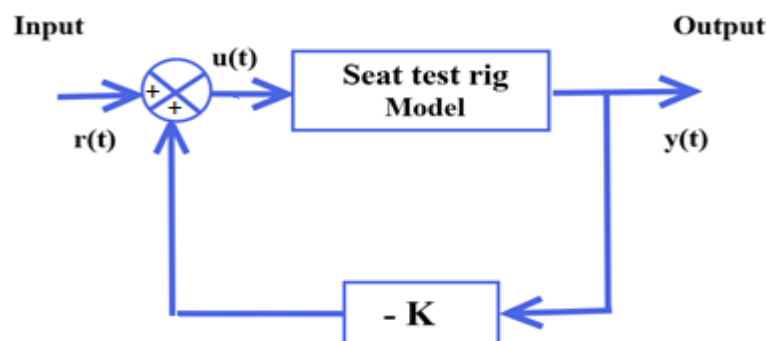


Figure 4–3: The LQR block diagram

The LQR technique relies on pole placements and the dominant second-order system's behavior. As mentioned above, the LQR control is full state feedback control, which means it is interest-only with the constraints related to the states of the systems. The LQR technique depends on the trade-off of the performance of the selected state with the level of control effort connected with the system's state. The solution of the LQR problem depends on cost and constraints connected with the states and system input [66].

However, a significant control signal is required to decrease the output controller energy. In-state feedback controller methods, to change poles of the system to a suitable location based on system output characteristics like settling time and overshoot, it was needed to select a feedback gain network. In addition, in the LQR control technique, a feedback gain is calculated to minimize a cost function, and that will be achieved three significant results as follows:

1. Adequately tracked to the input signal reference $r(t)$.
2. The state dynamics are kept under control while minimizing the cost function.
3. The energy is minimized through choosing K controller [K is the gain of LQR].

The stability of the passive seat system can be examined by the zeros-poles map as shown in Figure (4-4). The test rig model has two poles on the left side of the imaginary axis at -5.42 and -232 , and two complex conjugate poles at $-11 \pm 42i$, which has emergent positions and is affected by zero at -5 , this zero has tried to pull them to the right side of the imaginary axis to be unstable. This map clearly shows that the passive test rig system has critical stability, which needs to be enhanced to be stable by using the optimal control LQR technique.

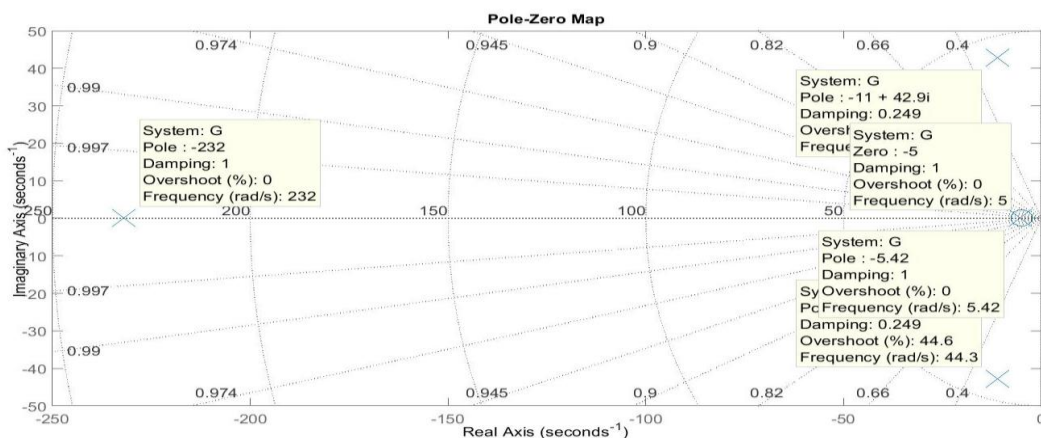


Figure 4-4: Poles-Zeroes map

The first step in LQR technique design is to derive the linear time-invariant system (LTI) and represent it in the state-space model. The LTI system is represented by a state-space model with (x), which is states of the system, and (\dot{x}) is the first derivative of those states, (u) inputs of the system and (y) outputs of the system as following shown:

$$\dot{x} = Ax + Bu$$

$$y = Cx + Du \quad \dots\dots\dots (4.5)$$

In this study, the LQR technique design aims to achieve ride comfort according to road disturbance and suspension travel constraints in terms of reducing the seat pan acceleration. So, the proposed control should be minimized this parameter. Therefore, four states are selected to construct the control, as follows:

$$x_1 = x_{sp} \quad , \quad x_2 = \dot{x}_{sp} \quad , \quad x_3 = x_{sb} \quad , \quad x_4 = \dot{x}_{sb}$$

Now, the test rig model will be represented in the state-space model by

Substituting x_1, x_2, x_3, x_4 in the equations (4.3) and (4.4), as follows:

$$\dot{x}_2 = \frac{-k_{sp}}{m_{sp}} x_1 - \frac{c_{sp}}{m_{sp}} x_2 + \frac{k_{sp}}{m_{sp}} x_3 + \frac{c_{sp}}{m_{sp}} x_4 + \frac{F_a}{m_{sp}} \quad (4.6)$$

$$\dot{x}_4 = \frac{k_{sp}}{m_{sb}} x_1 + \frac{c_{sp}}{m_{sb}} x_2 - \frac{k_{sb} + k_{sp}}{m_{sb}} x_3 - \frac{c_{sp}}{m_{sb}} x_4 + \frac{k_{sb}}{m_{sb}} x_b - \frac{F_a}{m_{sb}} \quad (4.7)$$

Then determine the matrixes as below:

$$A = \begin{bmatrix} 0 & 1 & 0 & 0 \\ \frac{-k_{sp}}{m_{sp}} & \frac{-c_{sp}}{m_{sp}} & \frac{k_{sp}}{m_{sp}} & \frac{c_{sp}}{m_{sp}} \\ 0 & 0 & 0 & 1 \\ \frac{-k_{sp}}{m_{sb}} & \frac{c_{sp}}{m_{sb}} & \frac{-k_{sb}-k_{sp}}{m_{sb}} & \frac{-c_{sp}}{m_{sb}} \end{bmatrix} \quad B = \begin{bmatrix} 0 \\ 0 \\ 0 \\ \frac{k_{sb}}{m_{sb}} \end{bmatrix}$$

$$C = \begin{bmatrix} \frac{-k_{sp}}{m_{sp}} & \frac{-c_{sp}}{m_{sp}} & \frac{k_{sp}}{m_{sp}} & \frac{c_{sp}}{m_{sp}} \\ 1 & 0 & 0 & 0 \end{bmatrix} \quad D = \begin{bmatrix} 1 & 0 & 0 & 0 \\ 0 & 0 & 0 & 0 \end{bmatrix} \quad (4.8)$$

Where:

A= state matrix

B= input matrix

C= output matrix

D= disturbance matrix.

The optimal control law for any $x(0)$ with zero references is:

$$u = -K_{LQR}x \quad (4.9)$$

Where $x(0)$ is the initial state, (u) is feedback law, K represents the LQR control gain matrix or optimal matrix connected with each state in the system.

As a result, the system will be examined in two cases. The first one is without disturbance, as illustrated in Figure (4-5). The second is with added disturbance to the system and makes the input reference equal to zero, as displayed in Figure (4-6).

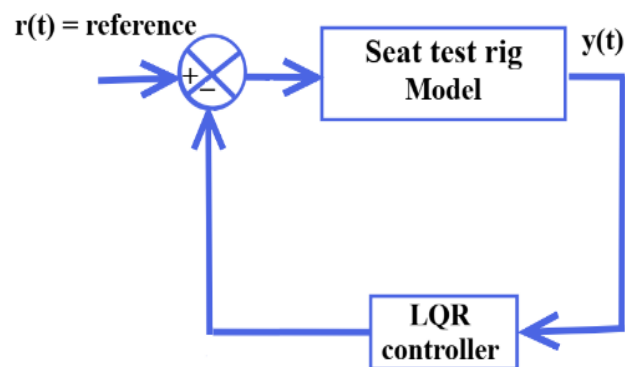


Figure 4-5: Controller design in case of without disturbance

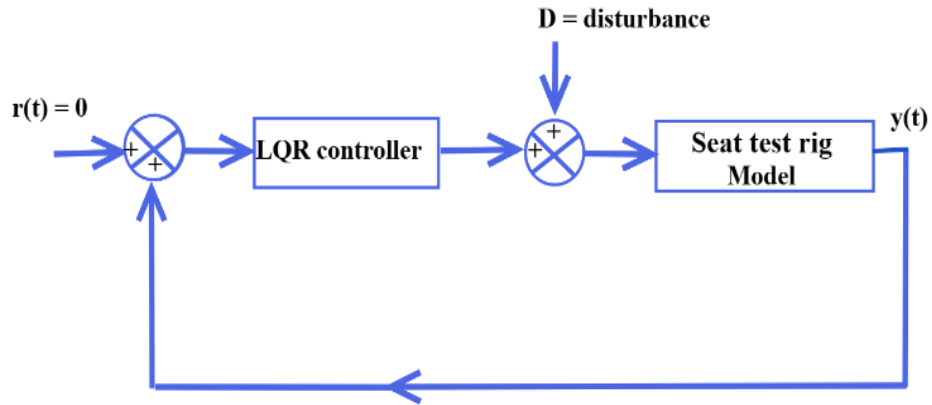


Figure 4–6: Controller design in case of adding disturbance

The performance index (J) represented the input limitation and required performance characteristics. Optimization of the LQR control system aims to determine the control input (u) to minimize the performance index [67].

$$J_{LQR} = \int_0^{\infty} (x^T Q x + u^T R u) dt \quad (4.10)$$

(x) is the state, while (u) is the control. The state weighting matrix Q ($n \times n$) and the control weighting matrix R ($r \times r$) are represented by Q and R , respectively.

The objective of the controller is to make the measured and controlled signal ($y = Cx$) small as possible. Frequently, the LQR control problem is described by a more general definition that consists of finding the control input to minimize the cost function:

$$J_{LQR} = \int_0^{\infty} (x^T * C^T \bar{Q} C * x + u^T * \rho \bar{R} * u) dt \quad (4.11)$$

Where:

$$Q = C^T \bar{Q} C, \text{ and } R = \rho \bar{R} \quad (4.12)$$

The ρ is a positive constant. The term $\int_0^\infty (x_{(t)}^T * C^T \bar{Q} C * x_{(t)})$ represent the energy of the output and the term $\int_0^\infty (u_{(t)}^T * \rho \bar{R} * u_{(t)}) dt$, represent the energy of the control signal. Restrictions on Q and R matrixes are symmetric positive definite matrixes [$Q=Q^T \geq 0$; $R=R^T \geq 0$] [68].

4.3.1 Design of LQR Controller

By substitution equation (3.5) into equation (3.9) (3.9), obtaining the relation below:

$$\dot{x} = Ax + Bu = Ax - BK_{LQR}x = (A - BK_{LQR})x \quad (4.13)$$

If the matrix $(A - BK_{LQR})$ stable or the eigenvalues of $(A - BK_{LQR})$ having negative real parts [63], and through substitution equation (4.9) into (4.10), the result is shown in the following equation:

$$J_{LQR} = \int_0^\infty (x^T Q x + x^T K_{LQR}^T R K_{LQR} x) dt$$

$$J_{LQR} = \int_0^\infty (x^T (Q + K_{LQR}^T R K_{LQR}) x) dt \quad (4.14)$$

To solve the problem of parameter optimization mentioned in equation (4.14), it should be beginning with the following equation:

$$x^T (Q + K_{LQR}^T R K_{LQR}) x = -\frac{d}{dt} (x^T P x) \quad (4.15)$$

The P is a positive, semi-definite matrix. Now by rearranging the equation (4.15) will be as follows:

$$\begin{aligned} x^T (Q + K_{LQR}^T R K_{LQR}) x &= -\dot{x}^T P x - x^T P \dot{x} \\ &= -x^T (A - BK_{LQR})^T P x + x^T P (A - BK_{LQR}) x \\ &= -x^T \left[(A - BK_{LQR})^T P + x^T P (A - BK_{LQR}) \right] x \end{aligned} \quad (4.16)$$

It demands that by comparing the right-hand side and left-hand side of the equation (4.16) and considering that, Therefore, equation (4.16) should be proven to be true for any $x(t)$, it required that:

$$(A - BK_{LQR})^T P - x^T P(A - BK_{LQR}) = -(Q + K_{LQR}^T R K_{LQR}) \quad (4.17)$$

The matrix $(A - BK_{LQR})$ is stable, and there is a positive definite matrix P that satisfies equation (4.13). So, the cost function (J_{LQR}) can be calculated as follows:

$$\begin{aligned} J_{LQR} &= \int_0^{\infty} (x^T (Q + K_{LQR}^T R K_{LQR}) x) dt \\ &= \left[-\frac{d}{dt} (x^T P x) \right] dx [-x^T P x]_0^{\infty} \\ &= -x^T(\infty) P x(\infty) + -x^T(0) P x(0) \end{aligned} \quad (4.18)$$

If $x(\infty) \rightarrow 0$ then all $(A - BK_{LQR})$ the eigenvalue is assumed to have a negative real part, so the equation (4.18) become as:

$$J_{LQR} = x^T(0) P x(0) \quad (4.19)$$

It was evidently seen that from equation (4.19) the J_{LQR} is only affected by P values since $x(0)$ is constant. As a result, it is set $x(0)$ concerning K to minimum J_{LQR}

$$\frac{\partial P}{\partial K} = 0 \quad (4.20)$$

As a result, by differentiation equation (4.17) in terms of K and substitution equation (4.20), the control equation will become as follows:

$$K_{LQR} = -R^{-1} B^T P \quad (4.21)$$

and,

$$u = -R^{-1} B^T P x \quad (4.22)$$

Where:

(u) is feedback low, K represents the LQR control gain matrix or optimal matrix connected with each state in the system.

The P is a positive, semi-definite matrix and satisfies the following equation.

$$PA + A^T P + Q - PBR^{-1}B^T P = 0 \quad (4.23)$$

Equation (4.23) is called (CARE) Continuous Algebraic Riccati Equation[69], the total derivative of it in [70].

The Riccati equation can be solved numerically or by using MATLAB m-file to find the P matrix and vector K.

To solve the optimal control LQR, it can be followed the following steps:

1. Model the cost function using equations (4.9) and (4.10) to find A, B, Q, R matrixes.
2. Solve the (CARE) in equation (4.23) to find the P matrix. the (A-BK) matrix or the system is stable when the matrix P is positive definite.
3. Finally, Substituting the P matrix in equation (4.21) to calculate K optimal gain matrix. it can be solved in MATLAB m-file by using the function

$$[K]=lqr(A, B, Q, R).$$

4.3.2 Determination of the Weight Matrices

For a successful LQR technique design, the Q and R parameters should be carefully chosen. These two matrixes determine the system energy expense and the existing error relative importance. Many methods determine the Q & R parameters. The hybrid with the rule of trial and error is usually used; this method allows the designer to offset the drawback of using one method alone.

In this system, it will be choosing a hybrid of Bryson's method to determine the initial weight matrixes \bar{Q} & \bar{R} . The use of trial and error is to the accurate tuning of these two matrixes' parameters and to achieve the best performance for the controller [71].

Bryson's method assumed the Q&R are diagonal matrices; thus, the weights Q_{ii} and R_{jj} are only concerned. This method suggested that the initial weight (diagonal elements) equals the reciprocals of the square of the value of the maximum acceptable time-domain response, which the designer permits [72]. Bryson's method for \bar{Q} matrix and \bar{R} the matrix can be written as:

$$\bar{Q}_{ii} = \frac{1}{\text{Max.}[x_i]^2} \quad \bar{R}_{jj} = \frac{1}{\text{Max.}[u_j]^2} \quad (4.24)$$

In Bryson's method, a simple approach was used for the single input to calculate the \bar{Q}_{ii} weight element of that most significant state and all other weight elements equal to unity and already \bar{R}_{jj} weight is unity in a single input.

In general, when the $\bar{R}_{jj} \gg \bar{Q}_{ii}$, the system is called expensive control. The control effort u is dominated in the cost function (J), and the controller system achieved stability with a bit of control energy.

When the $\bar{R}_{jj} \ll \bar{Q}_{ii}$, the system is called cheap control, where the output error y is dominated in the cost function (J), and no penalization to using a significant control signal(u). if the \bar{Q}_{ii} (weight element) chosen a big value, that means the needless state change to achieve stability to the system [63].

In this work, in order to design a controller for the test rig seat system, the R matrix has been chosen with 100 to examine the design and system response.

Furthermore, for Q, it has been chosen by using the dominate state, which is using the variable of(\ddot{x}_{sp}), and ($x_{sp} - x_{sb}$) to find the Q matrix by using Bryson's method and the result as follows:

$$\bar{Q} = \begin{bmatrix} 0.0011 & 0 \\ 0 & 0.001 \end{bmatrix}$$

$$Q = \begin{bmatrix} 130.8066706 & 26.15933413 & -130.7966706 & -26.15933413 \\ 26.15933413 & 5.231866825 & -26.15933413 & -5.231866825 \\ -130.7966706 & -26.15933413 & 130.7966706 & 26.15933413 \\ -26.15933413 & -5.231866825 & 26.15933413 & 5.231866825 \end{bmatrix}$$

4.3.3 Controllability and Observability of the System

In the closed-loop system, it is essential to ensure that each state that energy be minimized can affect by the input (or inputs) signal; this is the controllability issue. The system controllability suggests that the state can drive it to the origin by input in a finite time. If the state energy will be considered in cost function (J), it is essential to be controllable. The controllability can be calculated from the matrix as follows [63]:

$$C_m = [B \ AB \ AB^2 \ \dots \ AB^{n-1}] \quad (4.25)$$

The system is controllable if the rank of C_m is equal to n . For the seat test rig system, $n=4$ and the rank of $C_m=4$.

The system observability means that all-state information can able to be observed at the output within giving enough time. Observability can be calculated from the matrix as below:

$$O_m = [C \ CA \ CA^2 \ \dots \ CA^{n-1}]^T \quad (4.26)$$

The system is observable if the rank of O_m is equal to n . For the seat test rig system, $n=4$ and the rank of $O_m=4$.

Controllability and observability can be found by using MATLAB m-file function. Our system is controllable and observable.

4.3.4 LQR Controller with Integral Compensation Action

A regular control system should have zero references. Therefore, the test rig system used disturbances instead of the system input. The block diagram of the system with disturbance is shown in Figure (4-7).

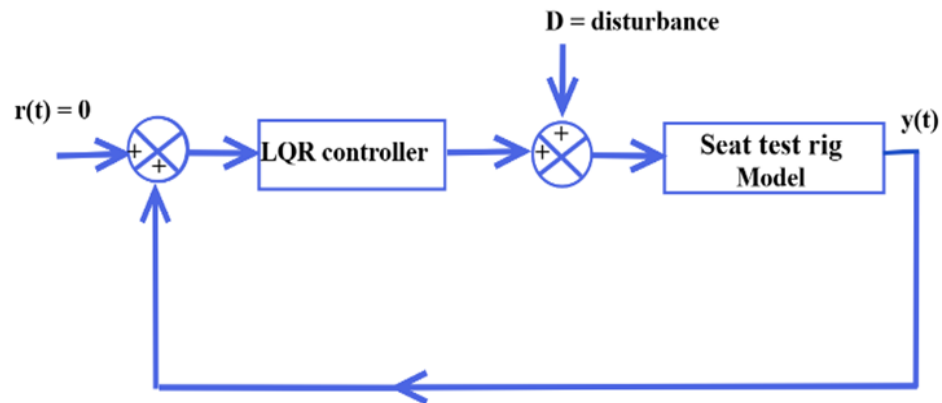


Figure 4–7: The test rig system with zero reference

A significant steady-state error was found with using the LQR controller, which affects the system's final value in terms of performance.

From Figure (4-8), it can be seen that the system response according to disturbance input, step input disturbance it takes a delay time of 0.1 s, and the final value of the seat pan displacement with steady-state is 0.1 m.

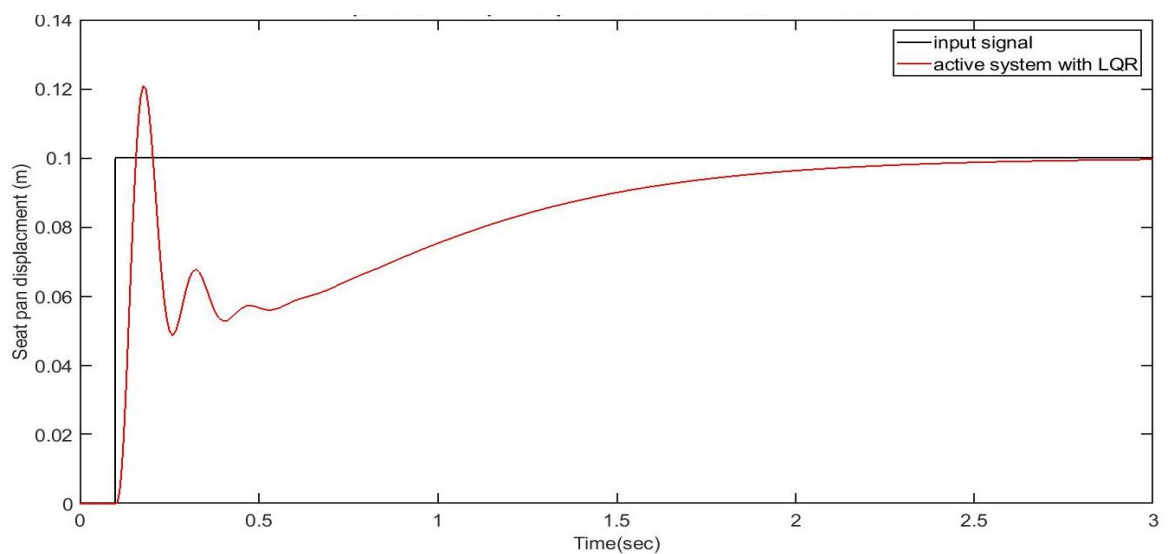


Figure 4–8: Step response of the active test rig with LQR control

Figure (4-8) shows a big value of steady-state error, and the system output did not go to the zero references. So, the modification of the LQR controller is required to reduce the steady-state error to zero. Many strategies, such as compensating for lead-lag and using a PI, PD, or PID controller, are utilized to improve optimal control systems. Additional poles, zeroes, or a combination of both are added to the system's poles in these methods, increasing the system's order and complexity [73]. In our system case, adding an integrator to the closed-loop system is recommended. As a result, it obtains the LQR regulators, in which the original system's state space is extended in proportion to the parameters that must be controlled, and the control law is determined as follows [74]:

$$u = -[K \ K_I] \begin{bmatrix} x \\ z \end{bmatrix} \quad (4.27)$$

Where: (z) is a new state variable added to our system, K_I is integrator gain.

$$z = \int e \, dt \quad (4.28)$$

The state-space for the new system becomes:

$$\begin{bmatrix} \dot{x}(t) \\ \dot{z}(t) \end{bmatrix} = \begin{bmatrix} A & 0 \\ -C & 0 \end{bmatrix} \begin{bmatrix} x(t) \\ z(t) \end{bmatrix} + \begin{bmatrix} B \\ 0 \end{bmatrix} u(t) \quad (4.29)$$

Figure (4-9) shows the active seat test rig system with the LQR controller and integrator Compensation.

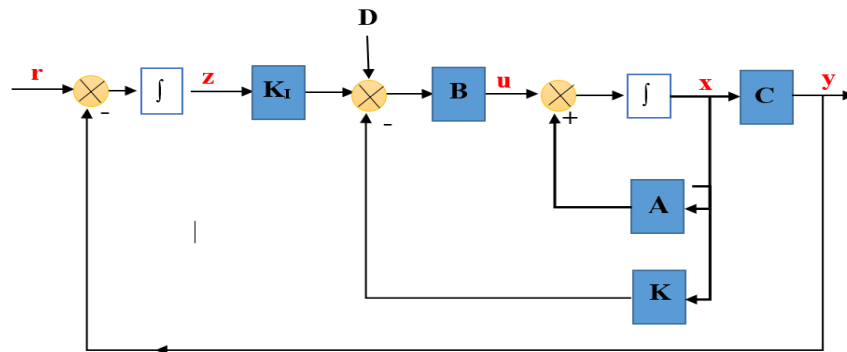


Figure 4–9: System with the LQR controller and integrator compensation

The improvement of system response according to adding the integral controller happened as shown in Figure (4-10), the steady-state error goes to zero.

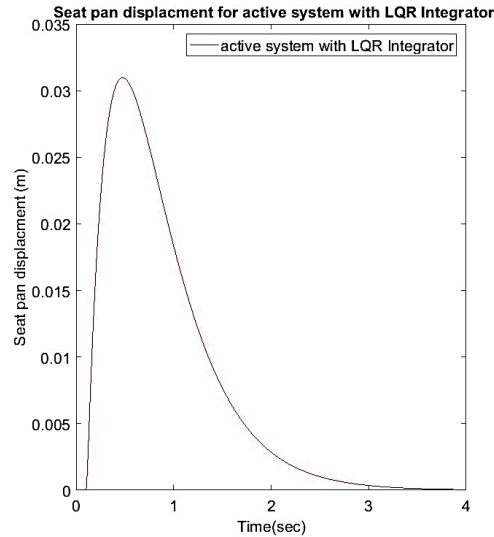


Figure 4–10: Step response of the active test rig with LQR control and integrator

4.4 Road Profile Generation

Road disturbances are the primary source of transmitted vibrations to vehicle drivers, which transmit through the vehicle body and then to the driver's seat. It is necessary to simulate the road disturbances to analyze the seat test rig suspension to reduce those vibrations. So, it was decided to use two types of road disturbance input to check the control action. The first type is a bump road profile [75], as shown in Figure (4-11). The road equation is:

$$y(t) = \begin{cases} (a(1 - \frac{\cos 8\pi t}{2}) & 0.25 \leq t \leq 0.5 \\ 0 & \text{otherwise} \end{cases} \quad (4.30)$$

where: (a) is the bump height =10 cm.

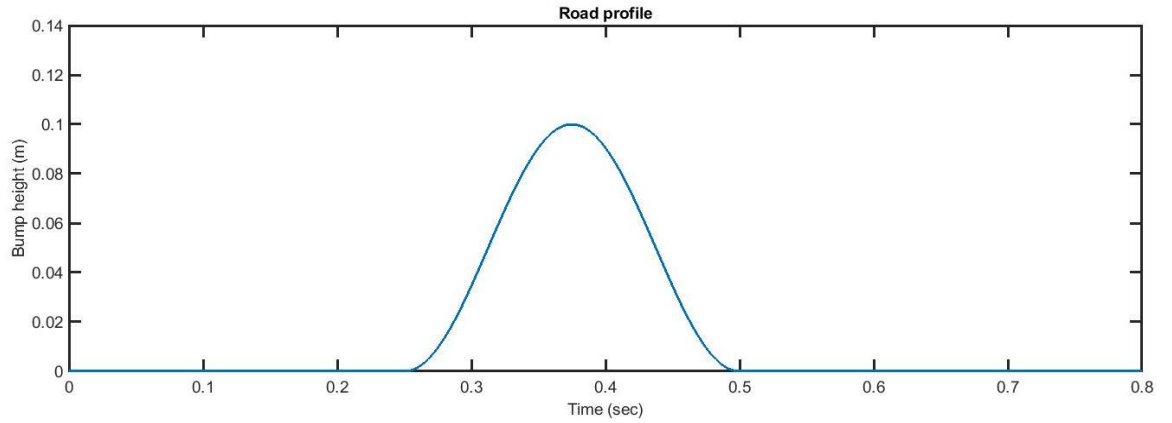


Figure 4–11: Bump road profile

The second one is a random road profile. The cause of the chosen random profile is that most road disturbance profiles are random, including frequencies sensitive to the human body. The following equation (equation (4.31)) can be used to generate the random profile in the time domain [76].

$$x_r(t) = \sum_{n=1}^N A_n \sin(nw_0t - \vartheta_n) \quad (4.31)$$

where:

$x_r(t)$ = road displacement. A_n = the amplitudes, and ϑ_n = random phase angel, its value between $(0,2\pi)$, $w_0 = V \Delta\Omega$ the fundamental temporal frequency (rad/sec).

$$A_n = \sqrt{\phi(\Omega_n) \frac{\Delta\Omega}{\pi}} \quad (4.32)$$

where:

Ω is angular spatial frequency = $2\pi/L$ (rad/m), Moreover, L is the wavelength.

The $\Delta\Omega = \frac{\Omega_N - \Omega_1}{N-1}$, $\Omega_1 = 0.2\pi$ and $\Omega_N = 6\pi$, these values were suggested by ISO 8608.

$\phi(\Omega_n)$ = the PSD (power spectral density) function of road roughness, and ISO 8608 suggests the following approximate formula:

$$\phi(\Omega) = \phi(\Omega_0) \left(\frac{\Omega}{\Omega_0} \right)^{-w} \quad (4.33)$$

where:

The Ω_0 = reference angular spatial frequency =1 rad/m. w = waviness, and it equal two for most roads. equation (4.31), (4.32), (4.33) solved in MATLAB with road roughness $3m^3$ a classed C according to ISO 8606 and vehicle speed 20 Km/h. Figure (4-12) shows the random road profile.

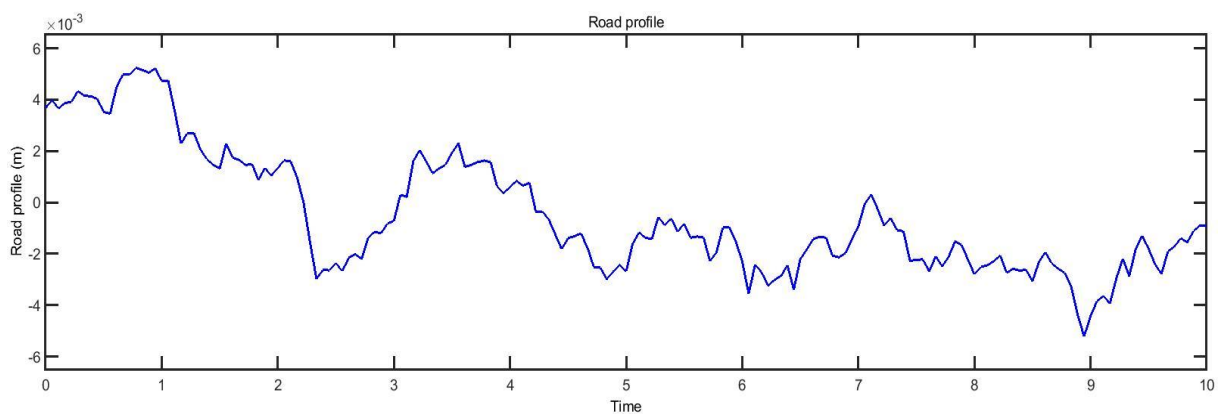


Figure 4–12: Random road profile

4.5 Summary

This chapter identified the mathematical model of the experimental passive test rig and showed how the test rig modeled with defined the parameters of actual works. As mentioned, the test rig model is considered linear and consists of two masses: the seat pan mass and the seat base mass, with the (spring and damper). This modeling will be helped to easily model and analysis of the active model.

Then, modeling the active suspension system and its importance, as a result, to reduce the vibration transmitted to the driver and provide the ride comfort experience using the optimal control technique (LQR). The Q&R weight matrixes consider the implementation point of the LQR controller; some methods were suggested to be calculated, but it decided to choose a hybrid of

Bryson's method with a trial-and-error method. The LQR controller with integrator compensation was used to improve the response of the active test rig system that was exposed to a disturbance road. Two road profiles were provided, which are random and bump disturbance helping in performing the test rig system. As will be shown in the next chapter, the proposed controller techniques are effectiveness, robustness, and power to improve comfortable rides were evaluated when the test rig model was subjected to different types of road profiles.

Chapter Five
Results and Discussion

Chapter 5. Results and Discussion

5.1 Introduction

In this chapter, it will be displayed and highlighted the results of experimental and simulation works. The comparison between the experimental and simulation results of the passive system responses will be demonstrated in the next section. The experimental results are measured using Arduino sensors then monitored through a GUI window. The theoretical results are founded by processing the mathematical model with MATLAB/Simulink environment. The active seat test rig is modeled through the covering design of the suggested LQR controller will be illustrated in this chapter. At the end of this chapter, the response enhancement of the seat driver's test rig relative to incorporated to use LQR controller was shown, the comprising between the passive and active seat test rig is performed.

5.2 Passive Test Rig Seat Performance Validation

This section illustrates the passive test rig seat's performance validation by comparing experimental and simulation response studies. The convergence of experimental performance with theoretical analysis is the essential aspect in determining the success of a design. As a result, the comparison between the theoretical and experimental results was vital.

5.2.1 Simulation and Experimental Verification

For the software section, MATLAB/SIMULINK is considered the main software to programing a theoretical work. A simulation environment prepper

to achieve analysis and monitoring [77]. The various dynamic systems can be modeled and simulated using SIMULINK as a graphical environment for programming language. The SIMULINK code is used to find the simulation system's dynamic performance, as the block diagram duplicated in Figure (5-1) shows. By using this code, it was easy to find the dynamic responses by employing the input signal, which was generated by an accurate eccentric cam profile in SOLIDWORKS as the system input.

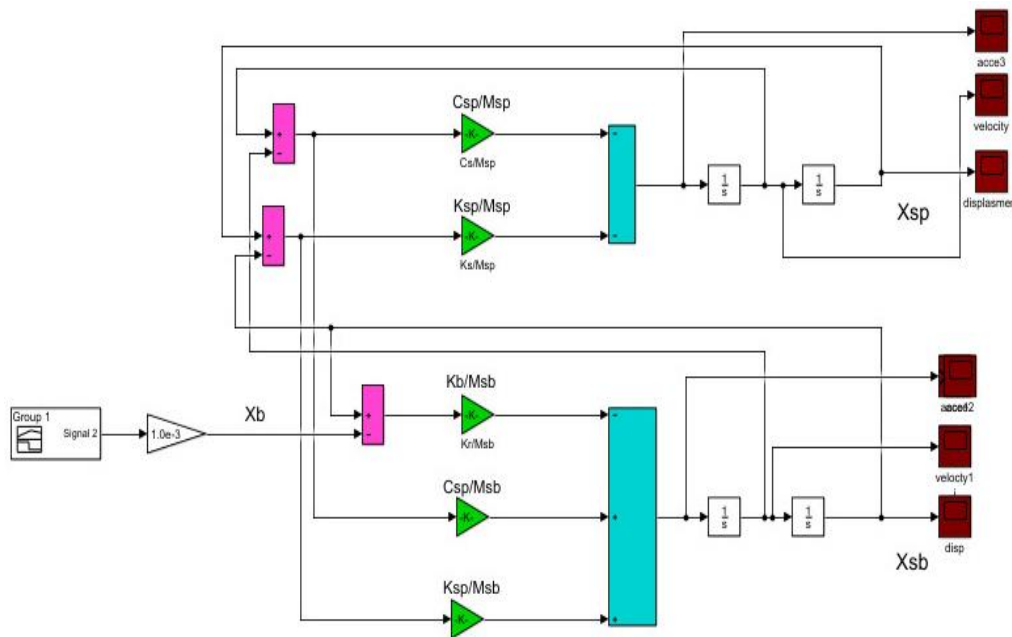


Figure 5–1: SIMULINK code of passive test rig model

The experimental analysis for the passive seat suspension system is performed using an Arduino Uno board with displacement and acceleration sensors. The dynamic results are monitored through the GUI window. Figure (5-2) shows the Arduino system and GUI window setup.

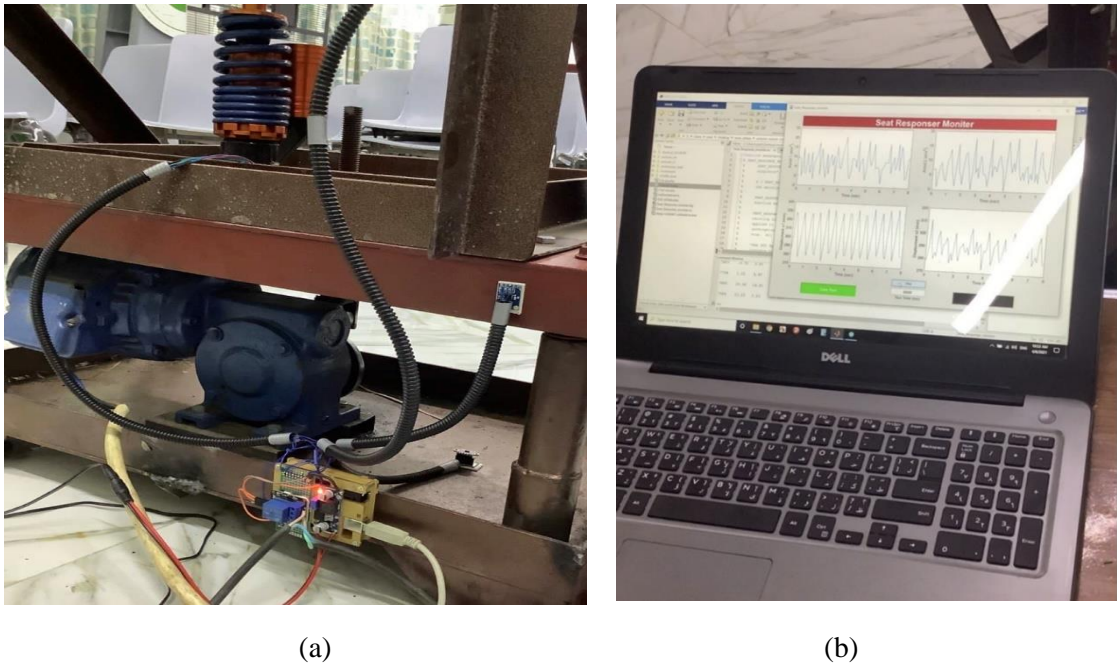


Figure 5–2: a) Setup of Arduino uno board with displacement and acceleration sensors b) GUI window with monitoring data

The passive seat suspension parameters are taken from the actual working driver's seat test rig. The used parameters in the following analysis are given in Table (5-1).

Table (5-1): The value of parameters of the active seat suspension

Parameter	value
m_{sp}	58 Kg
k_{sp}	20000 N\m
c_{sp}	4000 N.s\m
m_{sb}	21 Kg
k_b	150000 N\m

5.2.1.1 Passive Suspension Response

The results are validated by comparing the experimental and simulation results of displacement, velocity, and acceleration values for the seat pan, as will be shown in the following.

Figure (5-3) shows the system input, and the eccentric cam design will be used to create the input signal as possible to represent the real road and the simulated results. It is urgent to make a sensible comparison between them. The results verified by comparing them found that the experiment and simulation results are in good conformity.

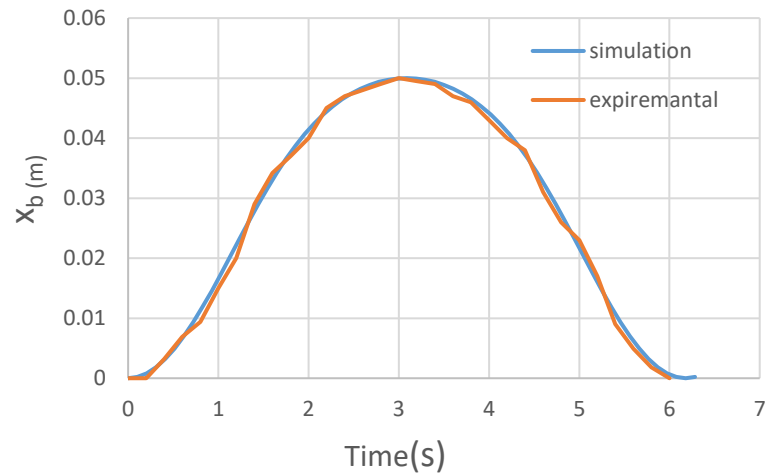


Figure 5–3: Experimental and simulation of system input

A comparison of the simulation and experimental results for the seat pan displacement has been conducted, as illustrated in Figure (5-4). It is eventually seen that a good agreement found between both.

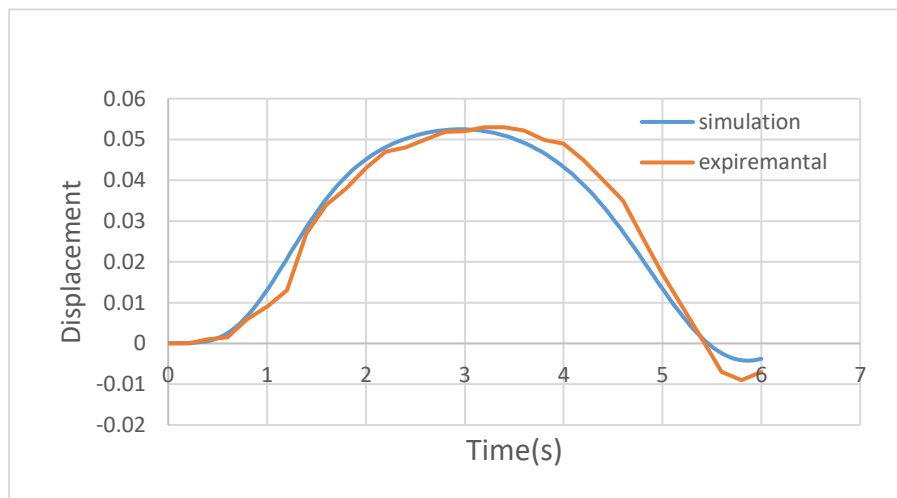


Figure 5–4: Simulated and experimental seat pan displacement results

While the comparison of the experimental and simulation results of the velocity of the seat pan is demonstrated in Figure (5-5), it is seen that a good agreement is between both, and that means the test rig construction used and the simulated model is accurate and sufficient.

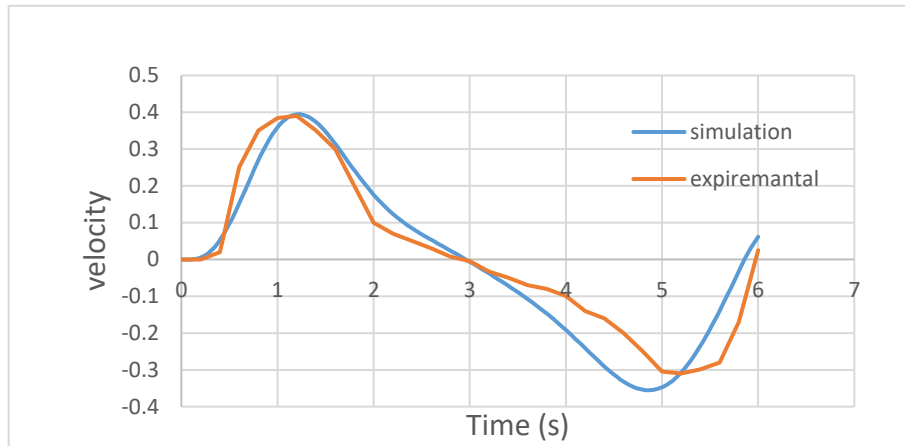


Figure 5-5: Experimental and simulation of seat pan velocity results

The comparative experimental and simulation results for seat pan acceleration are presented in Figure (5-6). It is vital to display the acceleration test rig behavior because acceleration is directly connected with the vibration. The acceleration data was filtered using the Excel program -Data analysis to overcome the noise caused by sensor sensitivity and working conditions.

As a result, the simulation and experimental work outcomes are slightly different, but this difference is acceptable within this system.

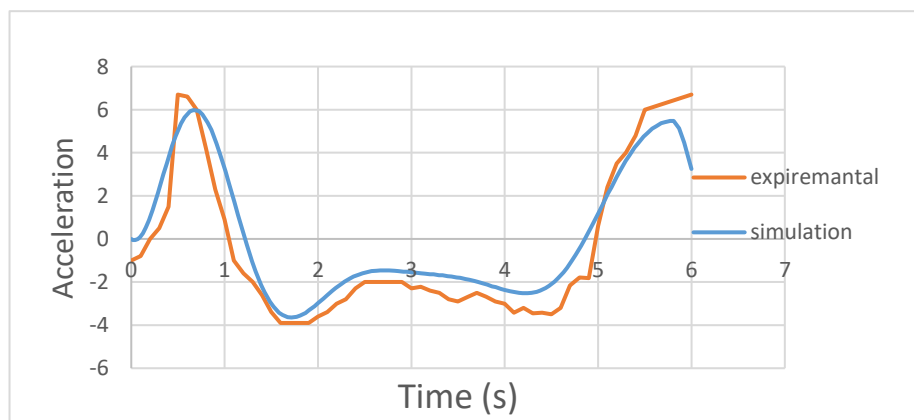


Figure 5-6: Experimental and simulation of seat pan acceleration results

5.3 Active System and LQR Controller Performance Validation

This section aimed to examine the active suspension of the seat test rig under various road excitations, such as bumps and random road profiles in the time domain, Figures (5-7) show the bump and random road profile. The essential concept in the ride is to be comfortable, safe, and have good handling. The ride comfort is related to the seat pan acceleration (reduction of vibration). Moreover, road handling and holding are related to suspension travel. Therefore, the proposed control (LQR controller) aims to enhance these quantities. Simulations of the test rig acceleration, velocity, and suspension travel in MATLAB m-file and Simulink environment are used to complete the design of LQR and perform results. The LQR controller design will be divided into two cases, as mentioned in chapter four: a system without disturbance and a system with disturbance.

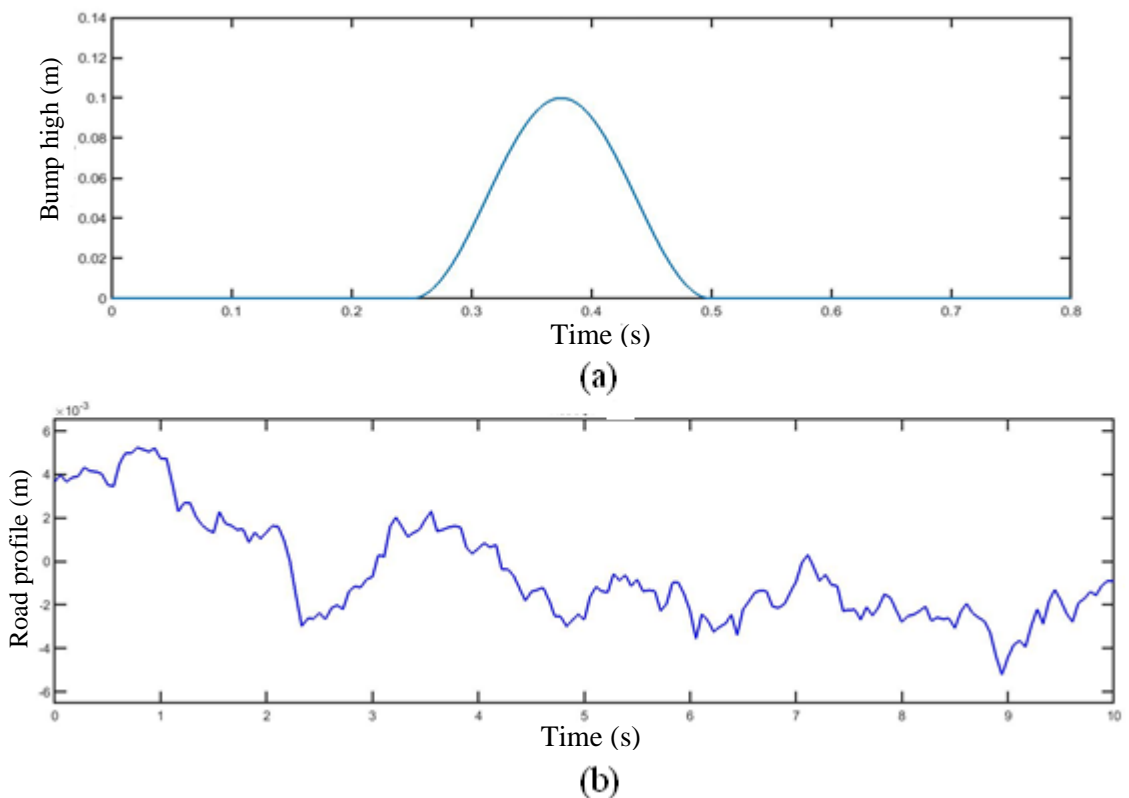


Figure 5–7: Road profiles a) Bump b) Random

5.3.1 Active System with LQR Controller Without Disturbance

MATLAB/Simulink environments were chosen for simulation works to check the performance of LQR controller design in terms of acceleration, velocity, and suspension travel to improve ride quality. The function $[K, E, P] = \text{lqr}[A, B, Q, R]$ evaluated the optimal LQR gain and completed the design. Figure (5-8) The Simulink code of the LQR controller for the active seat test rig system.

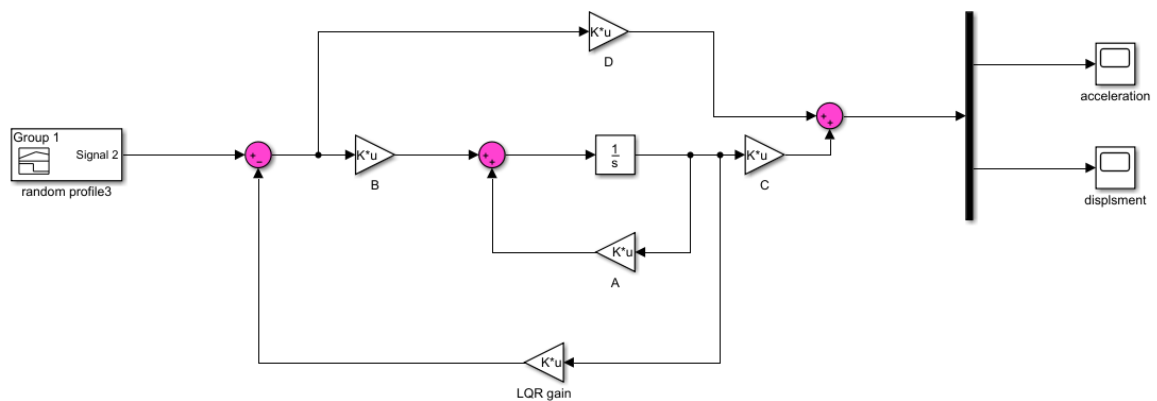
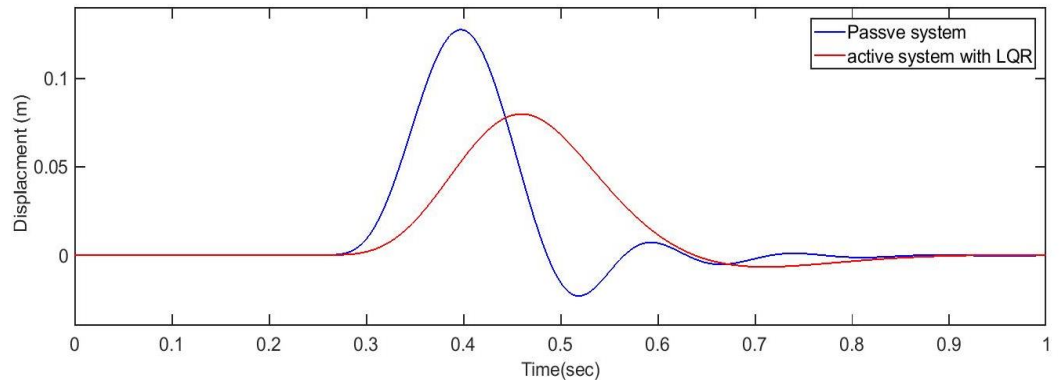


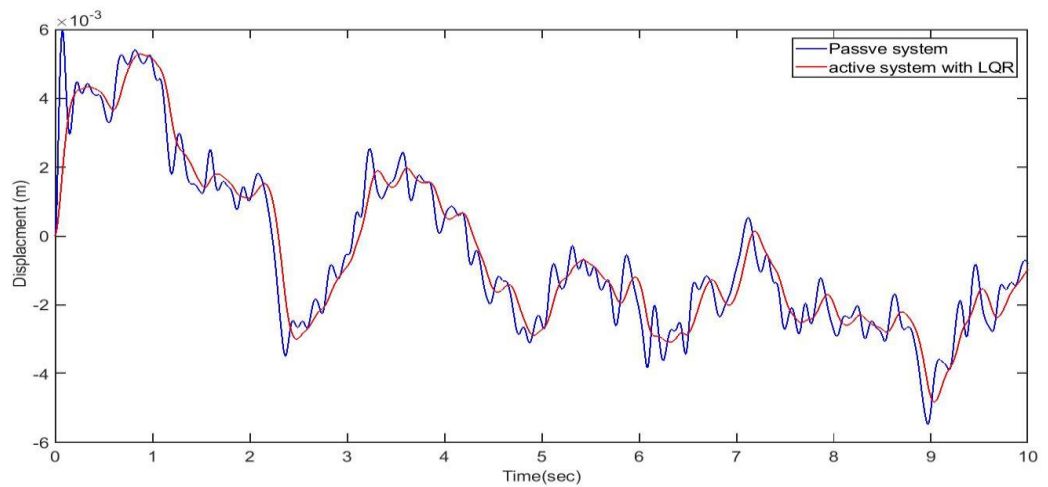
Figure 5–8: LQR control without disturbance for the active seat test rig

The controller design was vital to examine using the R and Q matrix as mentioned in chapter four with a disturbance matrix $D = 0$ to obtain the performance results for the seat test rig. The results will be reviewed for both bump and random road profiles.

Figure (5-9) shows the seat pan displacement in case of the bump and random road profile of the LQR controller compared to the passive response. According to a controller action, the displacement was reduced for bump by 50% and the random road profile by 33%, and this reduction was caused by damping force action.



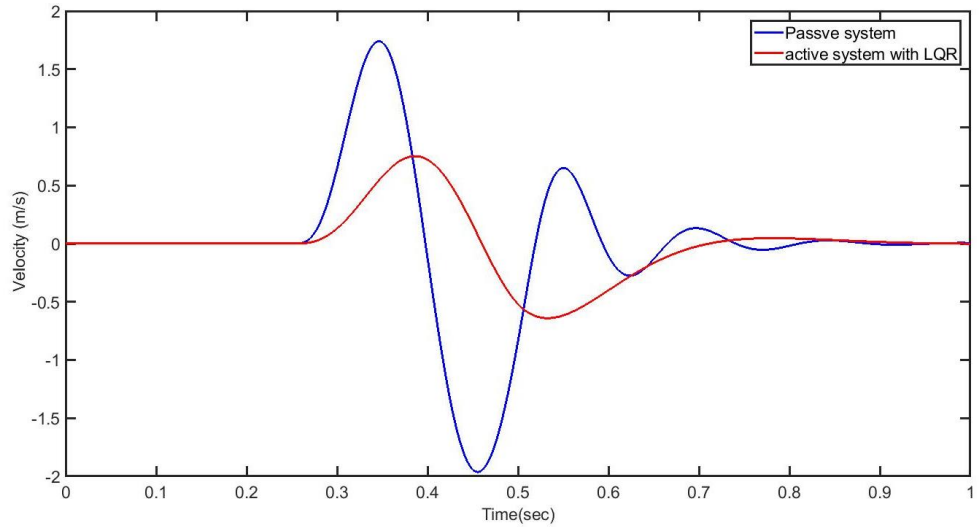
(a)



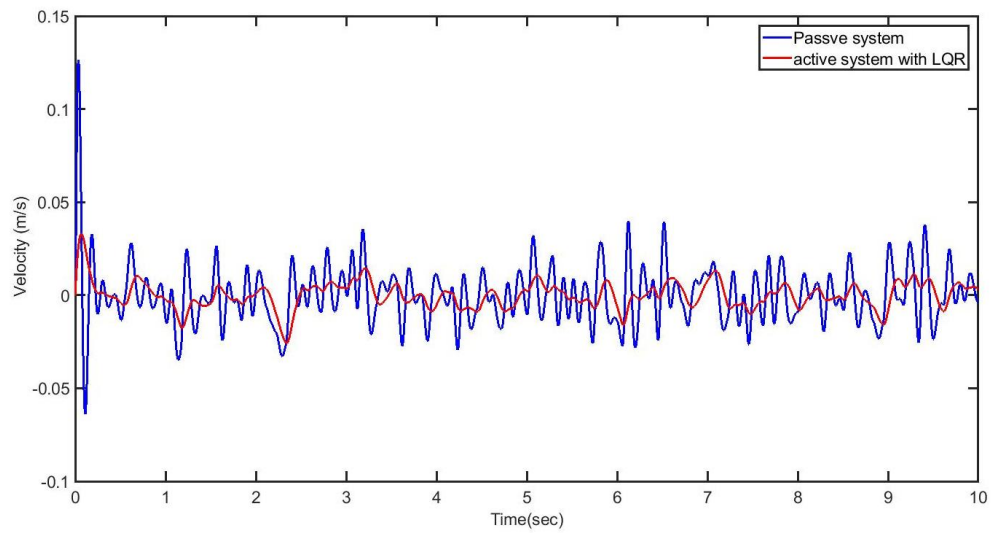
(b)

Figure 5–9: Seat pan displacement for a) Bump profile b) Random road profile

Figure (5-10) displays the behaviors of the seat pan velocity in case of the bump and random road profile of the LQR controller compared to the passive response. According to a controller action, the velocity was reduced for bump by 61% and for the random road profile by 80%, the enhancement of the overshoot and settling time are shown.



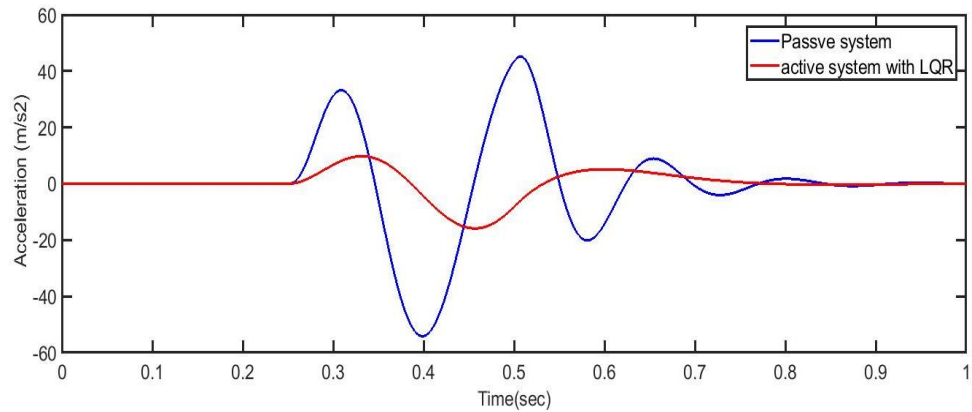
(a)



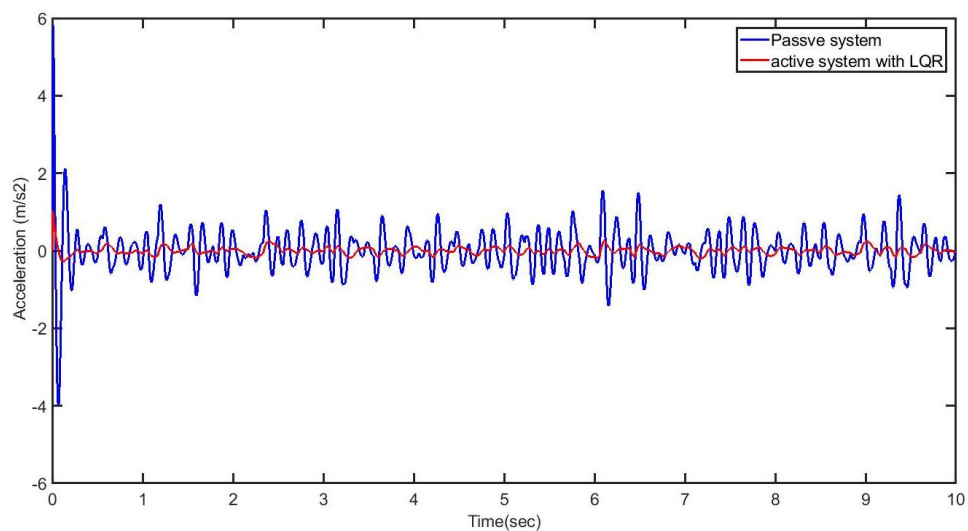
(b)

Figure 5–10: Seat pan velocity for a) Bump profile b) Random road profile

Figure (5-11) shows the response of the seat pan acceleration of the bump and random road profile of the LQR controller compared with the passive response. It can be seen that the reduction in acceleration for the bump by 71% and for the random profile is by 83%; this is relative to a controller action.



(a)



(b)

Figure 5–11: Seat pan acceleration for a) Bump profile b) Random road profile

Figure (5-12) show the suspension travels for bump road profiles. One of the cost effects of using an LQR controller is that the suspension travels will be increased due to the damping force's action, which is in the opposite direction of the suspension motion; the pan's displacement decreases, and the relative displacement between the seat base and seat pan increases. Therefore, the designer should be displayed this signal to find the limitation of the test rig system. Figure (5-12) shows that the suspension travels have a reasonable increase relative to a controller action by 57% for a bump profile.

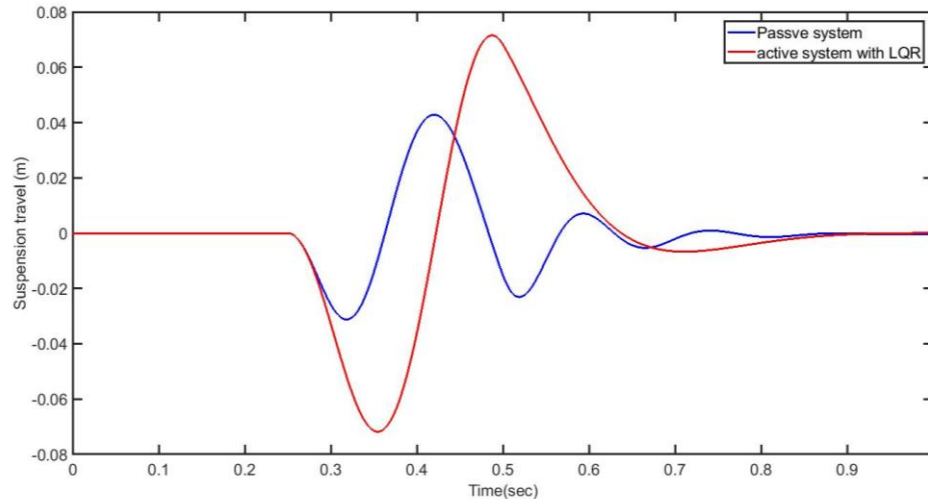


Figure 5–12: Seat suspension travel for Bump profile

Compared with the passive system, the active system results are significantly improved, so the vibration is reduced, and the stability increases. The LQR is effective in reducing the displacement, velocity and acceleration of the seat pan. As a result, LQR successfully eliminated the oscillations in signals and reached faster to a steady state.

5.3.2 Active System with LQR Controller with Disturbance

In this case, the reference input was assumed to be zero to consist of the term of regular controller. The input road profile was entered from the disturbance. Because the vehicle is exposed to the disturbance while driving, this simulation is quite close to reality.

The R-value and the Q matrix are used, as mentioned in chapter three with disturbance matrix $D = [1]$. Figure (5-13) shows the layout of the LQR controller model in Simulink/MATLAB.

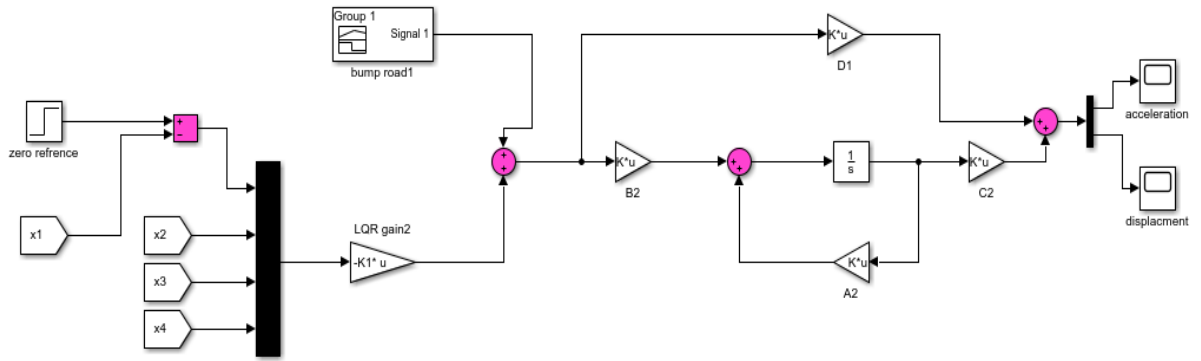


Figure 5–13: LQR control with disturbance for the active seat test rig

According to the second case, the comparison results of the active system through using the LQR controller with disturbance and passive system through considering the bump and random Profile inputs are shown in Figures (5-14) for seat pan displacement, according to a controller action, the displacement is valuable in reducing both bump and random road profiles. The percentage decreases in the seat displacement for a bump is 23% and for random profile is 20%. In this case, it can easily be observed that the output did not move to the reference value of zero.

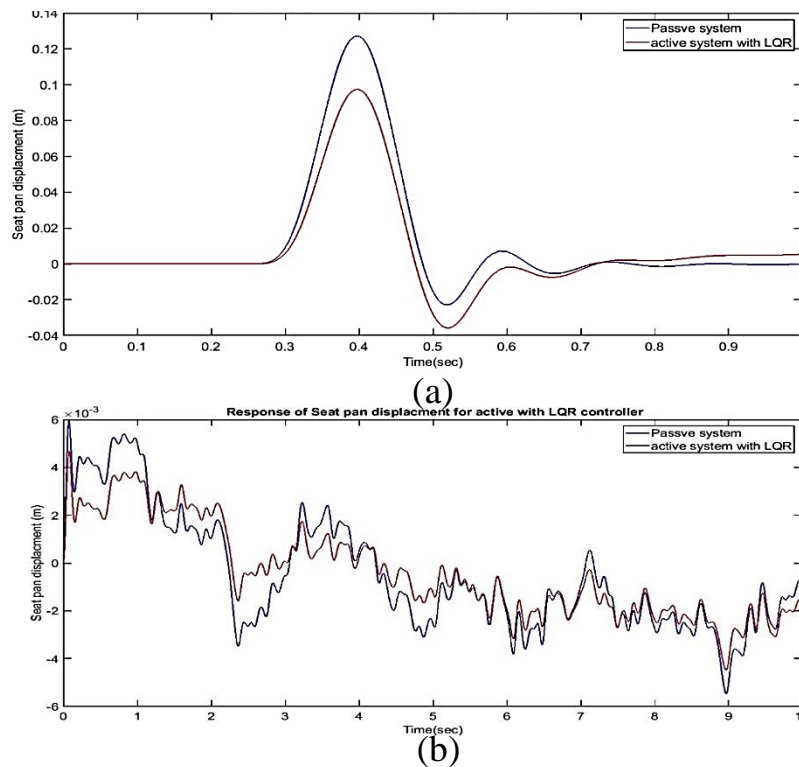
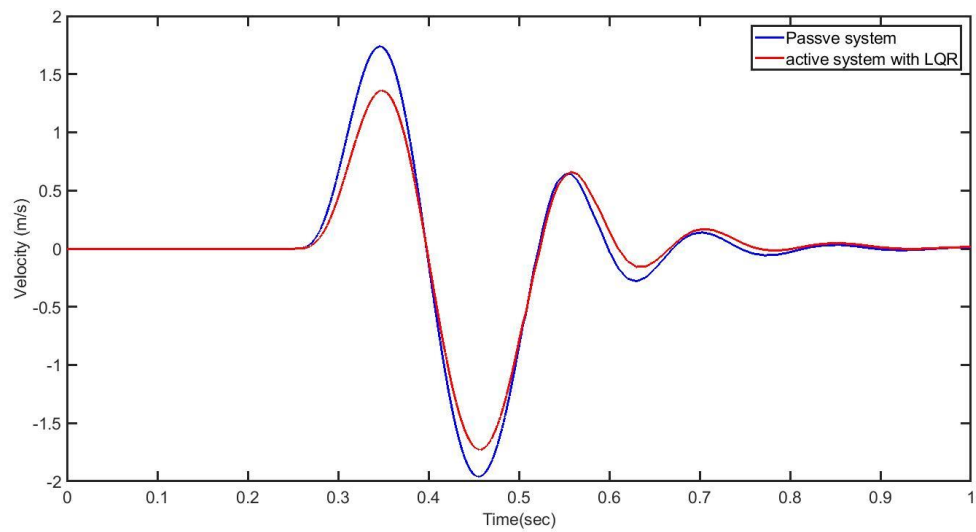
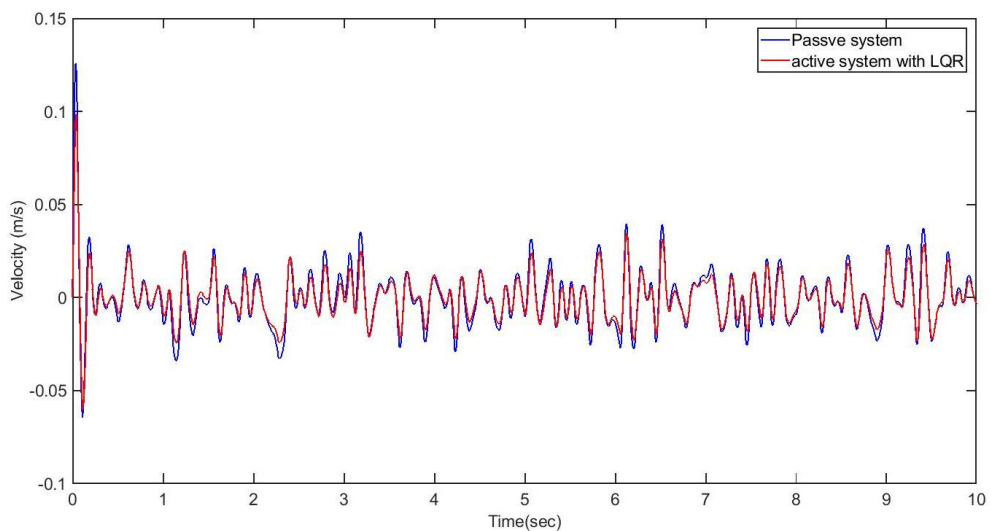


Figure 5–14: Seat pan displacement for a) Bump profile b) Random road profile

Figure (5-15) demonstrates the seat pan velocity behavior with considering the bump and the random road profile for the active seat test rig considered LQR controller and passive system. According to a controller action, the velocity is valuable in reducing both bump and random road profiles. The percentage decreases in the seat velocity for a bump is 18% and for random profile is 23%. In this case, it can easily be observed that the output did not move to the reference value of zero.



(a)

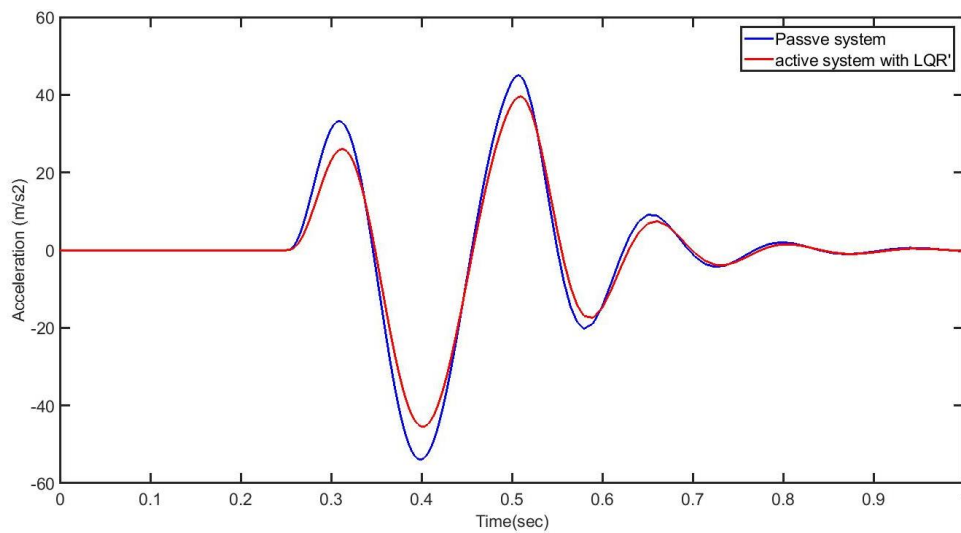


(b)

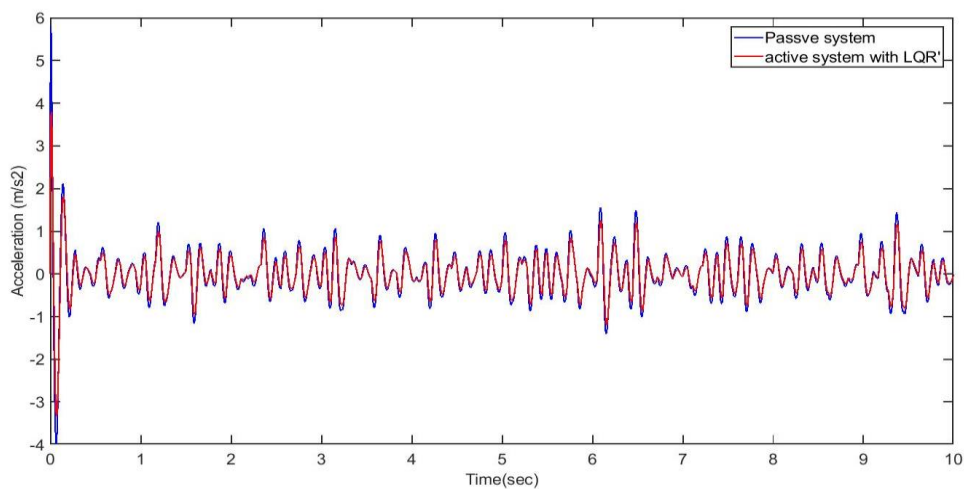
Figure 5–15: Seat pan velocity for a) Bump profile b) Random road profile

The seat pan acceleration with considering the bump and random road profile for the passive and active system considered LQR controller is compared in Figure (5-16). As a result of comparing the seat pan acceleration through considering the bump and random profiles, the controller action makes it possible to notice a reduction in acceleration for both profiles. The percentage reduction for a bump is 22% and for random is 32%.

It can see that another drawback found, the system has a big value of steady-state error that makes it critical stable.



(a)



(b)

Figure 5–16: Seat pan acceleration for a) Bump profile b) Random road profile

Figure (5-17) show the seat suspension travel. It has clearly been seen that the suspension travels have a small increase according to a controller action, and there is a cost-benefit of using LQR. The increasing percentage for a bump is 37%.

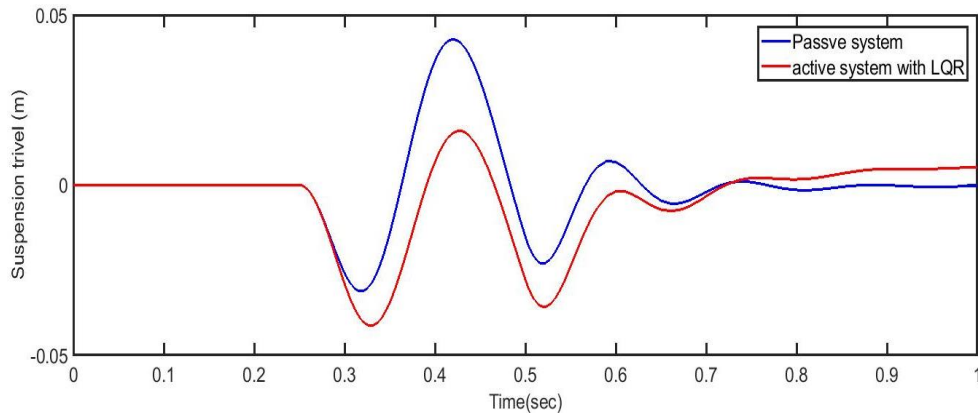


Figure 5–17: Seat suspension travel for bump profile

5.3.3 LQR Controller with Integrator Compensation

In the case of the LQR controller with disturbance, it can be shown that the LQR controller has a large steady-state error that has an effect on the final value of the test rig system. As shown in chapter four, it is required to make modifications to the LQR controller design to fix the steady-state error and drive it to zero. The suggested way to overcome this drawback is by considering the integrator controller; figure (5-18) shows the model of the LQR controller with Integrator Compensation.

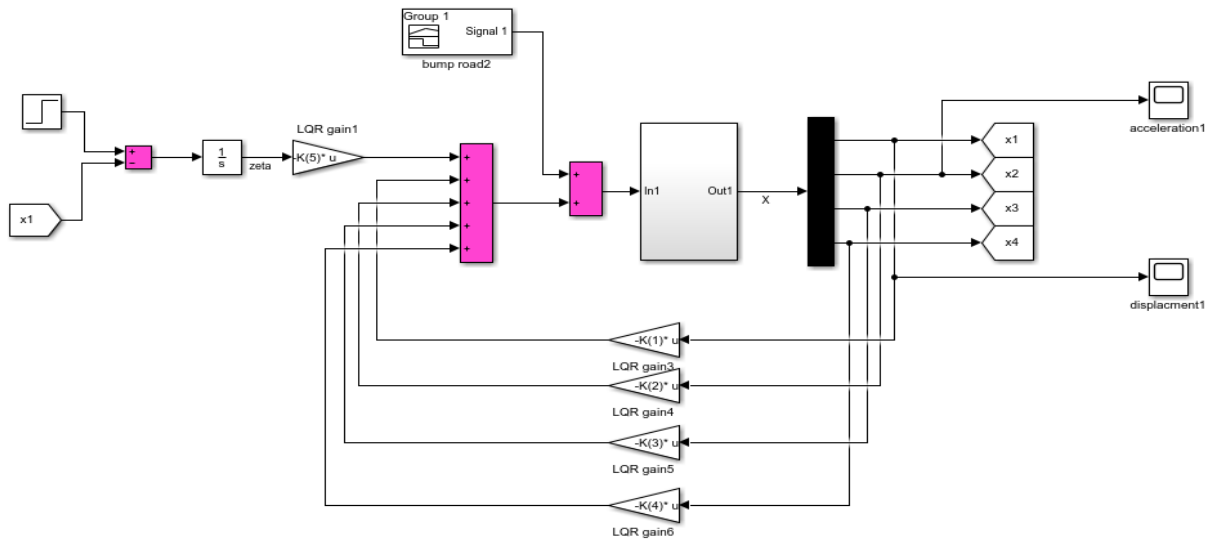


Figure 5–18: LQR control with integrator compensation for the active seat test rig

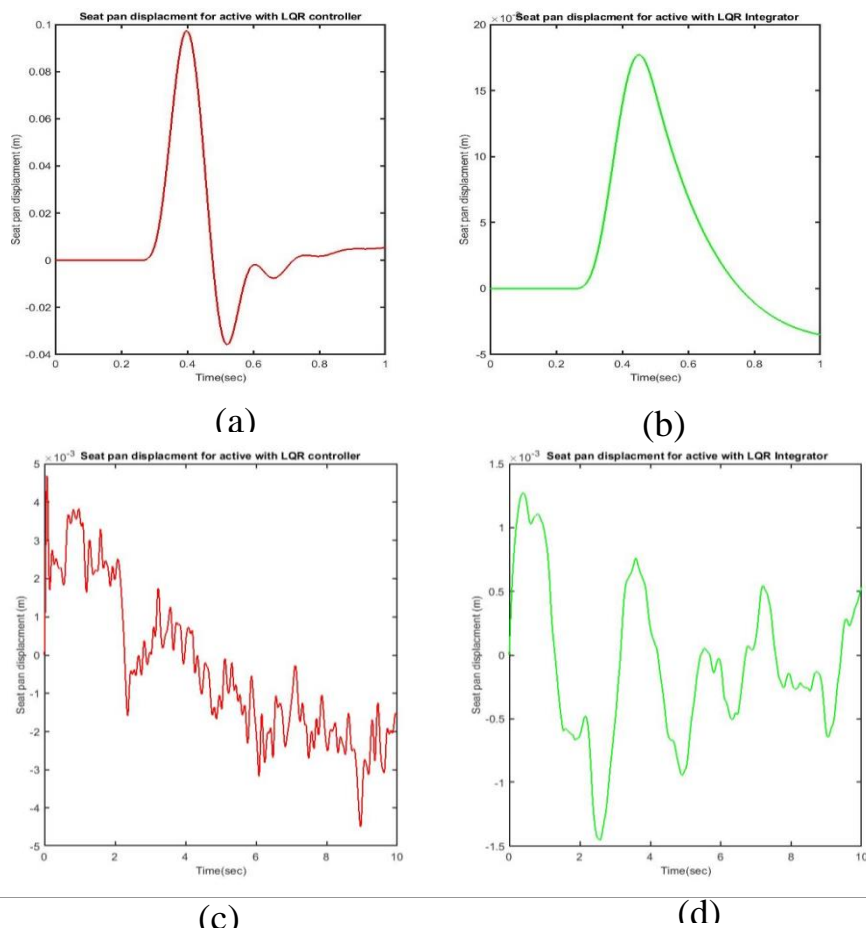


Figure 5–19: Seat pan displacement of a) Bump profile with LQR control b) Bump profile with LQR and an Integrator c) Random road profile with LQR control d) Random road profile with LQR and an Integrator

Figure (5-19) above shows the seat pan displacement behavior. According to the bump and the random road profile, the active system with an LQR controller was compared with the active system with an LQR controller and an integrator response. For the integrator compensation controller action, the displacement is reduced for a bumping road by 98% with zero steady-state error.

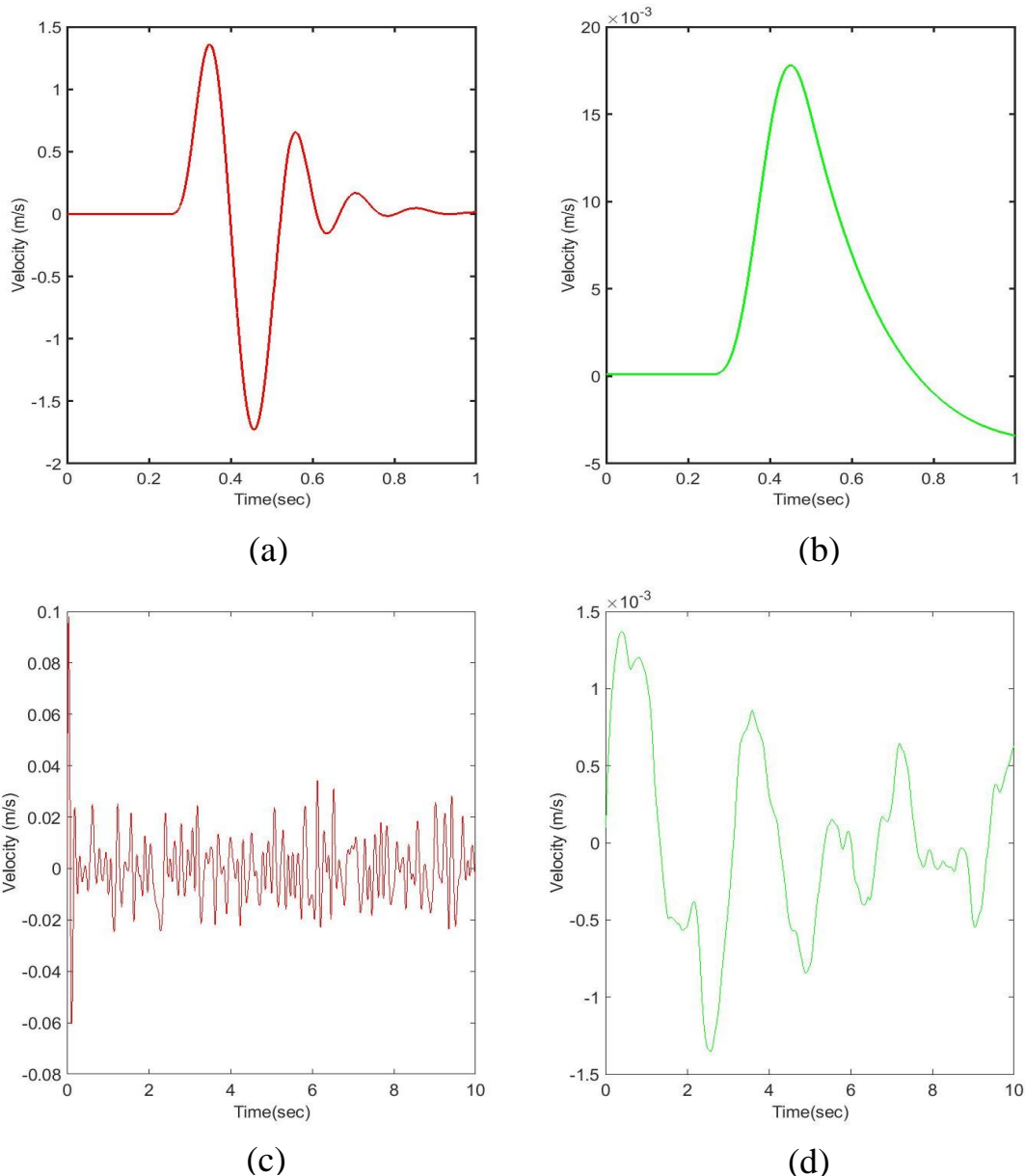


Figure 5–20: Seat pan velocity of a) Bump profile with LQR control b) Bump profile with LQR and an Integrator c) Random road profile with LQR control d) Random road profile with LQR and an Integrator

Figure (5-20) above, demonstrates the seat pan velocity behavior. According to the bump and the random road profile, the active system with an LQR controller was compared with the active system with an LQR controller and an integrator response. For the integrator compensation controller action, the velocity is reduced for a bumping road from 1.4 m/s to $17 \cdot 10^{-3} \text{ m/s}$, and the random road profile is from 1 m/s to $1.4 \cdot 10^{-3} \text{ m/s}$ with zero steady-state error. In general, the reduction percentage is by approximately 99%.

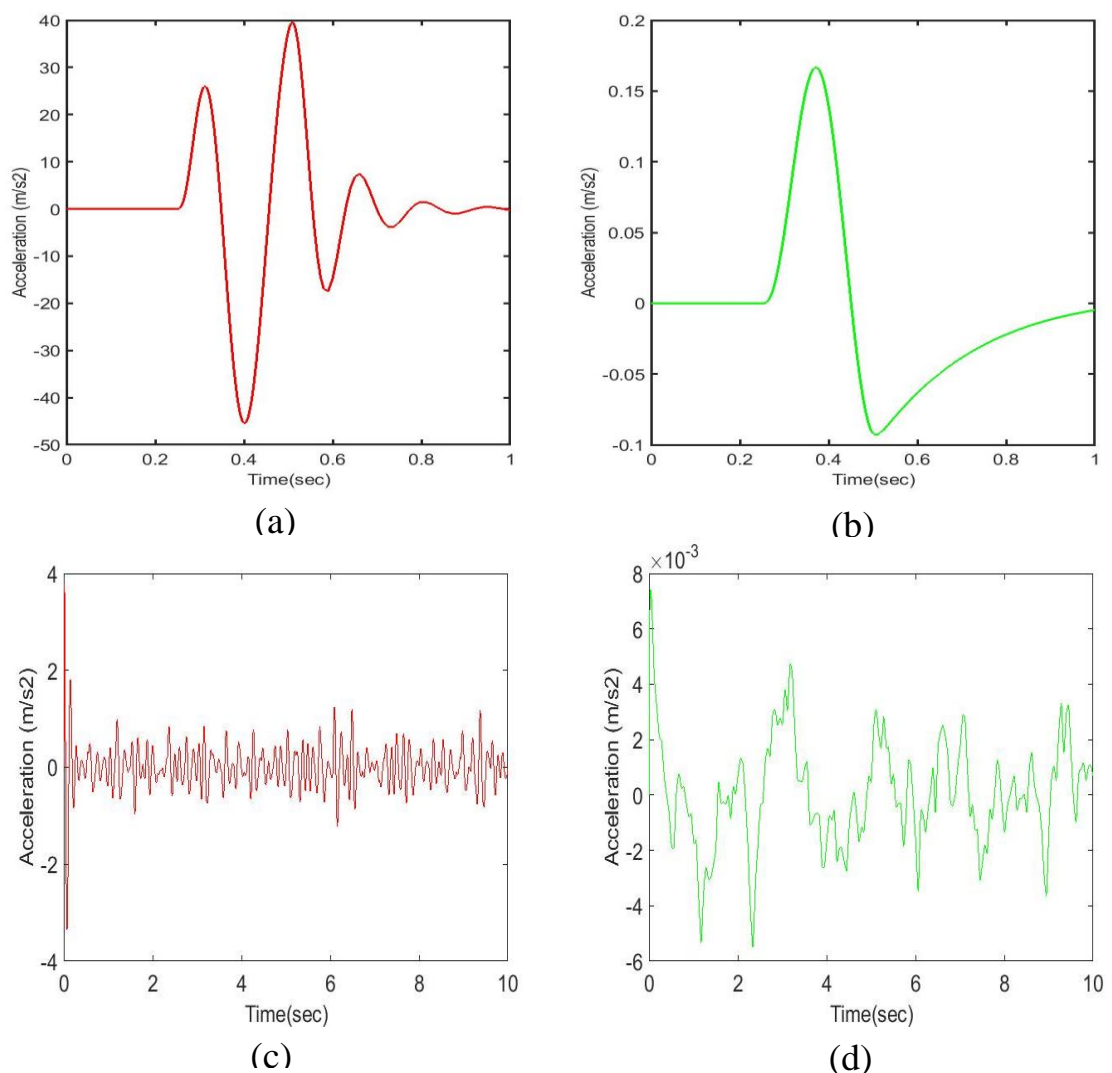


Figure 5–21: Seat pan acceleration of a) Bump profile with LQR control b) Bump profile with LQR and an Integrator c) Random road profile with LQR control d) Random road profile with LQR and an Integrator

Figure (5-21) displays the comparing of the seat pan acceleration of the bump and random road profiles for the active system with an LQR controller and the active system with an LQR controller with integrator action. It was found that a significant reduction in acceleration for both the bump and random profiles with considering the integrator compensation. There is 0% steady-state error, the acceleration of a bumpy road was lowered from 40 m/s to $0.17 \cdot 10^{-3}$ m/s² and for random road profiles from 1 m/s to $1.4 \cdot 10^{-3}$ m/s².

the comparison between the active system with the LQR controller only and the active system with LQR controller and integrator compensation for seat suspension travel shown in Figure (5-22). It has been seen that the suspension travels increase by approximately 200% relative to the action of the integrator compensation controller.

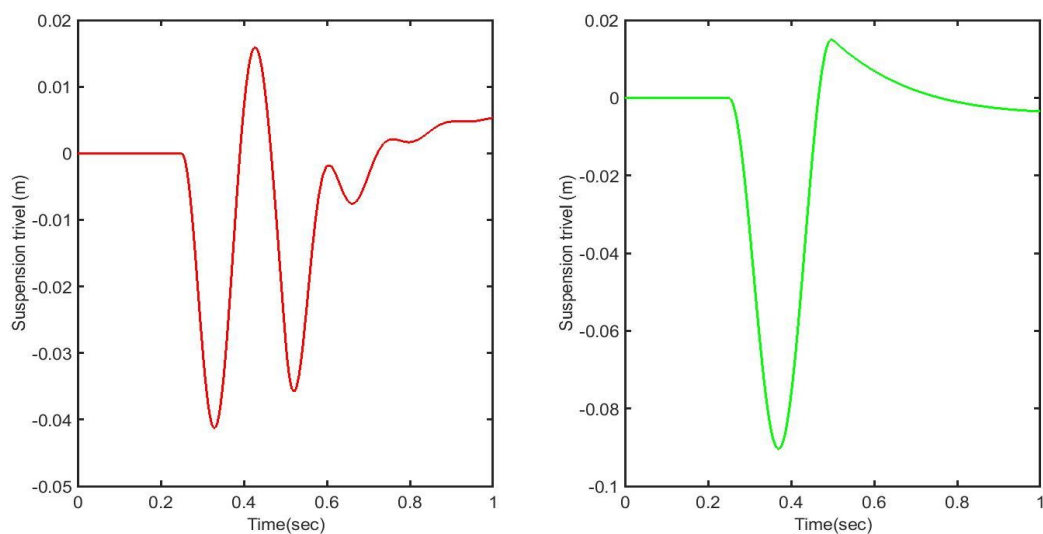


Figure 5–22: Seat suspension travel of

a) Bump profile with LQR control b) Bump profile with LQR and an Integrator

The active system with the LQR controller and integrator compensation has a better overall performance than the active system with the LQR controller only. It also has a good performance in terms of settling time and overshoot percentage. It can summarize the performance of the system in terms of seat

pan acceleration, velocity, displacement, and suspension travel in the table (5-2), and the performance of the system in terms of rising time, settling time, and percentage overshoot in the table (5-3) as follows:

Table 5-2: Performance of the system in terms of acceleration, velocity, suspension travel

Actions		Acceleration decrease		Velocity decrease		Displacement decrease		Suspension travel increase
		Bump	Random	Bump	Random	Bump	Random	Bump
Without Disturbance	Active with LQR Controller	71%	83%	61%	80%	50%	33%	57%
With Disturbance	Active with LQR Controller	22%	32%	18%	23%	23%	20%	37%
	Active with LQR Controller and Integrator	99.2%	99.5%	99.1%	99.3%	98%	98%	227%

Table 5-3: Performance of the system in terms of rising time, settling time, percentage overshoot

Actions		Rise time decrease	Settling time decrease	PO%
Without Disturbance	Active with LQR Controller	18.75%	23.49%	10
With Disturbance	Active with LQR Controller	18.75%	23.49%	20
	Active with LQR Controller and Integrator	100	23.83%	-70

To examine and characterize the performance of the driver's seat suspension system to improve ride quality by reducing the vertical vibration according to ISO 2631-1, it can evaluate the weighted-frequency RMS acceleration as in equation (5-1) [78].

$$a_{RMS} = \left[1/T \int_0^T a_w^2(t) dt \right]^{1/2} \quad (5-1)$$

Where T is the time period of suspension vibration and $a_w(t)$ is the frequency weighted vertical acceleration. The RMS value for vertical acceleration is shown in Table (5-4).

Table (5-4) : the RMS value of vertical acceleration for passive and active with LQR controller

Control Strategy	RMS seat acceleration (m/s ²)	
	Random	Bump
Passive system	0.37	0.42
LQR without disturbance	0.023	0.12
LQR with disturbance	0.034	0.23
LQR with disturbance and integrator	0.0051	0.036

The resulting values are defined by using the table (5-5) which shown the scale of the suggested discomfort.

Table (5-5): Uncomfortable reaction level to vibration values according to IOS 2631-1[78]

RMS acceleration(m/s ²) range	Level of Uncomfortable
Less than 0.315	Not uncomfortable
0.135-0.63	A little uncomfortable
0.5-1	Fairly uncomfortable
0.8-1.6	Uncomfortable
1.25-2.5	Very uncomfortable
Greater than 2	Extremely uncomfortable

Comparing the RMS acceleration values in Tables (5-4) and (5-5) shows that the active system with LQR has much lower RMS acceleration than that of the passive system.

In summary, using the LQR controller with the seat driver's test rig through an optimal choosing value of R and Q provides a good improvement in the performance of seat ride comfort, and clearly reduction of the vibration system, and achieved the stability to the system compared with the passive system. The LQR controller has the ability to find the best performance response in terms of the percentage of overshoot and the settling time in seat drive responses by reducing the velocity and acceleration of seat pan, and the steady-state error has the lowest value in the two cases.

Generally, in comparison to the passive seat suspension, the active seat system with the LQR controller technique achieved lower amplitude and faster response in terms of seat pan suspension travel, velocity, and acceleration, and all these led to riding comfort and a safe drive.

5.4 Summary

This chapter starts with reviewing the passive suspension system results of test rig. The simulation and experimental results show a good matching with little difference caused by sensors sensitivity, test environment. However, in general, the passive test rig is reliable and has a good performance.

The next section has shown the active LQR controller simulation results. The LQR design is divided into two cases: one without disturbance and the second with input disturbance. Although good performance in terms of displacement, velocity, and acceleration in the former case. Nevertheless, a little steady-state error is observed. The latter case results (with disturbance) have a big steady-state error. Therefore, an enhancement of its response is required by suggesting a suitable compensation. The results have been shown a big reduction in seat pan displacement, velocity, and acceleration. In general, the LQR control

without disturbance has a faster response than the LQR controller system with disturbance.

Finally, the proposed controller successfully enhanced the test rig system response to suspension travel, velocity, and acceleration. The LQR control is better in achieved comfort rides because the acceleration response is regarded with vibration reduction.

Chapter Six

Conclusion and Recommendation

Chapter 6. Conclusion and Recommendation

6.1 Conclusion

The following conclusions can be drawn by studying the construction of the driver's seat test rig with a simulation study of linear quadratic control.

1. From verification of the experimental passive test rig, it was found that there is a good agreement between the experimental and simulation results of displacement, velocity, and acceleration for the pan driver's seat. So, the dynamic response for the passive test rig is acceptable.
2. Consequently, the design driver's seat test rig is reliable, useable, and modifiable with a good performance, low cost, and practicable. So, the driver's seat can be developed especially for a heavy-duty vehicle.
3. Verifying the simulation design of the linear quadratic regulator control technique LQR for both methods was successfully used to drive the seat drive's system. It is obviously seen that the performance enhancement would achieve the seat system response in terms of the rise time by approximated 18.75%, settling time by approximated 23.49%, and percentage overshoot by approximated 10%. The LQR controller was examined by being subjected to the random and bump road profiles, and the controller action shows robustness and realizable.
4. The optimal LQR controller stabilizes the seat system compared to the passive system. Based on the results, the optimal LQR controller design accomplished the passive system by achieving the best ride comfort performance by significantly reducing seat pan acceleration by 83%. According to the RMS acceleration results, the active seat minimizes vertical seat acceleration more effectively than the passive suspension, achieving a more comfortable ride.

5. Depending on the results, this study will recommend using the design detail for manufacturing the heavy-duty vehicle driver's seat.

6.2 Recommendation

Based on the achieved work for this thesis, the following recommendations are suggested for future work.

1. It could be beneficial to develop the existing seat test rig by considering a hydraulic system with a computerizing system to generate the system inputs.
2. Also, the suspension system of the seat test rig can be developed by taking the active system instead of the passive system.
3. It can make the driver seat structure from lightweight and environmentally friendly materials that provide high vibration isolation.
4. The control actuating force for active suspension can be accounted for by considering different control techniques such as PID, sliding mode, and PA controller.

Reference

Reference

- [1] S. S. Jadhav and A. PShrotri, "S. S. Jadhav and A. PShrotri,2016. 'Suspension system with broad classification and various models: a review.' International Journal of Advanced Technology in Engineering and Science.Vol. No4, Isseu,No 2,Fabruary 2016."
- [2] T. Ram, M. Rao, G. V. Rao, R. Sreenivasa, and A. Purushottam, "Rao, T. R. M. R., Mohan, R., Rao, G. V., Rao, K. S., & Purushottam, A. (2010). Analysis of passive and semi active controlled suspension systems for ride comfort in an omnibus passing over a speed bump. International Journal of Research and Reviews in App," 2010.
- [3] Al-Zughaibi, Ali and Davies, Huw Charles 2015. Controller design for active suspension system of ¼ car with unknown mass and time-delay. World Academy of Science, Engineering and Technology International Journal of Mechanical, Aerospace, Industrial, Mechatronic and Manufacturing Engineering 9 (8) , pp. 1176-1181.
- [4] Braun, S. G., Ewins, D. J., Rao, S. S., & Leissa, A. W. (2002). Encyclopedia of Vibration: Volumes 1, 2, and 3. Appl. Mech. Rev., 55(3), B45-B45 .
- [5] Mihai, I., & Andronic, F. (2014). Behavior of a semi-active suspension system versus a passive suspension system on an uneven road surface
- [6] Alfadhli, A., Darling, J., & Hillis, A. (2018). Active Seat Suspensions for Automotive Applications (Doctoral dissertation, University of Bath) .
- [7] G. P. A. Koch, "Koch, G. (2011). Adaptive control of mechatronic vehicle suspension systems (Doctoral dissertation, Technische Universität München).2011 ..
- [8] Elattar, Y. M., Metwalli, S. M., & Rabie, M. G. (2016, April). PDF Versus PID Controller for active vehicle suspension. In The International Conference on Applied Mechanics and Mechanical Engineering (Vol. 17, No. 17th International Conference on Applied Mechanics and Mechanical Engineering, pp. 1-18). Military Technical College.
- [9] AbuShaban, M., Sabra, M., & Abuhadrous, I. (2012). A new control strategy for active suspensions using modified fuzzy and PID controllers. Proc. of the 4th IEC.
- [10] Aboud, W. S., Haris, S. M., & Yaacob, Y. (2014). Advances in the control of mechatronic suspension systems. Journal of Zhejiang University SCIENCE C, 15(10), 848-860.."
- [11] Jones, W. D. (2005). Easy Ride Bose Corp. uses speaker technology to give cars adaptive suspension. IEEE SPECTRUM, 42(5), 6-6.
- [12] van der Sande, T. P. J. (2011). Control of an automotive electromagnetic suspension system. Master's thesis, Eindhoven University of Technology.
- [13] G. Koch, E. Pellegrini, S. Spirk, N. Pletschen, and B. Lohmann, "Koch, G., Pellegrini, E., Spirk, S., Pletschen, N., & Lohmann, B. (2011). Actuator control for a hybrid suspension system. Lehrstuhl für Regelungstechnik.," Tech. Reports Autom. Control, no. 6, pp. 1–14, 2011, [Online]. Available: www.rt.mw.tum.de.
- [14] Al-Zughaibi, A., Xue, Y., Grosvenor, R. and Okon, A., 2019. Design and investigation of pole assignment controller for driving nonlinear electro hydraulic actuator with new active suspension system model. Proceedings of the Institution of Mechanical Engineers, Part D: Journal of Automobile Engineering, 233(13).
- [15] www.delphi.com. Status: 10/2010.

Reference

- [16] E. Guglielmino, T. Sireteanu, C. W. Stammers, G. Gheorghe, and M. Giuclea, “Guglielmino, E., Sireteanu, T., Stammers, C. W., Ghita, G., & Giuclea, M. (2008). Semi-active suspension control: improved vehicle ride and road friendliness. Springer Science & Business Media.” *Semi-active Suspension Control: Improved Vehicle Ride and Road Friendliness*. pp. 1–294, 2008, doi: 10.1007/978-1-84800-231-9.
- [17] N. Giorobtaini, A. Bemporad, H. E. Tseng, and D. Hrovat, “Giorobtaini, N., Bemporad, A., Tseng, H. E., & Hrovat, D. (2006). Hybrid model predictive control application towards optimal semi-active suspension. *International Journal of Control*, 79(05), 521-533.” *Int. J. Control*, vol. 79, no. 5, pp. 521–533, 2006, doi: 10.1080/00207170600593901.
- [18] Guo, S., Li, S., & Yang, S. (2006, December). Semi-active vehicle suspension systems with magnetorheological dampers. In *2006 IEEE International Conference on Vehicular Electronics and Safety* (pp. 403-406). IEEE.
- [19] Shen, C. and Liang, T., 2013. Design and implementation of a high-voltage generator with output voltage control for vehicle er shock-absorber applications. *Mathematical Problems in Engineering*, 2013, pp.1-6.
- [20] S. Surendran, “Analysis of Driver Seat Suspension using Electro- Rheological fluid damper for automotive ride comfort,” no. November 2016, 2017, doi: 10.13140/RG.2.2.34180.53129.
- [21] Jalili, N., 2002, “A Comparative Study and Analysis of Semi-Active Vibration-Control Systems,” *J. Vib. Acoust.*, 124(4), pp. 593–605.
- [22] D. Ning, S. Sun, H. Li, H. Du, and W. Li, “Ning, D., Sun, S., Li, H., Du, H., & Li, W. (2016). Active control of an innovative seat suspension system with acceleration measurement based friction estimation. *Journal of Sound and Vibration*, 384, 28-44.” *J. Sound Vib.*, vol. 384, pp. 28–44, 2016, doi: 10.1016/j.jsv.2016.08.010.
- [23] Zhao, L., Zhou, C., Yu, Y., & Yang, F. (2017). Hybrid modelling of driver seat-cushion coupled system for metropolitan bus. *Journal of Low Frequency Noise, Vibration and Active Control*, 36(3), 214-226.
- [24] Vér, I. L., & Beranek, L. L. (Eds.). (2005). *Noise and vibration control engineering: principles and applications*. John Wiley & Sons.
- [25] Adam, S. A., Jalil, N. A., Rezali, K. M., Ng, Y. G., & Sound and Vibration Research Group. (2020). The effect of posture and vibration magnitude on the vertical vibration transmissibility of tractor suspension system. *International Journal of Industrial E.*
- [26] Zhao, Y., & Wang, X. (2019). A review of low-frequency active vibration control of seat suspension systems. *Applied Sciences*, 9(16), 3326.
- [27] Appleyard, M., & Wellstead, P. E. (1995). Active suspensions: some background. *IEE Proceedings-Control Theory and Applications*, 142(2), 123-128.
- [28] M. Kawana and T. Shimogo, “Kawana, M., & Shimogo, T. (1998). Active suspension of truck seat. *Shock and vibration*, 5(1), 35-41.” *Shock and Vibration*, vol. 5, no. 1. pp. 35–41, 1998, doi: 10.1155/1998/579025.
- [29] Ning, D., Sun, S., Du, H., Li, W., & Li, W. (2018). Control of a multiple-DOF vehicle seat suspension with roll and vertical vibration. *Journal of Sound and Vibration*, 435, 170-191.

Reference

- [30] Braghin, F., Cheli, F., Facchinetti, A., & Sabbioni, E. (2011). Design of an active seat suspension for agricultural vehicles. In *Structural Dynamics*, Volume 3 (pp. 1365-1374). Springer, New York, NY.
- [31] Stein, G., 1997. A Driver's seat with active suspension of electro-pneumatic type. *Journal of Vibration and Acoustics*, 119(2), pp.230-235.
- [32] I. Maciejewski, L. Meyer, and T. Krzyzynski, "Maciejewski, I., Meyer, L., & Krzyzynski, T. (2010). The vibration damping effectiveness of an active seat suspension system and its robustness to varying mass loading. *Journal of sound and vibration*, 329(19), 3898-3914.," *Journal of Sound and Vibration*, vol. 329, no. 19. pp. 3898–3914, 2010, doi: 10.1016/j.jsv.2010.04.009.
- [33] Gan, Z., Hillis, A. J., & Darling, J. (2015). Adaptive control of an active seat for occupant vibration reduction. *journal of sound and vibration*, 349, 39-55.
- [34] Alfadhli, A., Darling, J., & Hillis, A. J. (2018). The Control of an Active Seat Suspension Using an Optimised Fuzzy Logic Controller, Based on Preview Information from a Full Vehicle Model. *Vibration*, 1(1), 20-40.
- [35] Anonymous, Bose Ride System [online], 2021. Available from: <http://www.boseride.com/seat-suspension-system> [Accessed 24/04/2015].
- [36] Kashem, S., Nagarajah, R., & Ektesabi, M. (2018). *Vehicle suspension systems and electromagnetic dampers*. Springer Singapore.
- [37] P. Eamcharoenying, "Eamcharoenying, P. (2015). Hybrid Numerical-Experimental Testing of Active and Semi-Active Suspensions (Doctoral dissertation, University of Bath).," 2015.
- [38] Sun, S. S., Ning, D. H., Yang, J., Du, H., Zhang, S. W., & Li, W. H. (2016). A seat suspension with a rotary magnetorheological damper for heavy duty vehicles. *Smart Materials and Structures*, 25(10), 105032.
- [39] X. Wu and M J G., (1997). A semi-active control policy to reduce the occurrence and severity of end-stop impacts in a suspension seat with an electrorheological fluid damper. *Journal of Sound and Vibration*, 203(5), 781-793.1997 ”,.
- [40] Choi, S. B., Nam, M. H., & Lee, B. K. (2000). Vibration control of a MR seat damper for commercial vehicles. *Journal of intelligent material systems and structures*, 11(12), 936-944.
- [41] S. J. McManus, K. A. St. Clair, P. É. Boileau, J. Boutin, and S. Rakheja, "McManus, S. J., Clair, K. S., Boileau, P. E., Boutin, J., & Rakheja, S. (2002). Evaluation of vibration and shock attenuation performance of a suspension seat with a semi-active magnetorheological fluid damper. *Journal of Sound and Vibration*, 253(1), 313-," in *Journal of Sound and Vibration*, May 2002, vol. 253, no. 1, pp. 313–327, doi: 10.1006/jsvi.2001.4262.
- [42] Hiemenz, G. J., Hu, W., & Wereley, N. M. (2008). Semi-active magnetorheological helicopter crew seat suspension for vibration isolation. *Journal of Aircraft*, 45(3), 945-953.
- [43] Tehrani, K. A., & Mpanda, A. (2012). *PID Control Theory, Introduction to PID Controllers-Theory, Tuning and Application to Frontier Areas*, Prof. Rames C. Panda (Ed.), ISBN: 978-953-307-927-1, InTech.
- [44] D. Karnopp, M. J. Crosby, and R. A. Harwood, "Karnopp, D., Crosby, M. J., & Harwood, R. A. (1974). Vibration control using semi-active force generators.," *ASME Pap*, no. 73-DET-122, pp. 619–626, 1973.

Reference

- [45] L. V. V. Gopala Rao and S. Narayanan, "Rao, L. G., & Narayanan, S. (2009). Sky-hook control of nonlinear quarter car model traversing rough road matching performance of LQR control. *Journal of Sound and Vibration*, 323(3-5), 515-529.," *J. Sound Vib.*, vol. 323, no. 3–5, pp. 515–529, Jun. 2009, doi: 10.1016/j.jsv.2009.01.025.
- [46] Gutierrez Soto, M., & Adeli, H. (2017). Recent advances in control algorithms for smart structures and machines. *Expert Systems*, 34(2), e12205.
- [47] H. Kwakernaak, "Kwakernaak, H. (1993). Robust control and H_∞ -optimization—tutorial paper. *automatica*, 29(2), 255-273.," *Automatica*, vol. 29, no. 2. pp. 255–273, 1993, doi: 10.1016/0005-1098(93)90122-A.
- [48] Emad Q. Hussien. an optimal control approach based on the spacecraft altitude by using h-infinity. 27 January 2018.
- [49] J. Liu, "Liu, J. (2017). Sliding mode control using MATLAB. Academic Press.," *Sliding Mode Control Using MATLAB*. pp. 1–332, 2017.
- [50] Alkhatib, R., & Golnaraghi, M. F. (2003). Active structural vibration control: a review. *Shock and Vibration Digest*, 35(5), 367.
- [51] R. Patel, D. Deb, R. Dey, and V. E. Balas, "Landau, I. D., Lozano, R., M'Saad, M., & Karimi, A. (2011). Adaptive control: algorithms, analysis and applications. Springer Science & Business Media.," *Intelligent Systems Reference Library*, vol. 161. pp. 53–65, 2020, doi: 10.1007/978-3-030-18068-3_5.
- [52] Anderson, E., How, J., How, J., & Anderson, E. (1997). Adaptive feedforward control for actively isolated spacecraft platforms. In *38th Structures, Structural Dynamics, and Materials Conference* (p. 1200).
- [53] W. S. Levine, "Levine, W. S. (Ed.). (2018). The Control Systems Handbook: Control System Advanced Methods. CRC press.," *The Control Handbook: Control System Fundamentals*, Second Edition. pp. 1–786, 2017, doi: 10.1201/b10383.
- [54] Lagaros, N. D. (Ed.). (2012). Design optimization of active and passive structural control systems. IGI global.
- [55] Cao, J., Liu, H., Li, P., & Brown, D. J. (2008). State of the art in vehicle active suspension adaptive control systems based on intelligent methodologies. *IEEE transactions on intelligent transportation systems*, 9(3), 392-405.
- [56] W. Levine, "Kirk, D. E. (2004). Optimal control theory: an introduction. Courier Corporation.," *IEEE Transactions on Automatic Control*, vol. 17, no. 3. pp. 423–423, 1972, doi: 10.1109/tac.1972.1100008.
- [57] Ali, S.A., Metered, H., Bassiuny, A.M., and Abdel-Ghany, A.M., 'Vibration Control of an Active Seat Suspension System Integrated Pregnant Woman Body Model,' *SAE Technical Paper* 2019-01-0172, 2019, doi:10.4271/2019-01-0172.
- [58] Emad Q. Hussien.2014. an optimal design for variable speed wind turbines based on LQG. *The Iraqi Journal for Mechanical and Material Engineering*, Vol.14, No1, 2014.
- [59] Metered, H. (2010). Modelling and control of magnetorheological dampers for vehicle suspension systems. The University of Manchester (United Kingdom).
- [60] Alfadhli, A., Darling, J., & Hillis, A. J. (2018). An active seat controller with vehicle suspension feedforward and feedback states: an experimental study. *Applied Sciences*, 8(4), 603.

Reference

- [61] <https://learn.adafruit.com/adafruit-analog-accelerometer-breakouts/calibration-and-programming>.
- [62] G. D'Emilia, D. Di Gasbarro, A. Gaspari, and E. Natale, "D'Emilia, G., Di Gasbarro, D., Gaspari, A., & Natale, E. (2017, August). Identification of calibration and operating limits of a low-cost embedded system with MEMS accelerometer. In *Journal of Physics: Conference Series* (Vol. 882, No. 1, p. 012006). IOP P," *J. Phys. Conf. Ser.*, vol. 882, no. 1, 2017, doi: 10.1088/1742-6596/882/1/012006.
- [63] Katsuhiko, O. (2010). *Modern control engineering*.
- [64] Nagarkar, M. P., Vikhe, G. J., Borole, K. R., & Nandedkar, V. M. (2011). Active control of quarter-car suspension system using linear quadratic regulator. *International Journal of Automotive and Mechanical Engineering*, 3(1), 364-372.
- [65] Kumar, M. S., & Vijayarangan, S. (2006). Linear quadratic regulator controller design for active suspension system subjected to random road surfaces. .
- [66] Doddabasappa, S. (2019). LQR control design for a DC-DC converter using sensitivity functions..
- [67] Maurya, V. K., & Bhangal, N. S. (2018). Optimal control of vehicle active suspension system. *Journal of Automation and Control Engineering*, 6(1). .
- [68] R. M. Murray, "Murray, R. M. (2009). Optimization-based control. California Institute of Technology, CA, 111-128.," *Optimization-Based Control*. pp. 2.1-2.19, 2010.
- [69] Thierry Miquel. *Introduction to Optimal Control*. Master. Introduction to optimal control, ENAC, France. 2020. hal-02987731 HAL .
- [70] Al-Zughaibi, A. (2019). *Automotive suspension system modelling and controlling* (Doctoral dissertation, Cardiff University).," p. 2019, 2019.
- [71] Okyere, E., Bousbaine, A., Poyi, G. T., Joseph, A. K., and Andrade., J. M. (2018) 'LQR controller design for quad-rotor helicopters', *The 9th International Conference on Power Electronics, Machines and Drives*. The Arena and Convention Centre, Liverpool, 1 .
- [72] Hussein, E. Q., Al-Dujaili, A. Q., & Ajel, A. R. (2020, July). Design of Sliding Mode Control for Overhead Crane Systems. In *IOP Conference Series: Materials Science and Engineering* (Vol. 881, No. 1, p. 012084). IOP Publishing. .
- [73] A. S. Shameem Banu, M. Mathuri, Y. Bineshlal, and S. Jayakumar, Åström, K. J., & Murray, R. M. (2003). *Analysis and Design of Feedback Systems: An Introduction for Scientists and Engineers*. Draft v01, 24., vol. 5, no. 5. 2014.
- [74] Mustapha Asslan.2021. *Application of Robust Control Methodologies to Control Micro Actuator Driven Systems*. Thesis for: Doctor of Philosophy (Engineering). University of Aleppo.
- [75] Fialho, I. J., & Balas, G. J. (2000). Design of nonlinear controllers for active vehicle suspensions using parameter-varying control synthesis. *Vehicle System Dynamics*, 33(5), 351-370.," p. 2000, 2000.
- [76] Tyan, F., Hong, Y. F., Tu, S. H., & Jeng, W. S. (2009). Generation of random road profiles. *Journal of Advanced Engineering*, 4(2), 1373-1378..

Reference

[77] Zaid Hikmat Rashid. Control And Dynamic Analysis of a Serial Type 6 Dof's Robotics Manipulator. University of Technology. Mechanical Engineering Department. Ph.D. Supervisor: Dr. Hassan M. Alwan. 2019. 135p .

[78] Yka Marjanen, "Validation and improvement of the ISO2631-1(1997) standard method for evaluation discomfort from whole- body vibration in a multi-axis environmental", PhD. thesis, Loughborough University, 2010.

Appendix

1- Specifications of Uno Board

Description	Value
Operating Voltage	5V
Input Voltage (recommended)	7~12V
Input Voltage (limits)	6~20V
Digital I/O Pins	14 (of which 6 provide PWM output)
Analog Input Pins	6
DC Current per I/O Pin	40mA
DC Current for 3.3V Pin	50mA
SRAM	2KB (ATmega328)
EEPROM	1KB (ATmega328)
Clock Speed	16MHz
Color	Blue

2- Specifications of GY-61 DXL335 3-Axis Accelerometer

Description	Value
Sensor Chip	ADXL335
Operating Voltage Range	3V ~ 5V
Supply Current	400uA
Interface	Analog quantity output
Full scale range	+/-3g
Operating Temperature	-40'C~ +85'C
Sensitivity	300mv /g;
Sensitivity of accuracy (%)	+/- 10
Application	Various electronic products or DIY project
Material	PCB + Brass
Dimensions	21 x 16 x 10 mm / 0.83 x 0.63 x 0.39 inch
Weight	2 g / 0.07 oz
Color	Blue

Appendix

3- Specifications of GY-VL53L0XV2 Laser Distance Sensor

Description	Value
Working voltage	3 ~ 5V
Communication method	IIC
Measurement of absolute distance	2m
size	25mm*10.7mm
Hole pitch	19.3mm

4- GY-61 DXL335 3-axis accelerometer calibration

$$\text{Actual reading} = \frac{\text{Original reading} - \text{Zero line}}{\text{Criterion}} * 9.81 \text{ m/s}^2 = \text{Sensitivity} \quad (1)$$

$$\begin{aligned} \text{Zero line} &= \frac{\text{Maximum reading} + \text{Minimum reading}}{2} \\ &= \frac{427 + 285}{2} \\ &= 356 \text{ mV} \end{aligned} \quad (2)$$

$$\begin{aligned} \text{Criterion}(\text{weight}) &= \frac{\text{Maximum reading} + \text{Minimum reading}}{2} \\ &= \frac{427 + 285}{2} \\ &= 71 \text{ mV} \end{aligned} \quad (3)$$

Substitute equations (3.2) and (3.3) into (3.1), then:

$$\text{Actual reading} = \frac{\text{Original reading} - 356}{71} * 9.81 \text{ m/s}^2 = 0.3 * \text{g} \quad (4)$$

Equation (4) represents the actual reading in m/s^2 . Where: original reading is a real-time reading during the test.

Appendix

5- LQR design code

% This program code to compute the response of seat pan test rig with passive system and active with LQR controller and LQR control with integrator

%% This program must run with simulink program which named (LQRdesign) at the same time

m1=58; %seat pan mass Kg

m2=21; %seat base mass Kg

k1=20000; % base stiffness N/m

k2=150000; % passive stiffness N/m

c1=4000; % passive damping N.s/m

A=[0 1 0 0;

-k1/m1 -c1/m1 k1/m1 c1/m1;

0 0 0 1;

k1/m2 c1/m2 (-k2-k1)/m2 -c1/m2];

B=[0 ;0 ;0 ;k2/m2];

C=[-k1/m1 -c1/m1 k1/m1 c1/m1 ;1 0 0 0];

D=[1 ;0];

poles=eig(A) %eigenvalue to check stability of passive system

Qm=[0.001 1 0 ; 0 0.001] %Bryson rule

Q=C'*Qm*C %state weight matrix

R=[100] % input weight matrix

[K1,p1,E1]=lqr(A,B,Q,R)

% for Integrator

A1=A;

A1(5,5)=0;

A1(5,1)=-1;

B1=B;

B1(5,1)=0;

C1=[-k1/m1 -c1/m1 k1/m1 c1/m1 0 ;1 0 0 0 0];

D1=[1 ;0];

Q1=diag([100 10 100 10 1000])

R1=[100]

[K,p,E]=lqr(A1,B1,Q1,R1)

Co=ctrb(A,B) % controllability of system

rank(Co)

Appendix

Ob=obsv(A,C)

rank(Ob)

poles =

1.0e+02 *
-2.3202 + 0.0000i
-0.0542 + 0.0000i
-0.1100 + 0.4286i
-0.1100 - 0.4286i

Qm =

0.0011 0
0 0.0010

Q =

130.7977 26.1593 -130.7967 -26.1593
26.1593 5.2319 -26.1593 -5.2319
-130.7967 -26.1593 130.7967 26.1593
-26.1593 -5.2319 26.1593 5.2319

R =

100

K1 =

-0.7222 -0.1337 0.7222 0.1984

p1 =

0.4015 0.0861 0.6768 -0.0101
0.0861 0.0211 0.1234 -0.0019
0.6768 0.1234 4.7173 0.0101
-0.0101 -0.0019 0.0101 0.0028

E1 =

1.0e+03 *
-1.6492 + 0.0000i
-0.0110 + 0.0125i
-0.0110 - 0.0125i
-0.0054 + 0.0000i

Q1 =

Appendix

100	0	0	0	0
0	10	0	0	0
0	0	100	0	0
0	0	0	10	0
0	0	0	0	1000

R1 =

100

K =

1.0439 0.1615 0.3834 0.2957 -3.1623

p =

62.9065 0.4292 0.8478 0.0146 -138.5549

0.4292 0.0661 0.0023 0.0023 -1.3909

0.8478 0.0023 44.9361 0.0054 -6.0236

0.0146 0.0023 0.0054 0.0041 -0.0443

-138.5549 -1.3909 -6.0236 -0.0443 767.5656

E =

1.0e+03 *

-2.2680

-0.0932

-0.0051

-0.0033

-0.0022

Co =

1.0e+10 *

0 0 0.0000 -0.0125

0 0.0000 -0.0125 2.8361

0 0.0000 -0.0001 0.0295

0.0000 -0.0001 0.0295 -6.8612

ans =

4

Ob =

1.0e+10 *

Appendix

```
-0.0000 -0.0000 0.0000 0.0000
0.0000 0 0 0
0.0000 0.0000 -0.0001 -0.0000
0 0.0000 0 0
-0.0023 -0.0004 0.0148 0.0004
-0.0000 -0.0000 0.0000 0.0000
0.5320 0.1041 -3.3681 -0.0916
0.0000 0.0000 -0.0001 -0.0000
```

ans =

4



وزارة التعليم العالي والبحث العلمي
جامعة كربلاء
كلية الهندسة
قسم الهندسة الميكانيكية

بناء جهاز اختبار مقعد السائق مع دراسة محاكاة للتحكم التربيعي الخطي

رسالة مقدمة الى قسم الهندسة الميكانيكية /جامعة كربلاء
كجزء من متطلبات نيل شهادة الماجستير في اختصاص
الميكانيك التطبيقي

من قبل الطالبة:

نور عباس حسين

بإشراف:

أ.د. عماد قاسم حسين

م.د. علي إبراهيم الزغبلي

2022م

الخلاصة

هناك اهتمام متزايد بتطوير نظام تعليق مقعد سائق المركبة الثقيلة لتقليل الاهتزازات المنقولة إلى جسم السائق. تحدث هذه الاهتزازات بسبب اثاره الطريق وتؤثر على كفاءة السائق وأدائه وصحته. لقد كان إنشاء وتطوير نظام تعليق مقعد السائق أمرًا حيويًا في السنوات الماضية، والذي حظي باهتمام كبير من قبل الباحثين والشركات للحصول على مزيد من الراحة والسلامة أثناء الركوب.

لذلك، في هذه الأطروحة تم تصميم وبناء مقعد اختبار بنظام تعليق سلبي من خلال إنشاء وتجميع الأجزاء باستخدام بعض النماذج المعتمدة عالميًا. ومن ثم تم إجراء تحليل لنظام تعليق المقعد السلبي. كذلك تم إجراء مقارنة بين المحاكاة والنتائج التجريبية للتحقق من فعالية جهاز الاختبار. وجد أن جهاز اختبار مقعد السائق المصنع نشط ومناسب ومنخفض التكلفة.

للحصول على صورة كاملة لأداء جهاز اختبار المقعد، تم اقتراح دراسة وتحليل نظام المقعد النشط من خلال تصميم جهاز تحكم (LQR منظم رباعي خطي) ومعرفة ما إذا كان التحسين في راحة الركوب الذي يحدث عن طريق تقليل الاهتزاز العمودي المنقول إلى المقعد. تم استخدام بيئة MATLAB / Simulink المختارة للمحاكاة للتحقق من أداء تصميم وحدة التحكم LQR. تم إجراء تحليل لنموذج جهاز اختبار مقعد السائق بمعادلة ذات درجتين من الحرية 2DOF. اظهرت نتائج المحاكاة أن وحدة التحكم LQR قوية ومناسبة ولديها إمكانية أفضل لتقليل التسارع الرأسي بنطاق تقريبي يبلغ 83% وتحقيق راحة الركوب، بتكلفة منخفضة لهذا النظام؛ عن طريق النظر في القيمة المثلى لمصفوفة وزن الإدخال R ومصفوفة وزن الحالة Q، الذين أثروا على إجراء التحكم.